NOTICE

The quality of this microform is heavily dependent upon the quality of the original thesis submitted for microfilming. Every effort has been made to ensure the highest quality of reproduction possible.

If pages are missing, contact the university which granted the degree.

Some pages may have indistinct print especially if the original pages were typed with a poor typewriter ribbon or if the university sent us an inferior photocopy.

Reproduction in full or in part of this microform is governed by the Canadian Copyright Act, R.S.C. 1970, c. C-30, and subsequent amendments.

AVIS

La qualité de cette microforme dépend grandement de la qualité de la thèse soumise au microfilmage. Nous avons tout fait pour assurer une qualité supérieure de reproduction.

S'il manque des pages, veuillez communiquer avec l'université qui a conféré le grade.

La qualité d'impression de certaines pages peut laisser à désirer, surtout si les pages originales ont été dactylographiées à l'aide d'un ruban usé ou si l'université nous a fait parvenir une photocopie de qualité inférieure.

La reproduction, même partielle, de cette microforme est soumise à la Loi canadienne sur le droit d'auteur, SRC 1970, c. C-30, et ses amendements subséquents.

Canada

Stabilities of Native Cytochromes c and Derivatives

Yazhen Hu

A Thesis

in

The Department

of

Chemistry and Biochemistry

Presented in Partial Fulfilment of the Requirements
for the Degree of Master of Science at
Concordia University
Montréal, Québec, Canada

March 1994

National Library
of Canada

Acquisitions and
Bibliographic Services Branch

395 Wellington Street
Ottawa, Ontario
K1A 0N4

Bibliothèque nationale
du Canada

Direction des acquisitions et
des services bibliographiques

395, rue Wellington
Ottawa (Ontario)
K1A 0N4

Your file Votre référence

Our file Notre référence

ISBN 0-315-90938-2

Canada

Abstract

Stabilities of Native Cytochromes c and Derivatives

Yazhen Hu

Stabilities of horse, tuna, Candida and Saccharomyces cytochromes c were investigated using spectroscopic probes. The integrated fluorescence intensity of Trp-59 was used to probe unfolding in urea and guanidine hydrochloride and the free energies of denaturation extrapolated to zero urea concentration ($\Delta G_{d,aq}$; kcal/mol) are 9.9 (horse), 8.9 (tuna), 8.1 (Candida) and 2.4 (Saccharomyces). For guanidine denaturation, the $\Delta G_{d,aq}$ values are ~1-2 kcal/mol lower but follow the same trend. The low $\Delta G_{d,aq}$ for the Saccharomyces protein was attributed to loss of a C-terminal helix-cap. Thermal stabilities as measured by fluorescence showed the same trend as the stabilities to denaturants. Fluorescence-monitored urea denaturation of horse cytochrome c derivatives yielded the following $\Delta G_{d,aq}$ values (kcal/mol): 9.9 (native), 5.4 (porphyrin; metal-free), 8.2 (Zn-substituted) and 10.5 (Co-substituted). This stability order correlates with the strength of the metal axial ligands.

695-nm absorbance was used to probe the Fe(III)-S(Met-80) bond. This is cleaved at high denaturant concentration, and changes in the Soret maxima revealed that axial-

ligand exchange occurs upon denaturation.

Local stabilities of the native cytochromes and the horse cytochrome c derivatives were examined by time-controlled tryptic digestion, followed by HPLC analysis. The results show that the local stabilities of the native cytochromes follow the order: horse > Candida > tuna, and those of horse c derivatives are: Co(III) > native [Fe(III)] > Zn(II) > porphyrin. The order of the observed local stabilities is interpreted in terms of the stability of the heme crevice and the Met-80 loop (segment 75-87).

Acknowledgements

I would like to take this opportunity to thank Dr. A.M. English for the chance to work in her laboratory and for her guidance throughout the course of this research.

I wish to thank Dr. R.H. Pallen and Dr. P.B.M. Joyce for being on my research committee and for their helpful suggestions during the course of my research. I would also like to thank Dr. M.J. Gresser (Merck-Frosst) for being an examiner and for taking the time to read this thesis.

I am grateful to all the graduate students, undergraduate students and postdocs who work in our laboratory for their friendship during my time at Concordia.

I am especially indebted to Mr. Bernard Gibbs (BRI) and Mr. George Tsaprailis for their assistance with the ES-MS measurements.

Finally, I dedicate this thesis to my husband Yongsheng Zhou for his love, support, encouragement and understanding during the course of my degree.

Table of Contents

1.0 Introduction 1

1.1 References 6

2.0 Relative stabilities of native cytochromes c 9

2.1 Introduction 9
2.2 Experimental 13
2.2.1 Materials 13
2.2.2 Methods 14
2.3 Results 20
2.4 Discussion 60
2.5 References 68

3.0 Relative stabilities of Fe, Co, Zn and porphyrin horse cytochromes c 72

3.1 Introduction 72
3.2 Experimental 73
3.2.1 Materials 73
3.2.2 Methods 73
3.3 Results 79
3.4 Discussion 106
3.5 References 112

4.0 Comparison of stabilities of native and derivatives of cytochrome c 114

5.0 Suggestions for future work 119

List of Figures

Figure 1.1:	Diagram of tuna cytochrome c	4
Figure 2.1:	Computer graphics display of the heme crevice of cytochrome c	10
Figure 2.2:	Method of ΔG_d calculation from fluorescence measurements	17
Figure 2.3:	FPLC cation-exchange chromatography of horse, tuna, Candida and Saccharomyces cytochromes c	21
Figure 2.4:	Relative fluorescence of horse, tuna, Candida and Saccharomyces cytochromes c vs. urea concentration	25
Figure 2.5:	Relative fluorescence of L-Trp vs. urea concentration	26
Figure 2.6:	Free energies of denaturation (ΔG_d) of horse, tuna, Candida and Saccharomyces cytochromes c vs. urea concentration	27
Figure 2.7:	Relative fluorescence of horse, tuna, Candida and Saccharomyces cytochromes c vs. guanidine hydrochloride concentration	29
Figure 2.8:	Relative fluorescence of L-Trp vs. guanidine hydrochloride concentration	30
Figure 2.9:	Free energies of denaturation (ΔG_d) of horse, tuna, Candida and Saccharomyces cytochromes c vs. guanidine hydrochloride concentration	31
Figure 2.10:	Relative fluorescence of horse, tuna, Candida and Saccharomyces cytochromes c vs. temperature	33
Figure 2.11:	Relative fluorescence of L-Trp vs. temperature	34
Figure 2.12:	Emission maxima vs. urea concentration for horse, tuna Candida and Saccharomyces cytochromes c	35

Figure 2.13: Emission maxima vs. guanidine hydrochloride concentration for horse, tuna, Candida and Saccharomyces cytochromes c 36

Figure 2.14: Soret maxima vs. urea concentration for horse, tuna Candida and Saccharomyces cytochromes c 37

Figure 2.15: Soret maxima vs. guanidine hydrochloride for horse, tuna, Candida and Saccharomyces cytochromes c 38

Figure 2.16: Soret absorption of horse and tuna cytochromes c in the presence and absence of urea 39

Figure 2.17: Determination of ΔA_{695} 42

Figure 2.18: The 695-nm absorption vs. urea concentration for horse, tuna, Candida and Saccharomyces cytochromes c 43

Figure 2.19: The 695-nm absorption vs. guanidine hydrochloride concentration for horse, tuna, Candida and Saccharomyces cytochromes c 45

Figure 2.20: Plot of ΔA_{695} vs. urea concentration for horse, tuna, Candida and Saccharomyces cytochromes c 47

Figure 2.21: Plot of ΔA_{695} vs. guanidine hydrochloride for of horse, tuna, Candida and Saccharomyces cytochromes c 48

Figure 2.22: Reversed-phase HPLC chromatograms of tryptic digests of horse cytochrome c 49

Figure 2.23: Relative peak areas of the HPLC bands of undigested horse, tuna, Candida and Saccharomyces cytochromes c vs. digestion time 50

Figure 2.24: ES-MS of undigested horse cytochrome c from 0, 1, 3, 7 and 18 h tryptic digests 52

Figure 3.1: Preparation of Zn-cyt c as monitored by Soret maxima 75

Figure 3.2: Preparation of Co-cyt c as monitored by Soret maxima 77

Figure 3.3: FPLC cation-exchange purification of por-cyt c 80

Figure 3.4: Soret absorption of the peaks from the FPLC purification of por-cyt c 81

Figure 3.5: FPLC cation-exchange purification of Zn-cyt c 83

Figure 3.6: Soret absorption of the peaks from the FPLC purification of Zn-cyt c 84

Figure 3.7: FPLC cation-exchange purification of Co-cyt c 85

Figure 3.8: Soret absorption of the peaks from the FPLC purification of Co-cyt c 86

Figure 3.9: ES-MS of Fe-, por-, Zn- and Co-cyts c 89

Figure 3.10: Integrated fluorescence of native and refolded horse cytochrome c vs. urea concentration 95

Figure 3.11: Relative fluorescence of native and partially refolded por-cyt c vs. urea concentration 96

Figure 3.12: Relative fluorescence of native and partially refolded Zn-cyt c vs. urea concentration 97

Figure 3.13: Relative fluorescence of native and partially refolded Co-cyt c vs. urea concentration 98

Figure 3.14: Relative fluorescence of Fe-, por-, Zn- and Co-cyts c vs. urea concentration 100

Figure 3.15: Free energies of denaturation (ΔG_d) of Fe-, por-, Zn- and Co-cyts c vs. urea concentration 101

Figure 3.16: Reversed-phase HPLC chromatograms of tryptic digests of Zn-cyt c 102

Figure 3.17: Relative peak areas of the HPLC bands of undigested Fe-, por-, Zn- and Co-cyts c vs. digestion time 103

Figure 3.18: Computer graphics display of horse cytochrome c showing the location of the 19 Lys residues 111

List of Tables

Table 2.1: Denaturation free energies ($\Delta G_{d,aq}$), m values and denaturant concentrations at half maximum fluorescence for native cytochromes c 58

Table 2.2: Denaturant concentration at half maximum fluorescence and at $\Delta A_{695} = 0$ 59

Table 3.1: MWs of Fe-, por-, Zn- and Co-cyts c as determined by ES-MS 104

Table 3.2: Denaturation free energies ($\Delta G_{d,aq}$), m values and urea concentrations at half maximum fluorescence for Fe-, por-, Zn- and Co-cyts c 105

List of Appendices

Appendix 1: Primary sequence alignment for cytochromes c 120

Appendix 2: Relative fluorescence values (%F) of native cytochromes c in urea 121

Appendix 3: Relative fluorescence values (%F) of horse cytochrome c derivatives in urea 125

Appendix 4: Relative fluorescence values (%F) of native cytochromes c in guanidine hydrochloride 128

Appendix 5: Determination of $\Delta G_{d,aq}$ and m values 132

1.0 Introduction

The thermodynamics of protein unfolding has been studied by many researchers[1,2]. These studies have focused primarily on the energetics of the transition between the folded and unfolded states and the mechanisms of stabilization of the structure of proteins. The unfolding transition of cytochrome c, a protein which plays a cental role in the mitochondrial electron-transfer chain, has been studied from both thermodynamic and kinetic points of view. Thermodynamic studies have assumed that unfolding involves a two-state transition such that no thermodynamically stable, partially folded states are significantly populated during the unfolding process[3].

It is possible to remove the heme iron from cytochrome c by brief exposure to hydrogen fluoride to generate metal-free porphyrin cytochrome c without disruption of the native tertiary structure. Protein-heme axial ligation can thus be selectively eliminated. Porphyrin cytochrome c can take up different metal ions into the porphyrin ring[4,5]. Derivatives prepared in this way and used in the present study include those containing Zn(II) and Co(III). The main reason for carrying out these modifications is to determine if the central metal influences the unfolding of the cytochrome c polypeptide. This work involves a comparison of the denaturation in urea of native horse ferricytochrome c, porphyrin cytochrome c, as well as its Co(III) and Zn(II) derivatives.

The free energy changes between the native (folded) state and the denatured (unfolded) state of the horse cytochrome c derivatives are determined to compare their relative conformational stabilities.

The free energy changes measured on denaturation of native cytochromes c from different sources are also reported in this study. These values will reveal the variation in conformational stability of cytochrome c with variation in amino acid sequence. Hence, a comparison of free energy changes from the two studies will indicate the relative importance of metal ligation and sequence on the conformational stability of cytochrome c. Cytochromes c from horse, tuna, Candida and Saccharomyces were chosen for this latter study. The horse and tuna cytochromes show ~82% homology, and Candida and Saccharomyces cytochromes show ~81% homology. There is significantly less homology between the yeast and horse cytochromes (~62%).

The fluorescence maxima (λ_m) of aqueous solutions of most native proteins at room temperature are in the range 330 to 340 nm. This emission is due to tryptophan (Trp) fluorescence, and the wavelength of maximum emission is dependent on environment of the indole ring. While Trps located inside the protein in a hydrophobic environment have λ_m at 330 to 340 nm, Trps on the surface in a highly polar, aqueous environment, exhibit λ_m at 350 nm. Thus, protein fluorescence shifts towards 350 nm under denaturing conditions[6], allowing the sensitivity of Trp residues to their environment to be used to monitor protein unfolding.

Figure 1.1[7], shows the heme packing in tuna cytochrome c and the interactions in the heme crevice. Bonds between the heme and four amino acids, Cys-14, Cys-17, His-

18 and Met-80, anchor the heme and, together with the extensive array of non-covalent side chain contacts, help to make the internal structure around the heme relatively rigid. All of the internal residues in Van der Waals contact with the heme are bulky hydrophobic groups (black dots, Figure 1.1). These hydrophobic groups help stabilize the structure of cytochrome c and control the redox potential.

Cytochrome c contains a Trp residue at position 59 at the lower left hand corner of the heme crevice[7] (Figure 1.1). The fluorescence of the native protein is highly quenched due to efficient energy transfer to the heme which is in close proximity. A dramatic increase in fluorescence and a red-shift in the λ_m of Trp from 330 to 350 nm is observed for cytochrome c upon denaturation. Thus, by monitoring the Trp fluorescence of cytochrome c in the presence of various concentrations of denaturant (urea and guanidine-HCl), the denaturation process may be followed by interpreting intensity changes in terms of variation in the heme to Trp-59 distance[8].

Fluorescence has also been used to monitor the kinetics of folding and unfolding of cytochrome c. The models used range from a single step process proposed by Schecther and Saludjian[9], to a three step process proposed by Myer[10] and Myer *et al.*[11], in which two intermediates are present. Heme absorbance at 400 nm versus time was also used to study folding and unfolding in 2.5 M guanidine hydrochloride[12]. The resultant semilogarithmic plot was biphasic[13], indicating that there are two steps in the folding - unfolding process of cytochrome c[12]. However the satisfactory fit of the thermodynamic data to a two-state transition[14] suggests that any kinetic intermediates formed rapidly decay and are not populated at equilibrium[15].

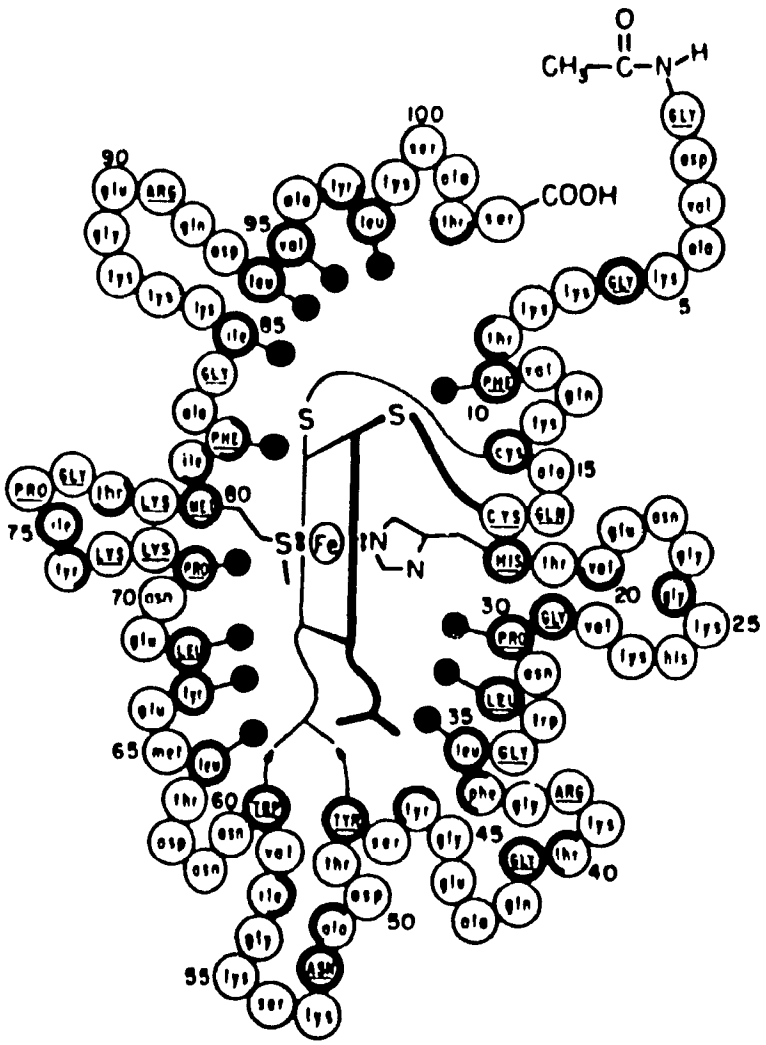

Figure 1.1: Diagram, from Dickerson *et al.* (1971), indicating the packing in the heme crevice. Heavy circles indicate side chains that are buried in the molecule. The black dots show residues whose side chains stack against the heme. Side chains present on the exterior of the molecule are shown by light circles, and those half buried by dark half-circles. Trp 59 is located in the lower left-hand corner of the heme crevice in the above diagram. The arrows indicate hydrogen-bonds between Trp 59, Tyr 48 and the propionic acid group of the porphyrin.

The free energy changes of denaturation reported here were monitored by measuring fluorescence intensity changes. The effects of temperature on cytochromes c fluorescence were also investigated to monitor the thermal stability of the proteins.

The iron present in the heme is coordinated to the four nitrogens of the porphyrin ring. The fifth and sixth axial positions are occupied by two strong field ligands, N from His-18 and S from Met-80[7]. The Fe(III)-S bond is relatively weak, compared to the bond between the Fe(III) and the imidazole N_3 on the right side of Figure 1.1. The Fe(III)-S bond of cytochrome c can be broken by high concentrations of denaturants and heating[16,17]. An absorption band at 695 nm is present when the Fe(III)-S bond is intact, and the protein is in its native conformation. Thus, this band has been used by a number of workers[18,19] as a sensitive marker for conformational change in the heme crevice of cytochrome c. The effects of denaturants on the absorbance at 695 nm should provide information on Fe(III)-S bond cleavage and the opening of the heme crevice in solution[20,21]. In this study, the dependence of the 695-nm absorbance on urea and guanidine hydrochloride concentrations was measured to probe the integrity of the heme crevice for horse, tuna and yeast cytochromes c.

The covalently-bound protoporphyrin IX heme prosthetic group is responsible for the intense band at 410 nm (Soret) and the visible (α,β) bands observed in the absorption spectrum of cytochromes c. These bands arise from allowed π-π^* porphyrin electronic transitions from the two highest filled molecular orbitals of a_{2u} and a_{1u} symmetry to the lowest empty orbital of e_g symmetry[22]. The porphyrin N atoms are strong-field ligands but are not strong enough to generate the low-spin state of Fe (III) or Fe(II). This

requires the addition of strong-field axial ligands to increase the ligand field strength. As a general rule, the ligand field of a 5-coordinated heme is rather weak, and this leads to the widely held view that the low-spin state requires 6-coordination. However, this is not always the case since a low-spin 5-coordination heme with a axial ligand has been described[23]. Nevertheless, the vast majority of low-spin hemes are 6-coordinate. Since the Soret shape and maximum are very sensitive to the axial coordination of the Fe(III) ion[24], we have studied this band as a function of urea and guanidine hydrochloride concentration to probe changes in heme axial ligation on denaturation.

Finally, protease digestion is used to analyze the relative local stability of the native cytochromes c and the horse cytochrome c derivatives. Following time-controlled tryptic digestion, the resultant digests were analyzed by high performance liquid chromatography (HPLC)[25]. Comparison of the results for the native cytochromes with those for the horse cytochrome derivatives will shed light on the relative importance of sequence and metal ligation on local stabilities.

1.1 References

1) Kawaguchi, H. and Noda, H. *J. Biochem.* **1977**, *81*, 1307.

2) Privalov, P.L. *Adv. Protein Chem.* **1979**, *33*, 167.

3) Cantor, C.R. and Schimmel, P.R. *Biophysical Chemistry*. W.H. Freeman and Company, San Francisco. **1980**, Part III, p. 1075.

4) Dickinson, L.C. and Chien, J.C.W. *Biochem.* **1975**, *14*, 3526.

5) Vanderkooi, J.M.; Adar, F. and Erecinska, M. *Eur. J. Biochem.* **1976**, *64*, 381.

6) Burstein, E.A.; Vedenkina, N.S. and Ivkova, M.N. *Photochem. Photobiol.* **1973**, *18*, 263.

7) Dickerson, R.E.; Takano, T.; Eisenberg, D.; Kallai, O.B.; Samson, L.; Cooper, A. and Margoliash, E. *J. Biol. Chem.* **1971**, *246*, 1511.

8) Tsong, T.W. *J. Biol. Chem.* **1974**, *249*, 1988.

9) Schechter, E. and Saludjian, P. *Biopolymers*, **1967**, *5*, 788.

10) Myer, Y.P. *Biochem.* **1968**, *7*, 765.

11) Myer, Y.P.; MacDonald, L.H.; Verma, B.C. and Pande, A. *Biochem.* **1980**, *19*, 199.

12) Ikai, A. and Tanford, C. *Nature*, **1971**, *230*, 100.

13) Raffery, S.P.; Pearce, L.L.; Barker, P.D.; Guillement, J.G.; Kay, C.M.; Smith, M. and Mauk, A.G. *Biochem.* **1990**, *29*, 9365.

14) Pearce, L.L.; Gärtner, A.L.; Smith, M. and Mauk, A.G. *Biochem.* **1989**, *28*, 3125.

15) Creighton, T.E. *Protein Folding*. W.H. Freeman and Company, New York. **1992**, p. 197.

16) Schejter, A.; Luntz, T.L.; Koshy, T.I. and Margoliash, E. *Biochem.* **1992**, *31*, 8336.

17) Kuroda, Y. *Biochem.* **1993**, *32*, 1219.

18) Schejter, A.; George, P. *Biochem.* **1964**, *3*, 1045.

19) Kaminsky, L.S.; Wright, R.L. and Davison, A.J. *Biochem.* **1971**, *10*, 458.

20) Kaminsky, L.S.; Miller, V.J. and Davison, A.J. *Biochem.* **1973**, *12*, 2215.

21) Stellwagen, E. *Biochem.* **1968**, 7, 2893.

22) Schomacker, K.T. and Champion, P.M. *J. Chem. Phys.* **1986**, 84, 5314.

23) English, D.R.; Hendrickson D.N.; Suslick, K.S.; Eigenbrot, J.C.W. and Scheidt, W.R.

J. Am. Chem. Soc. **1984**, *106*, 7258.

24) Stallard, B.R.; Callis, P.R.; Champion, P.M. and Albrecht, A.C. *J. Chem. Phys.* **1984**, *80*, 70.

25) Endo, S.; Nagayama, K. and Wada, A. *J. Biomol. Struct. Dynam.* **1985**, *3*, 409.

2.0 Relative stabilities of native cytochromes c

2.1 Introduction

As shown in Figure 1.1, and in more detail in Figure 2.1, Trp-59 is hydrogen bonded to heme propionate-7 (HP-7) in cytochrome c. The fluorescence will increase with increased distance between Trp-59 and the heme. In order to investigate the stability of cytochrome c, we have used fluorescence to probe its unfolding transition in the presence of denaturants[1,2]. We have undertaken studies of the denaturation equilibria of cytochromes c from four species: horse, tuna, Candida *krusei* and Saccharomyces *cerevisiae.*

The stability of the folded conformation of a protein appears to depend on its primary structure in a complex manner[3,4]. Cytochrome c is an excellent system for examining the relationship between sequence and stability since proteins from a large variety of sources are available. Also the Saccharomyces protein has been cloned[5] which has allowed mutants to be prepared and examined[6,7]. Studies to date clearly indicate that cytochromes c from different species have different conformational stabilities. Cytochromes from horse, tuna, Candida and Saccharomyces were chosen for this study because there are large phyletic distances among these species[8] and because all of these cytochromes c are commercially available.

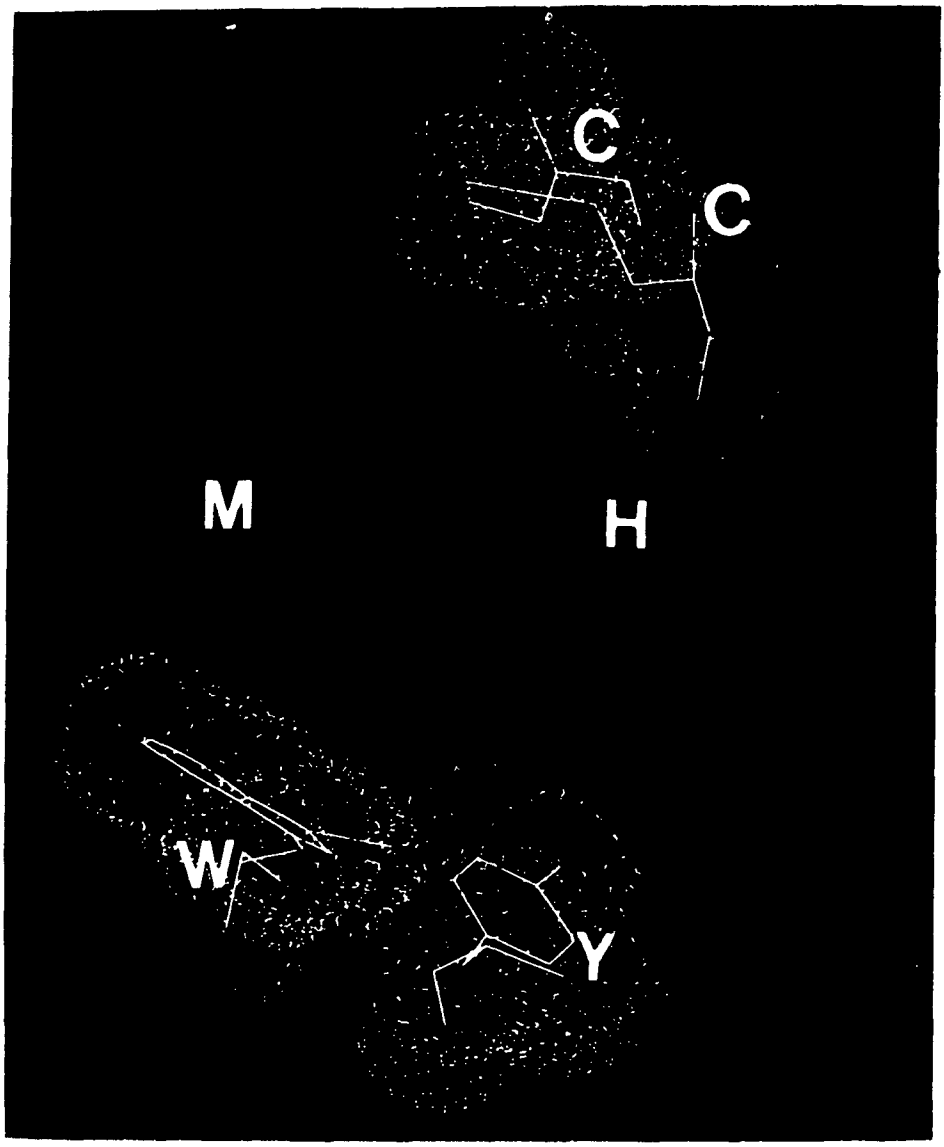

Figure 2.1: Computer graphics display of heme iron ligands to N-His-18 and S-Met-80, and the heme vinyl covalent bonds to Cys-14 and Cys-17. Two hydrogen-bonds connect the heme propionates to Trp-59 and Tyr-48. This molecular graphics image was produced using the MidasPlus software system[36] from the Computer Graphics Laboratory, University of California, San Francisco.

A large number of reagents affect protein stability when added to the aqueous solvent. Those that decrease protein stability are termed denaturants, the best known of which are urea and guanidine hydrochloride[9,10,11,12].

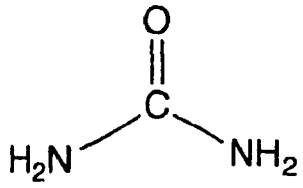

Urea

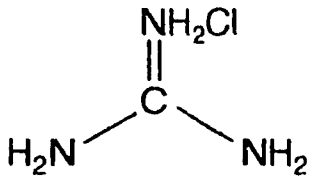

Guanidine hydrochloride

These compounds were considered to act as denaturants by breaking protein hydrogen bonds and to interact with peptide groups in unfolded proteins through hydrogen bonding[13]. However, it has been suggested that these denaturants are probably no more potent in hydrogen bonding than water[14].

Fe-S(Met-80) ligation through sulfur is common to all cytochromes c (Figure 2.1). The Fe(III)-S bond, as mentioned above, has been shown to give rise to a Fe-cyt c absorption band at 695 nm which can be used as a measure of the integrity of Fe(III)-S bond[15,16]. The 695-nm band can be abolished at neutral pH by increasing the denaturant (urea or guanidine hydrochloride) concentration[17]; this spectroscopic modification is fast and reversible. In this study, we examine the 695-nm band at various denaturant concentrations to compare the relationship between the strength of the Fe-S bond and the global conformation of cytochrome c. Limited data on the effects of denaturants and

temperature on the 695-nm absorbance have been reported previously[15,16,18].

The temperature at which different proteins unfold varies enormously. Most proteins unfold at high temperatures, but some unfold at very low temperatures. Cytochromes c are stable at relatively high temperatures (50-80 °C)[19], and 695-nm absorption measurement show that the Fe(III)-S bond is also cleaved at high temperatures around neutral pH[15]. Fluorescence measurements have not been used to date to probe the thermal stabilities of cytochromes c. Fluorescence intensities were measured for the native cytochromes c between 10 and 95 °C and results are reported here.

Proteolytic digestion has been used to probe local stabilities of proteins. Proteases can only cleave at locally unfolded regions of a polypeptide; thus, protease susceptibility requires local conformational instability. Studies on the local stabilities of native cytochromes c have been previously reported[3]. We have repeated these experiments to confirm the literature results since we wish to compare local stabilities of the native cytochromes with those of the derivatives under identical conditions. Trypsin, which cleaves at Arg and Lys residues, is one of the most widely use specific proteolytic enzymes[20]. Arg and Lys residues are relatively conserved in cytochromes c from very different sources, and play a key role in the binding of cytochrome c to its biological partners. Time dependence of tryptic digestion is used to probe the local stability of the different cytochromes. Trypsin is maximally active at pH 8.0, but in our case, we wanted slower digestion under more physiological conditions. Thus, 50 mM sodium phosphate with 0.2 M KCl buffer (pH 7.0) was used for our digestion (proteolytic) studies, which were carried out at 37 °C. The areas of the undigested cytochrome c peaks from a C-18

reversed-phase HPLC column were measured to determine the extent of tryptic digestion versus time[21]. The local stabilities of the different cytochromes c obtained by this method are compared to the global stabilities which were obtained from the fluorescence studies in denaturants. The undigested cytochrome c peaks from the HPLC were collected and the molecular weight was confirmed by electrospray mass spectrometry (ES-MS). Electrospray is a gentle method of ionization that produces intact, multiply protonated gas-phase ions directly from protein molecules in solution[22]. Electrospray ionization combined with quadrupole mass spectrometry has been very successful in obtaining molecular weights of cytochromes c[23] and this is exploited here.

2.2 Experimental

2.2.1 Materials

Horse cytochrome c (type III or type VI), tuna cytochrome c (type XI), Candida *krusei* cytochrome c (type VII), Saccharomyces *cerevisiae* cytochrome c (type VIII-B or type VIII-A) and L-tryptophan (L-Trp) were obtained from Sigma. Sodium phosphate, potassium chloride, potassium ferricyanide, acetonitrile and trifluoroacetic acid were purchased from Fisher Scientific. Guanidine hydrochloride and urea were obtained from Sigma and Anachemia, respectively. All solutions were made using distilled water (specific resistance 18 MΩ cm) from a Barnstead nanopure system.

2.2.2 Methods

Purification of cytochromes c: Cytochromes c were purified using a Pharmacia fast protein liquid chromatography (FPLC) system. The system consisted of a MV-7

valve, a LCC-500 Plus programming unit, two P-500 pumps, and a UV-M1 monitor connected to a HR cell. The detection wavelength used was 280 nm. Buffers were filtered using 0.45 μM filters, and the solutions were degassed by sonication or vacuum for a period of about 30 min prior to use. Cation-exchange was performed on a Mono S 10/10 column. 500 μl cytochrome c (15 ~ 30 mg/ml) were introduced into the system and elution was carried out using 20 mM sodium phosphate buffer (pH 7.0) with a gradient of 0 to 0.6 M KCl (horse and tuna cytochromes) and 0 to 1.2 M KCl (Candida and Saccharomyces cytochromes) at a flow rate of 1.0 ml/min. The chart recorder speed was 0.5 cm/ml.

Denaturation of cytochromes c in denaturants: The concentration of each cytochrome c was determined using a millimolar extinction coefficient of 106 $(mM\ cm)^{-1}$ at the Soret maxima of 410 nm[24]. The concentration of L-Trp was determined using an extinction coefficient of 5.6 $(mM\ cm)^{-1}$ at 280 nm[25]. Guanidine hydrochloride and urea solutions of known concentration were prepared by weight. Urea concentrations were from 0 to 9.0 M in 50 mM sodium phosphate, 0.2 M KCl buffer (pH 7.0), and guanidine hydrochloride concentrations were from 0 to 6.0 M in 100 mM sodium phosphate buffer (pH 7.0). The proteins were allowed to denature for at least 10 min in the presence of urea or guanidine hydrochloride at ambient temperature prior to obtaining fluorescence and absorption spectra.

Free energy of denaturation: Unfolding of native cytochromes c in urea and guanidine hydrochloride has been shown to be reversible[26]. It is assumed that unfolding is a two-state phenomenon, with only the folded (native, n) and unfolded (denatured, d)

state present. Thus at 50% unfolding, 50% of the molecules are native (n) and 50% are denatured (d). For a two-state transition, the equilibrium constant between the native and denatured states can be measured directly from the average fraction of unfolded molecules in the transition region[27].

Fluorescence intensities (F), were determined at various urea or guanidine hydrochloride concentrations. F_n and F_d indicate the values of F in the absence of denaturant and after saturation with denaturant, respectively (Figure 2.2). Thus, the equilibrium constant between the denatured (cyt c_d) and native (cyt c_n) states is given by:

$$K_d = [\text{cyt } c_d]/[\text{cyt } c_n] = (F - F_n)/(F_d - F) \qquad (2.1)$$

The free energy change on denaturation (ΔG_d). can be determined using the formula,

$$\Delta G_d = - RT\ln K_d \qquad (2.2)$$

The most pertinent value of ΔG_d is that under normal conditions: aqueous solutions in the absence of denaturant at room temperature ($\Delta G_{d,aq}$). This value can be estimated by extrapolation. In the unfolding transition region the value of ΔG_d is generally found to vary linearly with denaturant concentration so that

$$\Delta G_d = \Delta G_{d,aq} - m.[\text{denaturant}] \qquad (2.3)$$

where $\Delta G_{d,aq}$ is the free energy of denaturation extrapolated to 0 M denaturant. Equations 2.1 and 2.2 can be combined to give the following form:

$$\Delta G_d = -RT\ln[(F - F_n)/(F_d - F)] \quad (2.4)$$

Figure 2.2 shows the use of linear extrapolation to calculate F_n and F_d in the transition range. Using the observed % fluorescence (F), and the extrapolated F_n and F_d values, ΔG_d was calculated at each denaturant concentration. A plot of ΔG_d vs. denaturant concentration yields $\Delta G_{d,aq}$ (intercept) and the parameter m (slope).

Thermal denaturation of cytochromes c: 2.0 μM cytochromes c solutions were prepared in 100 mM sodium phosphate (pH 7.0) buffer. The temperature of fluorometer sample compartment was controlled from 10 to 95 °C.

Fluorescence measurements: Fluorescence measurements were performed on FPLC-purified cytochrome c samples containing 2.0 μM protein. All measurements were performed using a Shimadzu Model RF-5000 fluorometer with excitation and emission slit widths of 5 nm, and an excitation wavelength of 280 nm. The emission of the blank was subtracted from that of the protein samples to correct for any background fluorescence from the buffer, urea or guanidine hydrochloride at each temperature examined. In all the cases, the emission intensity was integrated (using the integration mode of the fluorometer) over the region 315 to 400 nm following subtraction of the blank. The integrated intensity obtained for 2.0 μM L-Trp under identical conditions was taken to be 100%. Correction for inner filter effects was accomplished using the

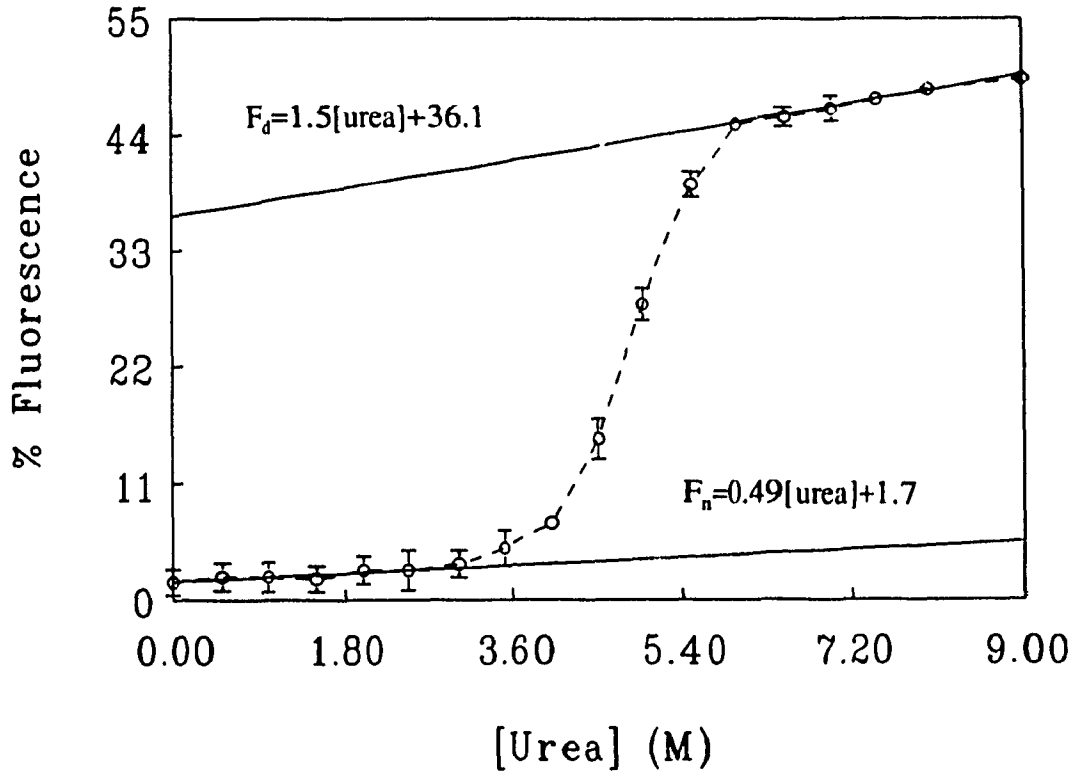

Figure 2.2: Urea unfolding of Candida cytochrome c as monitored by fluorescence intensity, F. The equations for F_n and F_d obtained by least squares analysis give the variation of F for the native and denatured states, respectively, with urea concentration. These values and the meas ıred F values in the transition region (3.5 ~ 5.5 M urea) were put into equation 2.4 to obtain ΔG_d.

relationship[28] (Lakowicz, 1983):

$$F_c = F \text{ antilog}[(A_{ex} + A_{em})/2] \qquad \textbf{(2.5)}$$

where F is the observed fluorescence, F_c is the corrected fluorescence, A_{ex} is the absorbance of the solution at the excitation wavelength, and A_{em} is the absorbance of maximum emission wavelength.

Soret band maximum of cytochrome c: Soret absorbance of FPLC-purified 2.0 μM samples were detected using a Philips Pu 8710/01 spectrophotometer and Falcon Scan software with a band width of 2.0 nm and a scan speed of 250 nm/min. Cytochromes c were unfolded at 25 ± 1 °C in urea with 50 mM sodium phosphate buffer (pH 7.0) containing 0.2 M KCl, or in guanidine hydrochloride with 100 mM sodium phosphate buffer (pH 7.0).

695-nm absorbance of cytochromes c: Absorbance readings were taken at 25 ± 1 °C on FPLC-purified 30 μM cytochrome c in 50 mM sodium phosphate buffer (pH 7.0) with 0.2 M KCl and different urea concentrations, and in 100 mM sodium phosphate buffer (pH 7.0) with different guanidine hydrochloride concentrations. Potassium ferricyanide (30 μM) was added to the samples to ensure that only the Fe(III) form was present. The Philips Pu 8710/01 spectrophotometer and Falcon Scan software were also used for these measurements. The wavelength range was scanned from 600 to 800 nm at a speed of 250 nm/min.

Analysis of local stability of cytochromes c by HPLC: 10 mg/ml of trypsin was

dissolved in 10 mM HCl and the cytochromes c were dissolved in 50 mM sodium phosphate buffer (pH 7.0) with 0.2 M KCl. The trypsin and cytochrome c solutions were mixed and incubated at 37 °C for 0, 1, 4, 7, 18 h. The trypsin to cytochrome c ratio was 1:50 (W:W) and the concentration of cytochrome was ~2 mg/ml. Digestion was terminated by adding 5.0 M HCl. The HPLC system (LKB Bromma) consisted of a 2249 gradient pump, a Vydac 218TP54 reversed-phase C-18 column (0.46x25 cm), a 2141 variable wavelength monitor, and a 100-µl injection loop. All HPLC solutions were filtered through 0.2-µM nylon membrane filters (Gelman Sciences) on a Millipore filtration system and degassed for about 1 h before use. 100 µl of cytochrome c (0.5 µg/µl) were injected onto the column at 25 °C. The eluent was 0.1% trifluoroacetic acid (pH 2.5) with a gradient of 20 to 80% acetonitrile over 15 min, and a flow rate of 1.0 ml/min at 15 ± 0.3 MPa pressure. The eluted samples were detected by their absorbance at 210 (peptide backbone) and 410 nm (Soret band), and the absorbance vs. elution time was plotted using Maxima software (Waters). The undigested horse cytochrome c peaks were collected to confirm the MW of the protein present by ES-MS.

Electrospray mass spectrometry of horse cytochrome c peaks from HPLC: A triple quadrupole mass spectrometer (API III, Sciex) was used for all the MS experiments. The instrument has a mass-to-charge (m/z) range of 2400 and is fitted with a pneumatically-assisted electrospray interface. Multiply charged cytochrome c ions were generated by spraying the sample solution through a stainless steel capillary held at a high potential of +4.8 kV. The sample solution was delivered to the sprayer by a syringe infusion pump (Model 22, Harvard Apparatus) through a fused silica capillary of 100-µm

i.d. The liquid flow rate was set at 2.0 ~ 3.0 µl/min for sample introduction, and the potential on the sampling orifice of the instrument was set at +100 V. The m/z scale was first checked with lysozyme (14,310 Da), and then MW determinations on the cytochrome c peaks in 10% acetic acid (pH 2.2) were performed using the same parameters.

2.3 Results

FPLC cation-exchange chromatography: Commercial cytochrome c contains some deamidated forms (Gln → Glu and Asn → Asp). Since native cytochrome c is more positively charged it binds more tightly to a cation-exchange column than the deamidated forms. Figure 2.3 shows the chromatograms of the commercial cytochromes c. As can be seen from this figure, the proteins were eluted at high salt, with the deamidated forms first, followed by the native form. Candida and Saccharomyces cytochromes c were eluted at higher salt concentration compared to horse and tuna cytochromes c, implying that the exposure of positive charges are different among these proteins. Native, monomeric Saccharomyces cytochrome c is in the band at 0.86 M KCl; the second band at 0.92 M KCl contains a dimeric form due to disulfide bond formation between Cys-102 residues. SDS-PAGE with and without β-mercaptoethanol, which reduces disulfide bonds, was used to confirm the presence of monomeric and dimeric forms of Saccharomyces cytochrome c. The purified cytochromes c were collected and concentrated by ultrafiltration using an Amicon stirred cell and YM 10 filter. Rechromatography of the cytochromes indicated the absence of deamidated forms since they yielded a single band on FPLC (Mono S) or HPLC (C-18). Also, SDS-PAGE shows

Figure 2.3: FPLC cation-exchange chromatography (Mono S, HR 10/10) of commercial (a) horse, (b) tuna, (c) Candida and (d) Saccharomyces cytochromes c. The column was equilibrated with 20 mM sodium phosphate buffer (pH 7.0) and elution was with a KCl gradient (dashed line) in 20 mM sodium phosphate buffer (pH 7.0). Flow rate, 1.0 ml/min; fraction size, 4.0 ml.

(a)

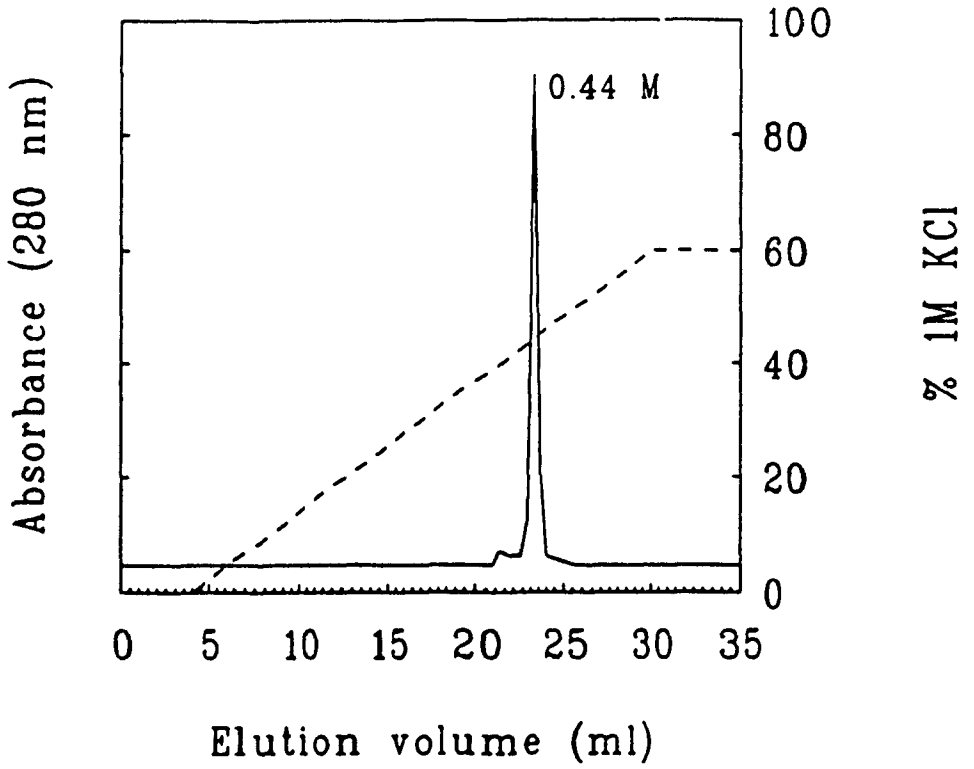
0.44 M
Absorbance (280 nm)
% 1M KCl
100
80
60
40
20
0
0 5 10 15 20 25 30 35
Elution volume (ml)

(b)

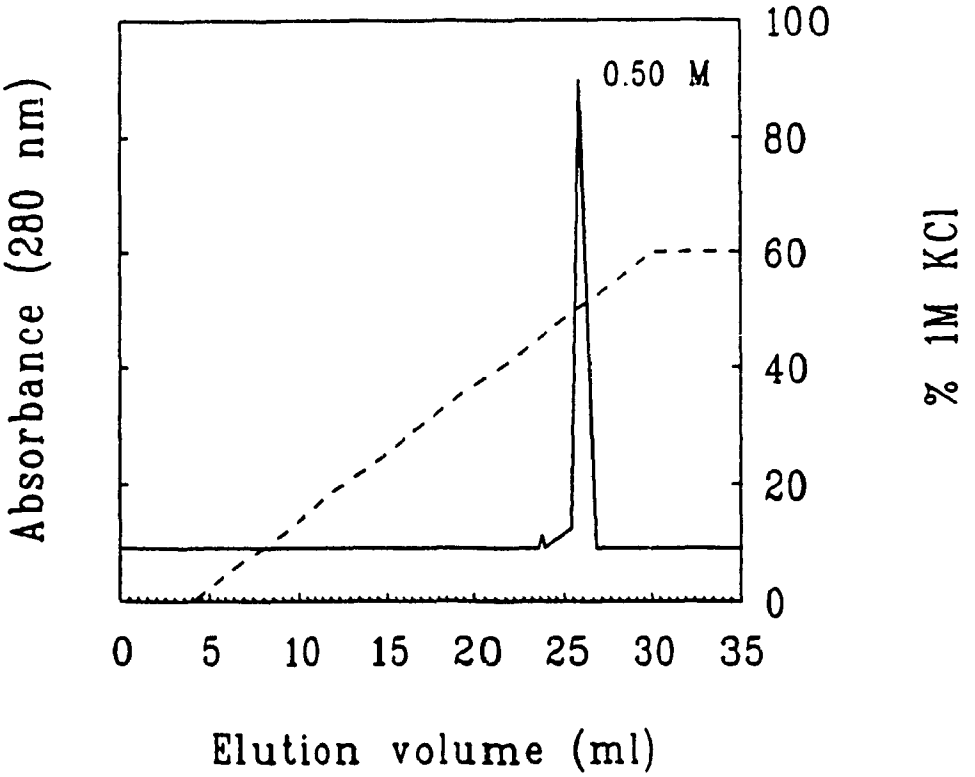
0.50 M
Absorbance (280 nm)
% 1M KCl
100
80
60
40
20
0
0 5 10 15 20 25 30 35
Elution volume (ml)

(c)

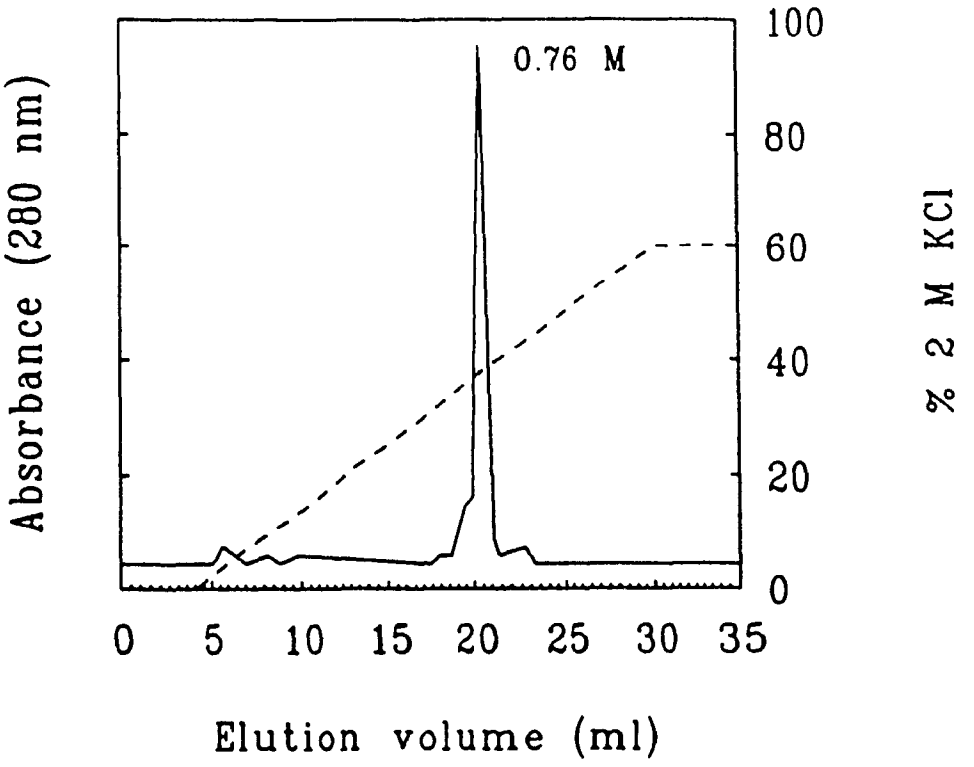
0.76 M
Absorbance (280 nm)
% 2 M KCl
0 5 10 15 20 25 30 35
0 20 40 60 80 100
Elution volume (ml)

(d)

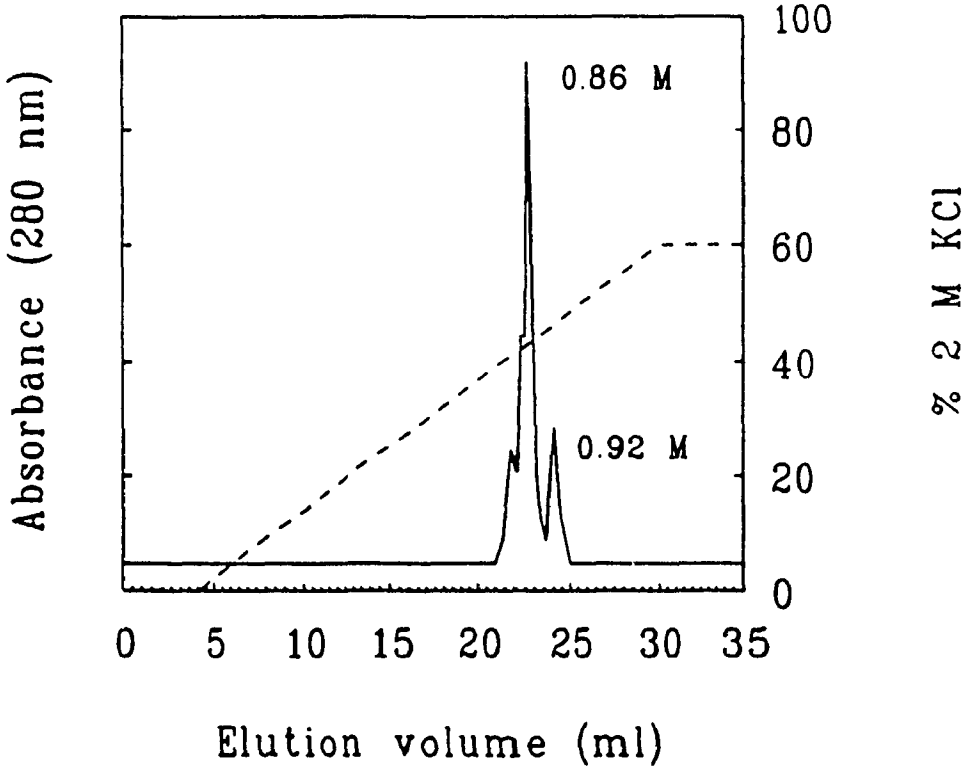
0.86 M
0.92 M
Absorbance (280 nm)
% 2 M KCl
0 5 10 15 20 25 30 35
0 20 40 60 80 100
Elution volume (ml)

only one band after FPLC for horse, tuna and Candida cytochromes c, while that of Saccharomyces cytochrome c contains two bands, with MWs corresponding to the monomer and dimer. A separate SDS-PAGE study indicated that dimerization is time dependent in buffer with 13.4% dimer forming in 60 min in ~0.1 mM Saccharomyces cytochrome c solutions. Previous work showed that both monomer and dimer have similar unfolding curves in denaturants[29], so the denaturation studies were carried out here on mixtures of the two forms.

Fluorescence of cytochromes c in urea: Trp fluorescence of cytochrome c is quenched by heme in the folded state. The conformation of cytochrome c changes from a folded state to an unfolded state at high urea concentration. The change in relative fluorescence of 2.0 μM cytochromes c vs. urea concentration is given in Appendix 2 and plotted in Figure 2.4, where the fluorescence of 2.0 μM L-Trp in urea is taken as 100%. The variation in L-Trp fluorescence vs. urea concentration is shown in Figure 2.5, which reveals that the fluorescence of L-Trp also increases with urea concentration. The maximum relative fluorescence of horse, Candida and Saccharomyces cytochromes c is about 50%, while that of tuna cytochrome c is around 75% (relative to 2.0 μM L-Trp) due to the presence of two Trp residues in its polypeptide.

The unfolding transition occurs at different urea concentrations for the four cytochromes c. Figure 2.2 shows how the F_d, F_n and hence the ΔG_d values were determined from the % fluorescence intensities (F), and Figure 2.6 shows plots of ΔG_d vs. urea concentration. The intercepts of these plots denote the free energy changes in the aqueous solvent ($\Delta G_{d,aq}$) and the slopes denote the parameter m (Equation 2.3). Table 2.1

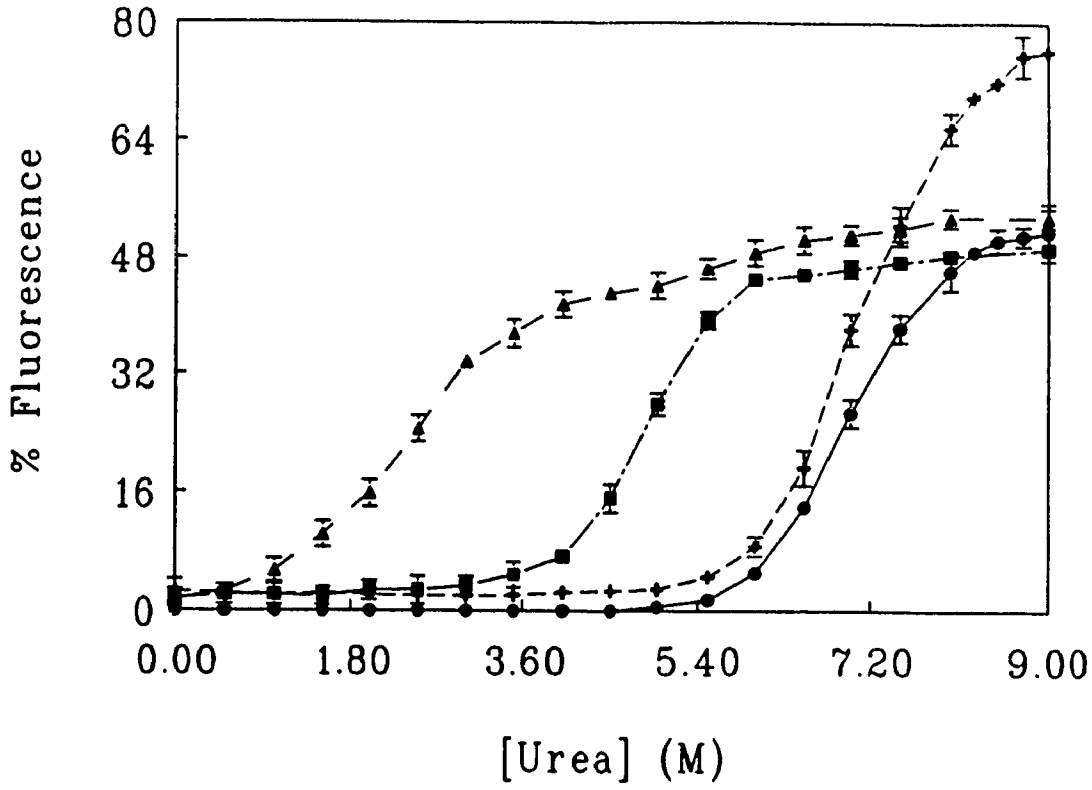

Figure 2.4: Relative integrated fluorescence (%) of 2.0 μM horse (●), tuna (+), Candida (■) and Saccharomyces (▲) cytochromes c vs. urea concentration at pH 7.0. Each data point represents the integrated emission from 315 to 400 nm. The excitation wavelength was 280 nm and excitation and emission slits were set at 5 nm. The samples were buffered with 50 mM sodium phosphate buffer (pH 7.0) containing 0.2 M KCl, at 25 ± 1 °C. The fluorescence of 2.0 μM L-Trp at the same concentration of urea was taken as 100%. Error bars were obtained from an average of 3 to 5 trials.

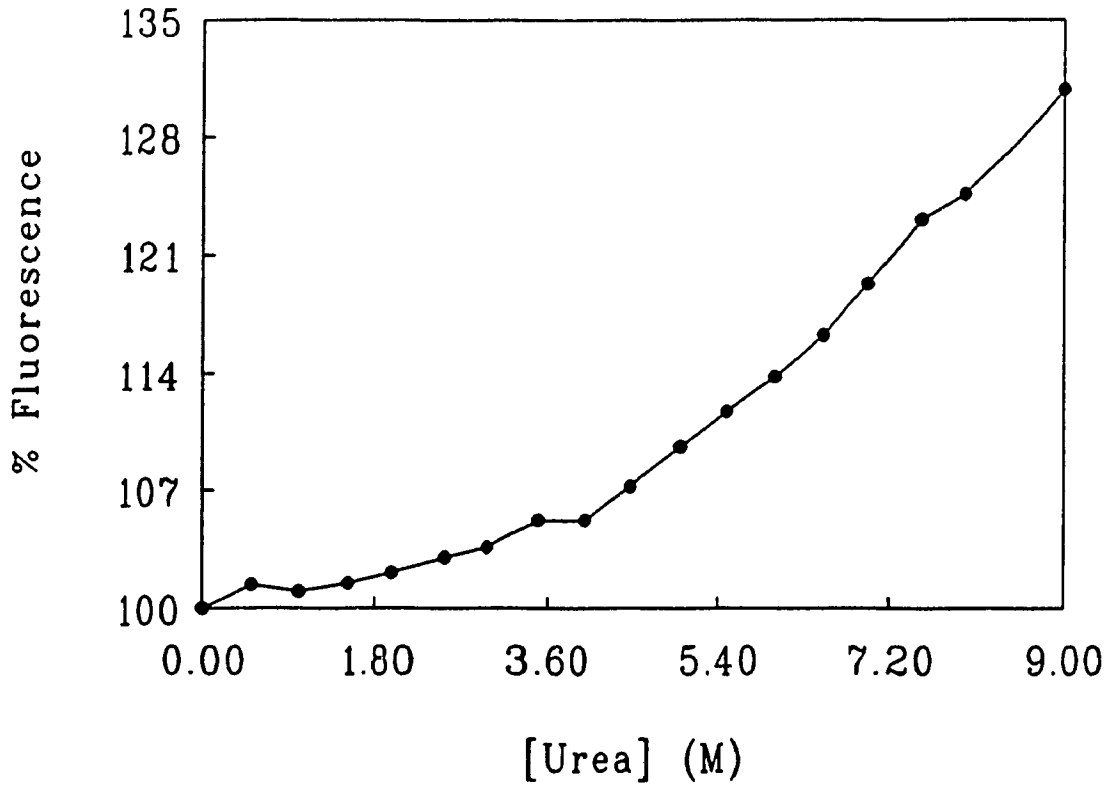

Figure 2.5: Relative integrated fluorescence (%) of 2.0 μM L-Trp vs. urea concentration at pH 7.0. L-Trp was in 50 mM sodium phosphate buffer, pH 7.0, containing 0.2 M KCl. The fluorescence of 2.0 μM L-Trp in buffer with no added urea was taken as 100%. See caption to Figure 2.4 for further experimental details.

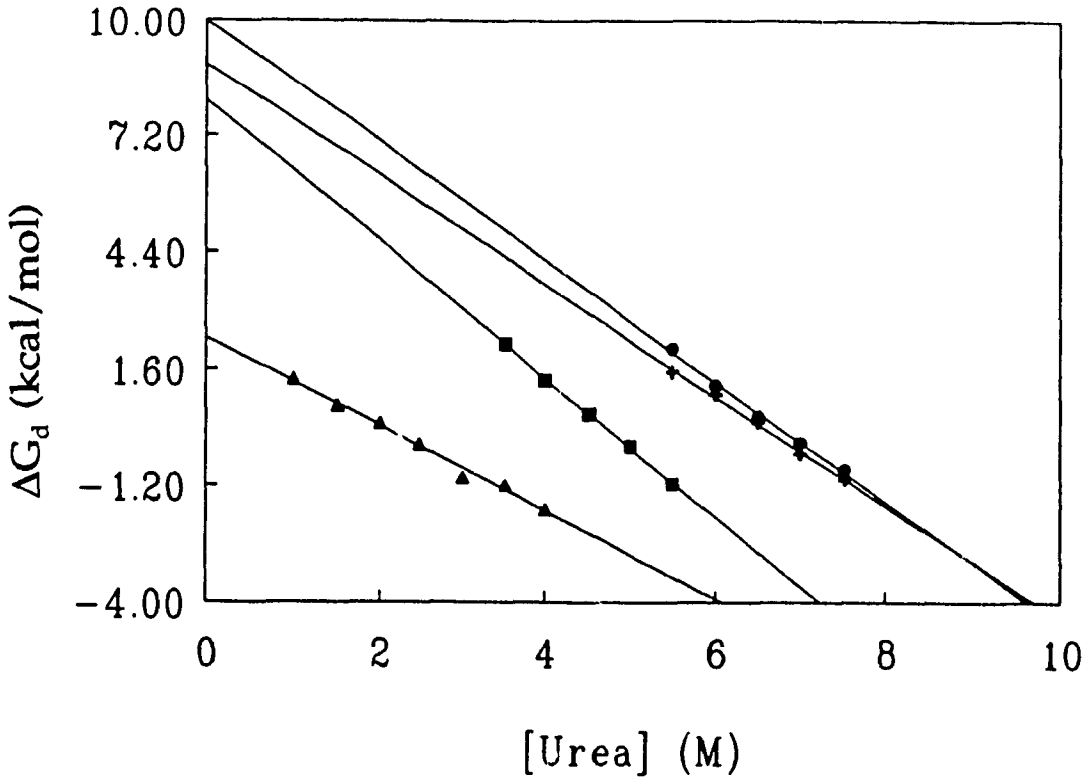

Figure 2.6: Free energies of denaturation (ΔG_d) of horse (●), tuna (+), Candida (■) and Saccharomyces (▲) cytochromes c vs. urea concentration. ΔG_d values were calculated using Equation 2.4 and the data in Appendix 2. The intercept and slope of each plot gives $\Delta G_{d,aq}$ and m, respectively (Equation 2.3).

summarizes the $\Delta G_{d,aq}$ and m values and also lists the concentration of urea at half maximum fluorescence for each species of cytochrome c.

Fluorescence of cytochromes c in guanidine hydrochloride: The relative fluorescence of the four cytochromes c in guanidine hydrochloride solutions is given in Figure 2.7. As shown in this figure, the % fluorescence increases with increasing concentration of denaturant, and the maximum fluorescence of horse, Candida and Saccharomyces cytochromes c is about 70% in 6.0 M guanidine hydrochloride, while that of tuna cytochrome c is more than 100% because it contains two Trp residues. In these experiments, the fluorescence of 2.0 μM L-Trp in guanidine hydrochloride is taken as 100%, and the dependence of L-Trp fluorescence on the guanidine hydrochloride concentration is shown in Figure 2.8. It is of interest that L-Trp fluorescence decreases with increased guanidine hydrochloride concentration, while an increase is seen with increasing urea (Figure 2.5).

The dependence of ΔG_d on the concentration of guanidine hydrochloride is shown in Figure 2.9. The intercepts of the plots yield $\Delta G_{d,aq}$, the free energy of denaturation of cytochrome c in aqueous solvent and the slopes give the parameter m. These data are also listed in Table 2.1.

Effect of temperature on the fluorescence of cytochromes c: Figure 2.10 shows the effect of temperature on the fluorescence of the cytochromes c. The temperature of 2.0 μM solutions of the proteins in 100 mM sodium phosphate buffer at pH 7.0 was gradually increased from 10 to 95 °C. The interval between consecutive readings, including the time necessary for temperature change and equilibration, was 10 min. The

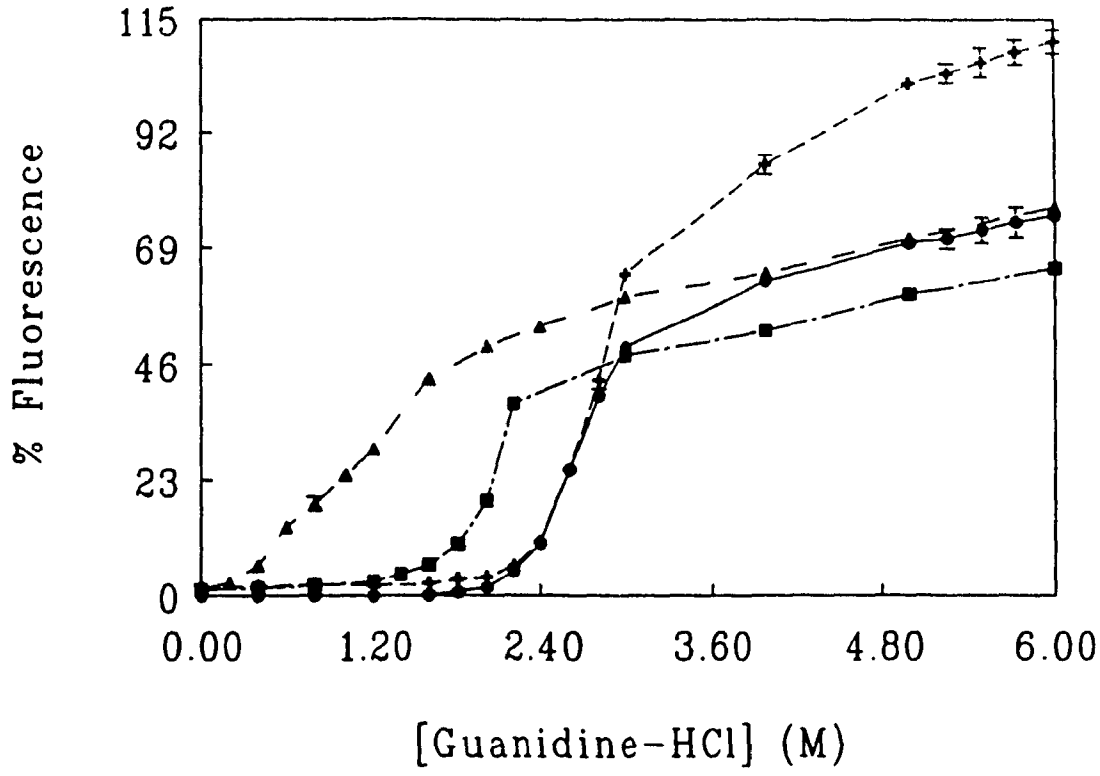

Figure 2.7: Relative integrated fluorescence (%) vs. guanidine hydrochloride concentration for 2.0 μM horse (●), tuna (+), Candida (■) and Saccharomyces (▲) cytochromes c in 100 mM sodium phosphate buffer, pH 7.0, 25 ± 1 °C. The fluorescence of 2.0 μM L-Trp in the same concentration of guanidine hydrochloride was taken as 100%. See caption to Figure 2.4 for further experimental details. The error bars were obtained from an average of 3 trials.

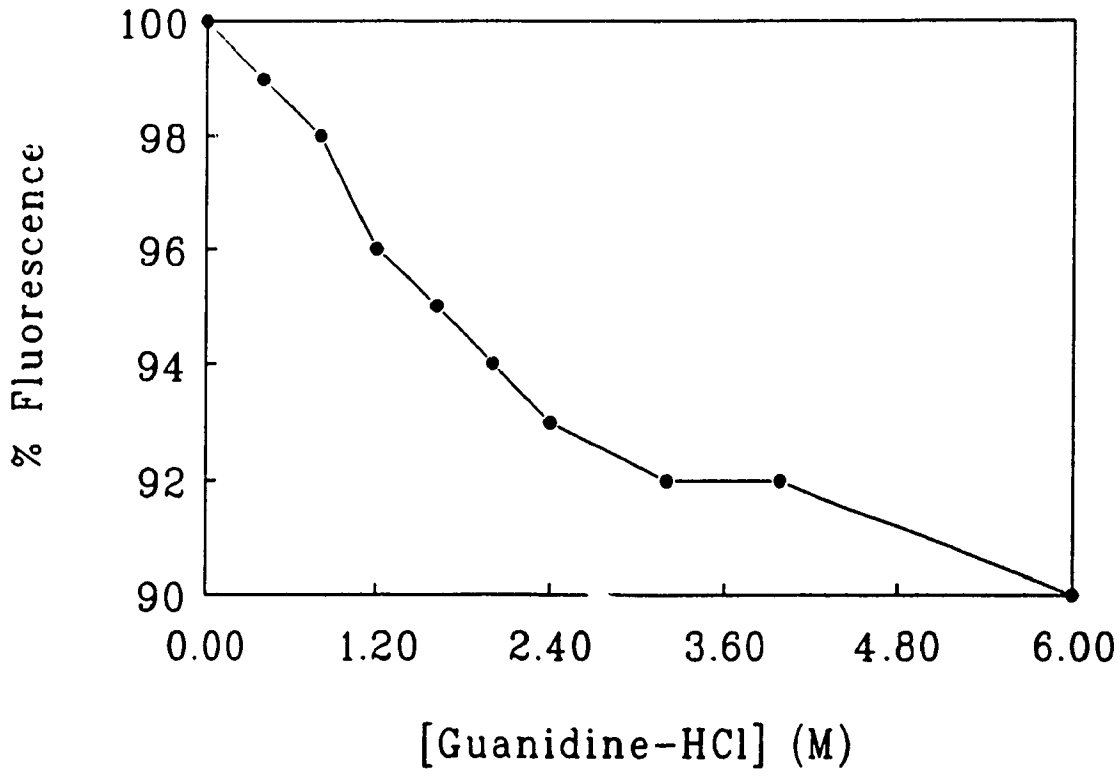

Figure 2.8: Relative integrated fluorescence (%) of 2.0 μM L-Trp vs. guanidine hydrochloride concentration in 100 mM sodium phosphate buffer, pH 7.0. The fluorescence of 2.0 μM L-Trp in buffer with no added guanidine hydrochloride was taken as 100%. See caption to Figure 2.4 for further experimental details.

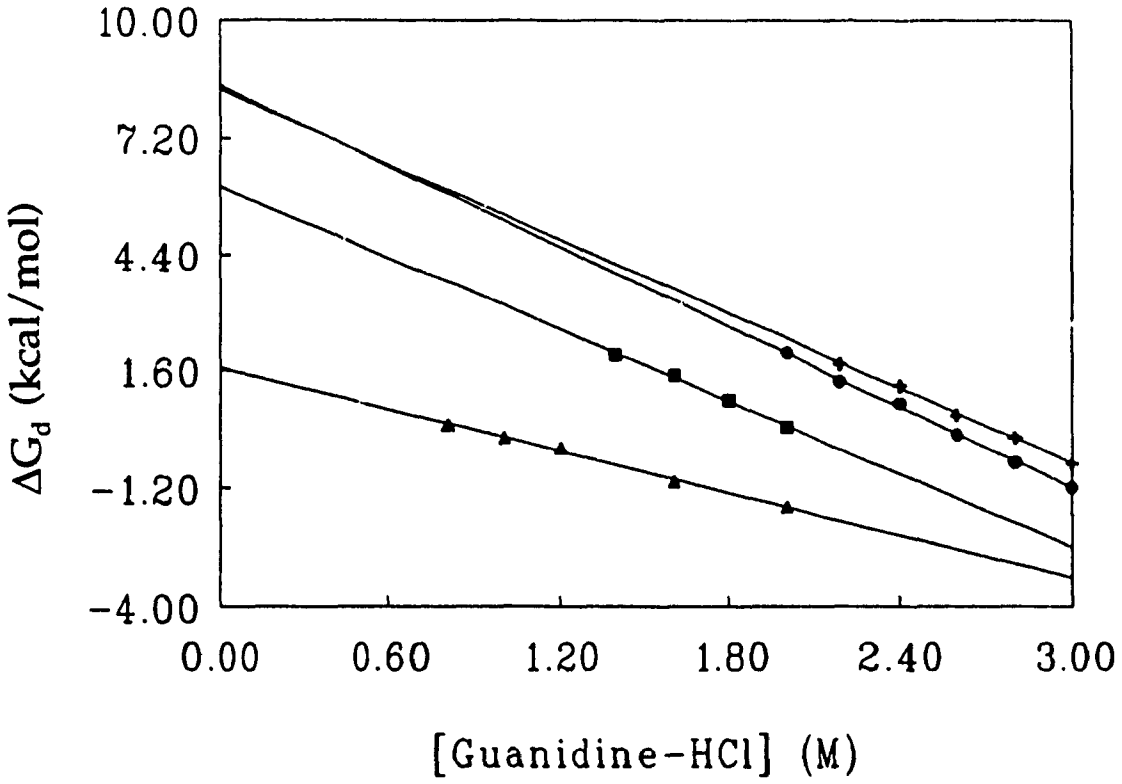

Figure 2.9: Free energies of denaturation (ΔG_d) of horse (●), tuna (+), Candida (■) and Saccharomyces (▲) cytochromes c vs. guanidine hydrochloride concentration. ΔG_d values were using Equation 2.4 and the data in Appendix 4. The intercept and slope of each plot gives $\Delta G_{d,aq}$ and m, respectively (Equation 2.3).

fluorescence of 2.0 μM L-Trp at the same temperature was taken as 100%. The relative fluorescence of L-Trp vs. temperature is shown in Figure 2.11, and as can be seen from this figure the fluorescence intensity is strongly temperature dependent.

Fluorescence maxima in denaturants: The Trp emission maximum of cytochrome c may range from 330 to 350 nm, depending on whether the environment of the indole ring is hydrophobic or hydrophilic. For single Trp-containing proteins, such as cytochromes c (except the tuna cytochrome which contains two Trps), the emission spectrum reflects the environment of that single fluorophore. The emission maxima of all the cytochromes c red-shift at high urea and guanidine hydrochloride concentrations as shown Figures in 2.12 and 2.13, respectively. The yeast cytochromes' emission maxima red-shift at relatively low concentrations of urea and guanidine hydrochloride, while the horse and tuna maxima red-shift at higher concentrations of denaturants. Also, the yeast cytochromes c exhibit emission maxima at ~340 nm in solutions containing 0 - 2 M urea whereas the horse and tuna cytochromes have emission maxima at ~330 nm. This is due to the presence of 0.2 M KCl in the buffer used for the urea denaturation studies, since in the absence of added KCl and denaturant, all cytochromes c exhibit the same emission maxima (Figure 2.13).

Soret absorption in denaturants: In Figures 2.14 and 2.15, the Soret absorption maxima of the cytochromes c are displayed as a function of urea and guanidine hydrochloride concentration, respectively. The Soret maxima are blue-shifted by ~ 2 - 3 nm for horse, Candida and Saccharomyces cytochromes c in 9.0 M urea, but a larger shift (8 nm) is observed for tuna cytochrome c under the same conditions. Similar trends

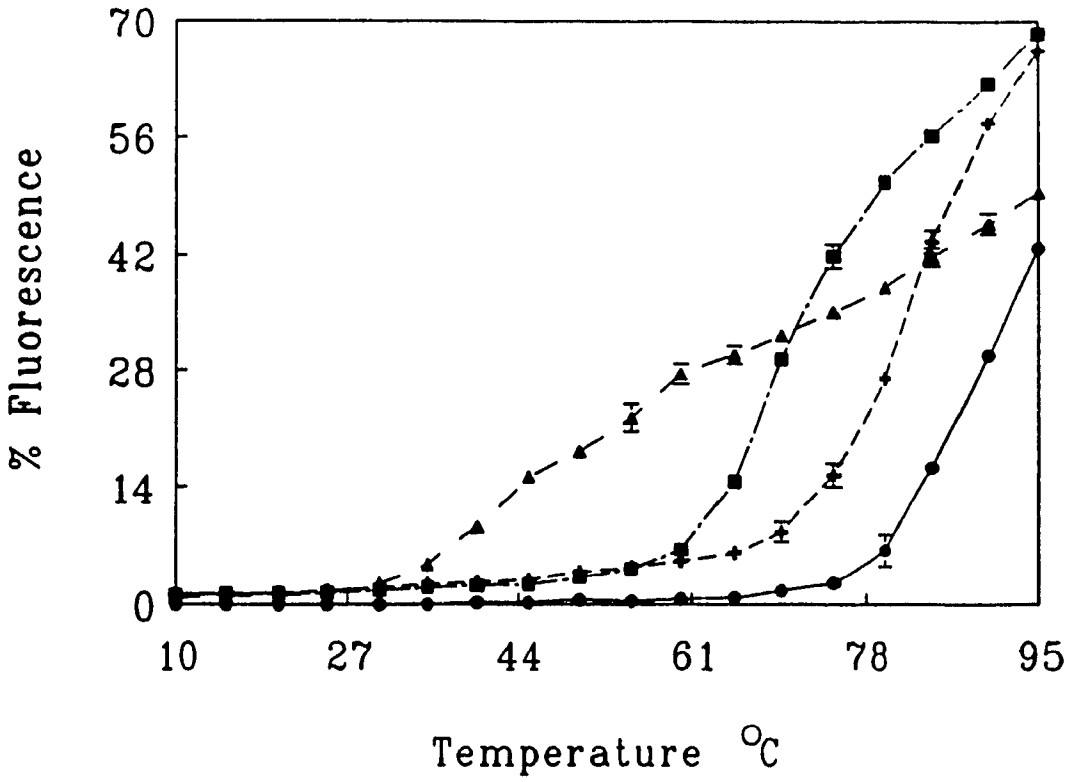

Figure 2.10: Thermal denaturation of cytochromes c. Relative integrated fluorescence (%) of 2.0 μM horse (●), tuna (+), Candida (■) and Saccharomyces (▲) cytochromes c in 50 mM sodium phosphate buffer, pH 7.0, containing 0.2 M KCl. The integrated emission of 2.0 μM L-Trp at the same temperature was taken as 100%. See caption to Figure 2.4 for further experimental details. The error bars were obtained from an average of 3 trials.

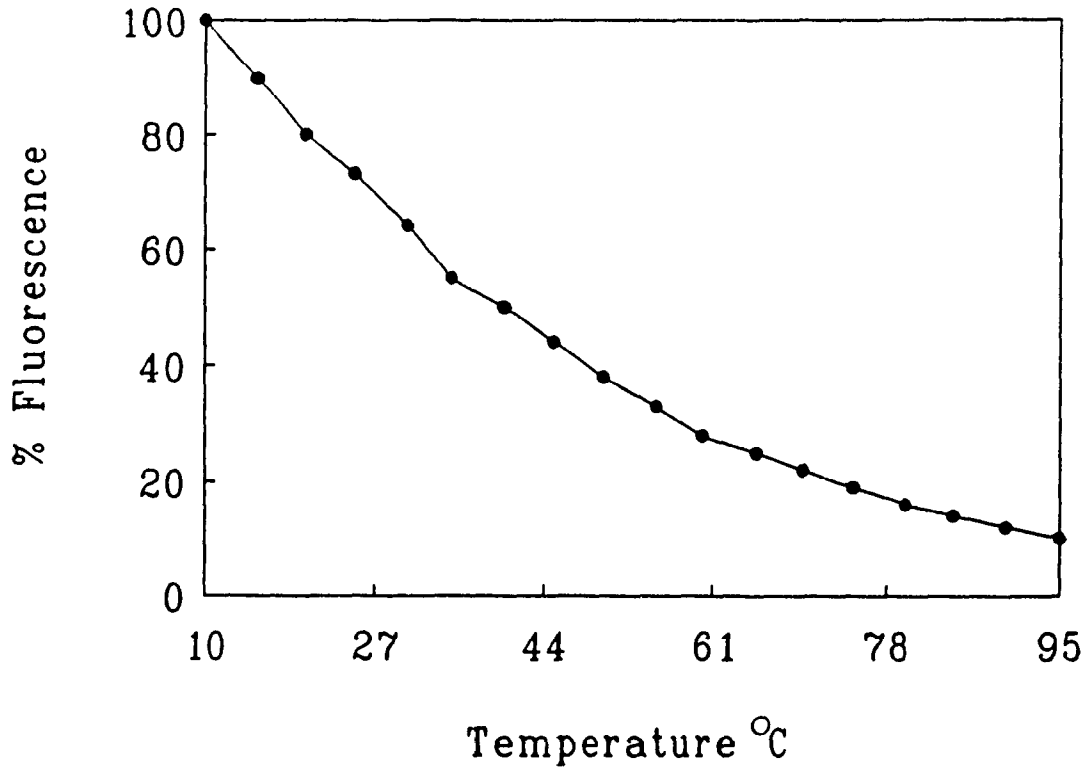

Figure 2.11: Relative integrated fluorescence of 2.0 μM L-Trp in 50 mM sodium phosphate buffer, pH 7.0, containing 0.2 M KCl, vs. temperature. Fluorescence of 2.0 μM L-Trp at 10 °C was taken as 100%.

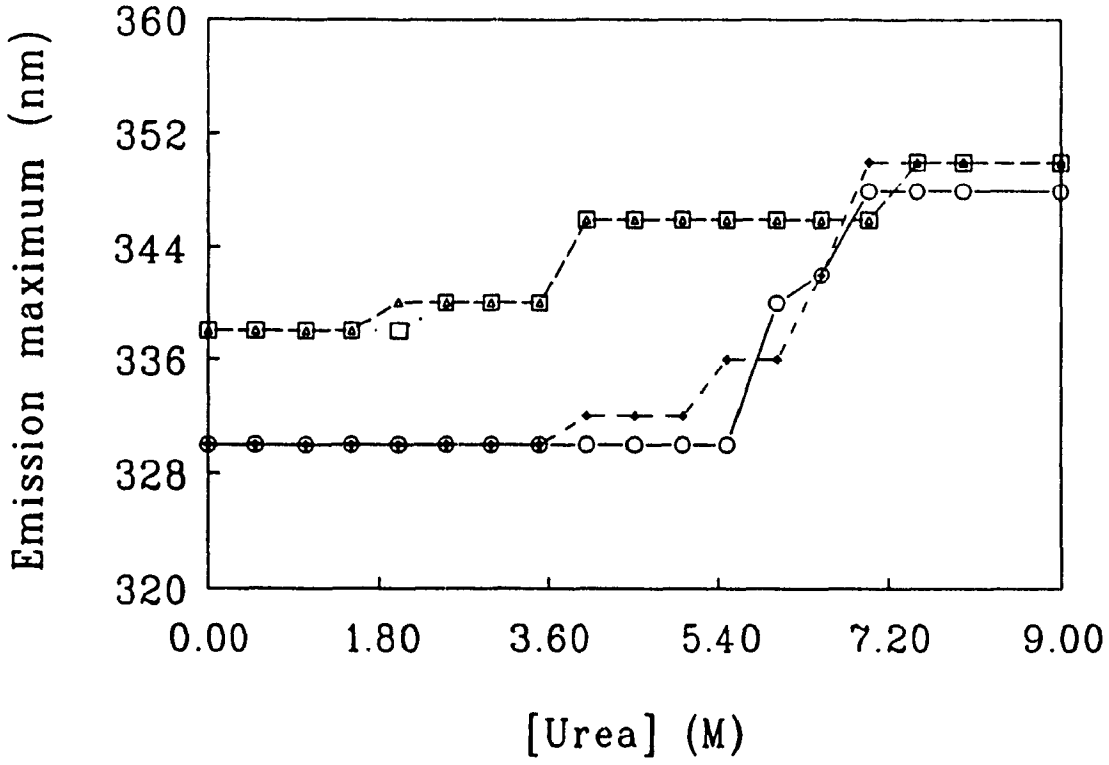

Figure 2.12: Emission maxima vs. urea concentration of 2.0 μM horse (○), tuna (+), Candida (□) and Saccharomyces (△) cytochromes c in 50 mM sodium phosphate buffer, pH 7.0, containing 0.2 M KCl, 25 ± 1 °C. The excitation wavelength was 280 nm and excitation and emission slits were 5 nm.

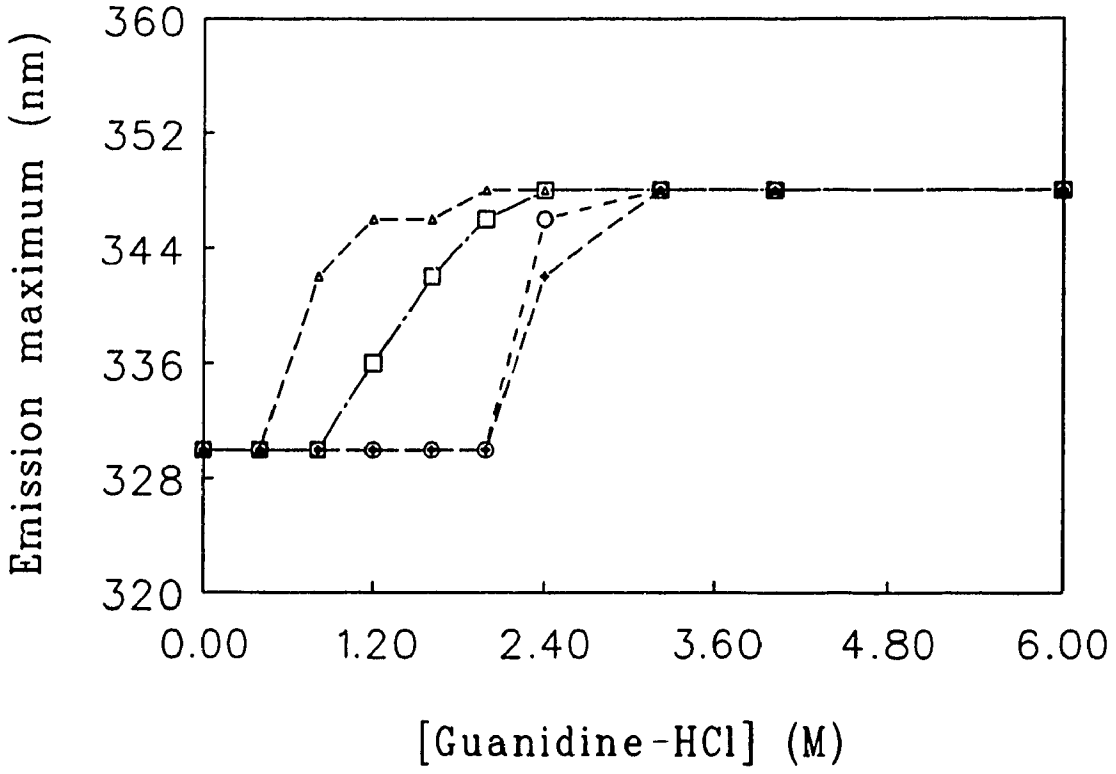

Figure 2.13: Emission maxima vs. guanidine hydrochloride concentration of 2.0 μM horse (○), tuna (+), Candida (□) and Saccharomyces (△) cytochromes c in 100 mM sodium phosphate buffer, pH 7.0, 25 ± 1 °C. The excitation wavelength was 280 nm and excitation and emission slits were 5 nm.

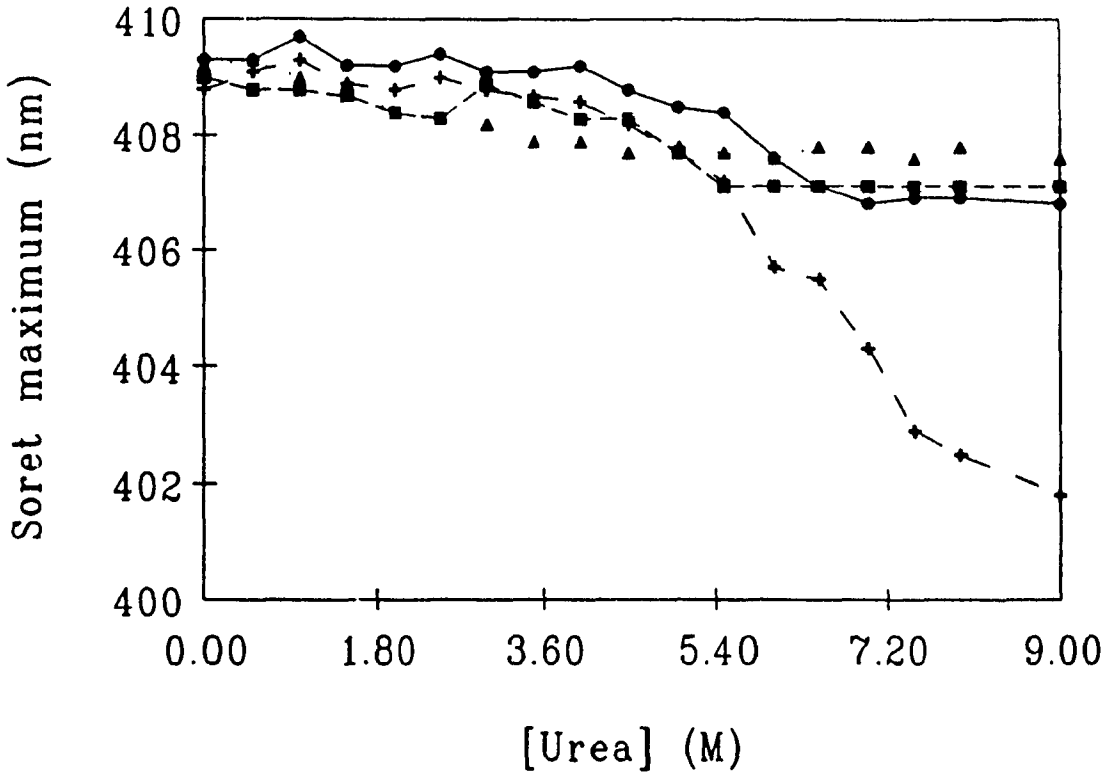

Figure 2.14: Soret maxima vs. urea concentration of 2.0 μM horse (●), tuna (+), Candida (■) and Saccharomyces (▲) cytochromes c in 50 mM sodium phosphate buffer, pH 7.0, containing 0.2 M KCl, 25 ± 1 °C. The Soret absorption was scanned from 250 nm to 500 nm at a speed of 250 nm/min.

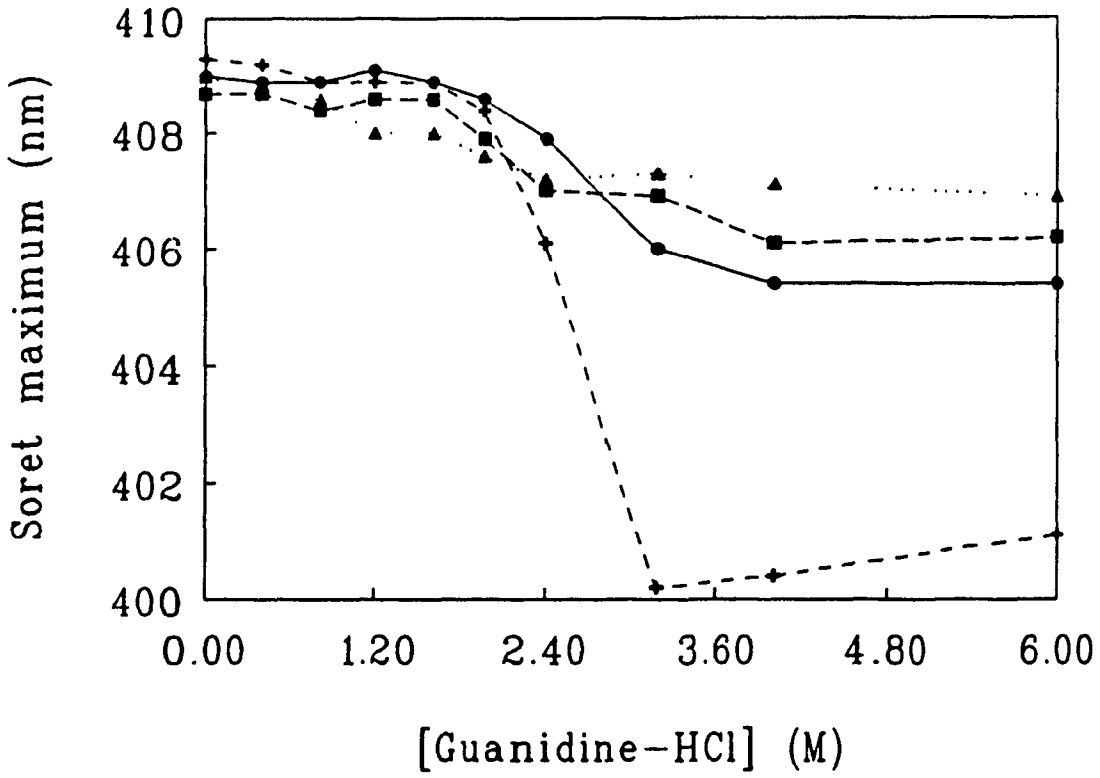

Figure 2.15: Soret maxima vs. guanidine hydrochloride concentration of 2.0 μM horse (●), tuna (+), Candida (■) and Saccharomyces (▲) cytochromes c in 100 mM sodium phosphate buffer, pH 7.0, 25 ± 1 °C. The Soret absorption was scanned from 250 nm to 500 nm at a speed of 250 nm/min.

Figure 2.16: Soret absorption of horse (solid line) and tuna (dashed line) cytochromes c in 50 mM sodium phosphate buffer, pH 7.0, containing 0.2 M KCl. (a) Without urea; (b) with 9.0 M urea.

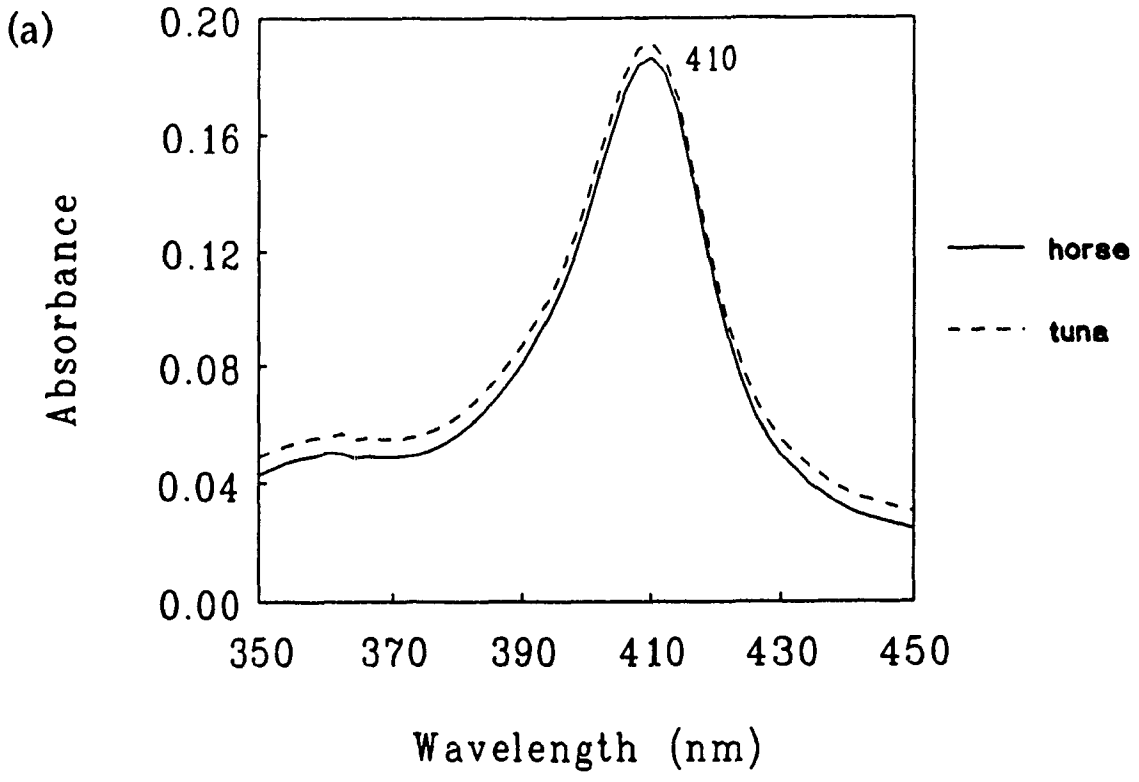
(a)
0.20
0.16
0.12
0.08
0.04
0.00
Absorbance
410
350
370
390
410
430
450
Wavelength (nm)
horse
tuna

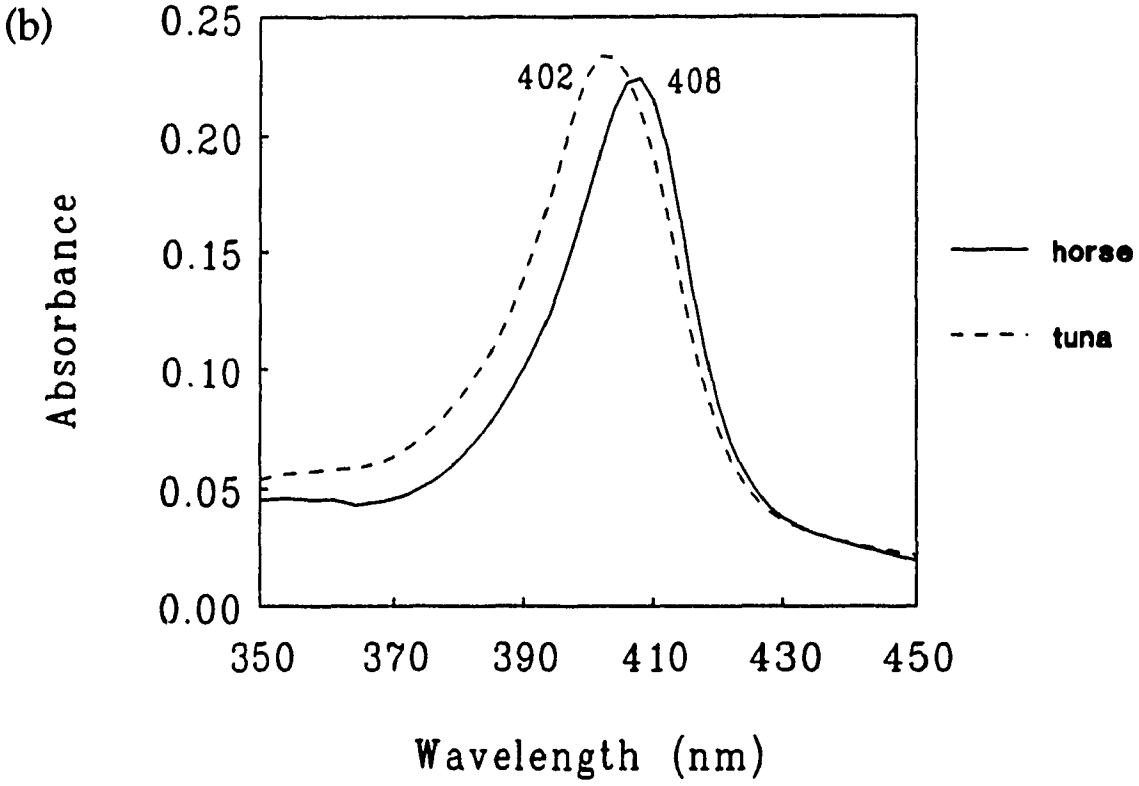
(b)
0.25
0.20
0.15
0.10
0.05
0.00
Absorbance
402
408
350
370
390
410
430
450
Wavelength (nm)
horse
tuna

are observed in guanidine hydrochloride, where small blue-shifts (2-3 nm) are observed for the same three cytochromes c, and the tuna cytochrome again displays a large blue-shift (8-9 nm) at high guanidine hydrochloride concentration. Figure 2.16 compares the Soret absorption of horse and tuna cytochrome c in the presence and absence of urea.

695-nm absorption in denaturants: The 695-nm absorption band of horse cytochrome c is displayed in Figure 2.17. The effects of increasing denaturant concentration at pH 7.0 on this band of the four ferricytochromes c are shown in Figures 2.18 and 2.19. Figures 2.20 and 2.21 display the observed 695-nm absorbance change (ΔA_{695}), which was measured as shown in Figure 2.17, vs. urea and guanidine hydrochloride concentrations, respectively.

Analysis of local stability of cytochromes c by HPLC: The time evolution of tryptic digestion of cytochromes c was analyzed by HPLC. Figure 2.22 shows the chromatograms obtained for digests of horse cytochrome c, and similar chromatograms were obtained for the other cytochromes. The absorbance at 210 nm was taken as 100% at zero time and the relative absorbance of bands containing undigested proteins are plotted vs. digestion time in Figure 2.23. The local stabilities of the cytochromes c are in the order: horse > Candida > tuna. Attempts to analyze the local stability of Saccharomyces cytochrome c was not successful because the dimer and monomer have different retention time on the C-18 column (not shown). The resultant chromatogram was not sufficiently reproducible to allow the time course of tryptic digestion of this protein to determined.

Determination of MW of undigested horse cytochrome c by ES-MS: The

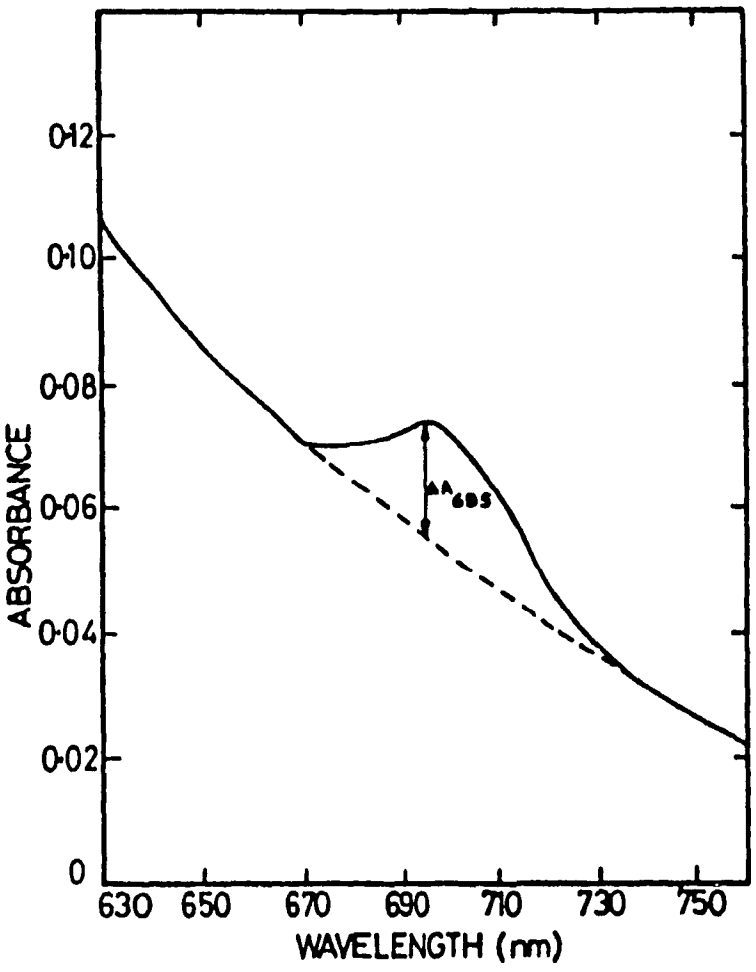

Figure 2.17: 695-nm absorption of ferricytochrome c indicating the determination of ΔA_{695}. This figure was adopted from Kaminsky *et al. Biochem.* **1973**, *12*, 2214.

Figure 2.18: Absorption spectra of 30 μM (a) horse, (b) tuna, (c) Candida and (d) Saccharomyces ferricytochromes c in 50 mM sodium phosphate buffer, pH 7.0, containing 0.2 M KCl and the urea concentrations indicated on the spectra. Scan speed was 250 nm/min, 25 ± 1 °C.

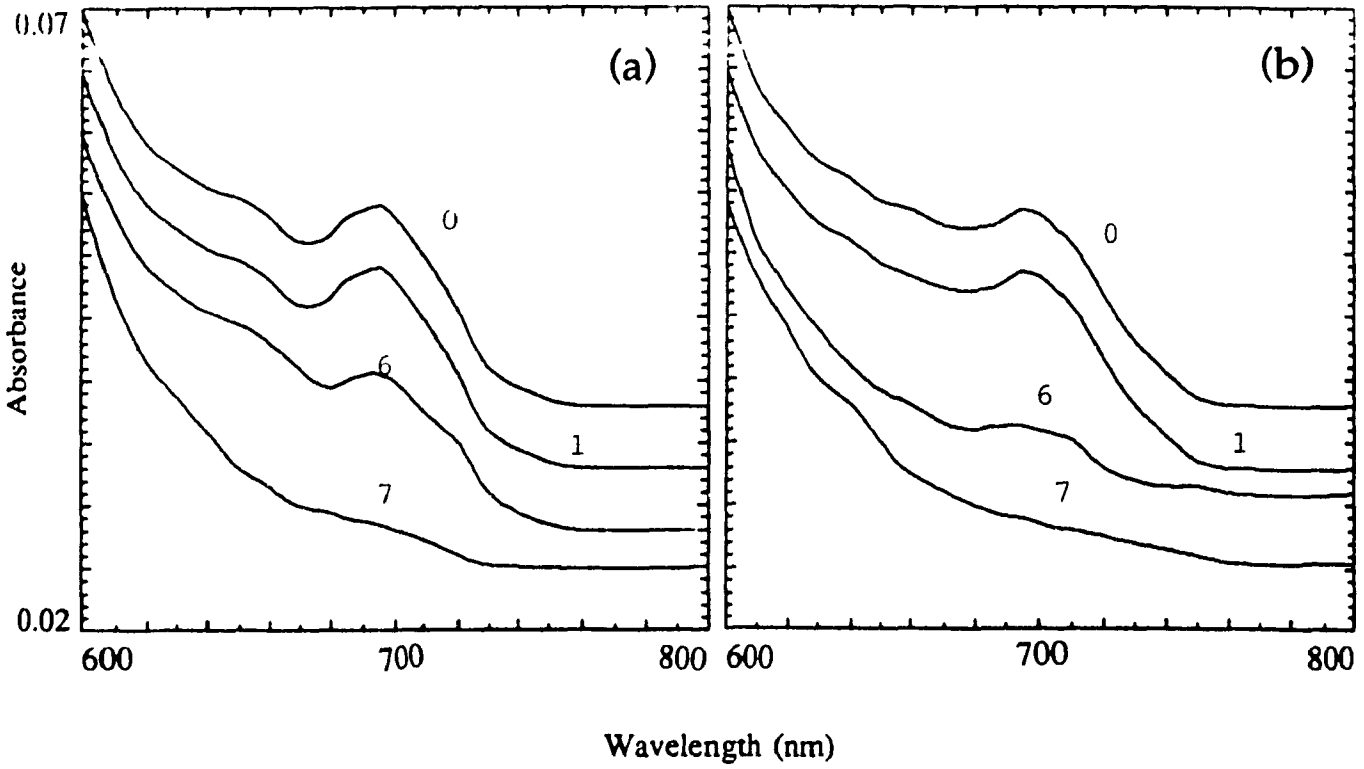
0.07
0.02
Absorbance
(a)
(b)
0
1
6
7
600
700
800
Wavelength (nm)

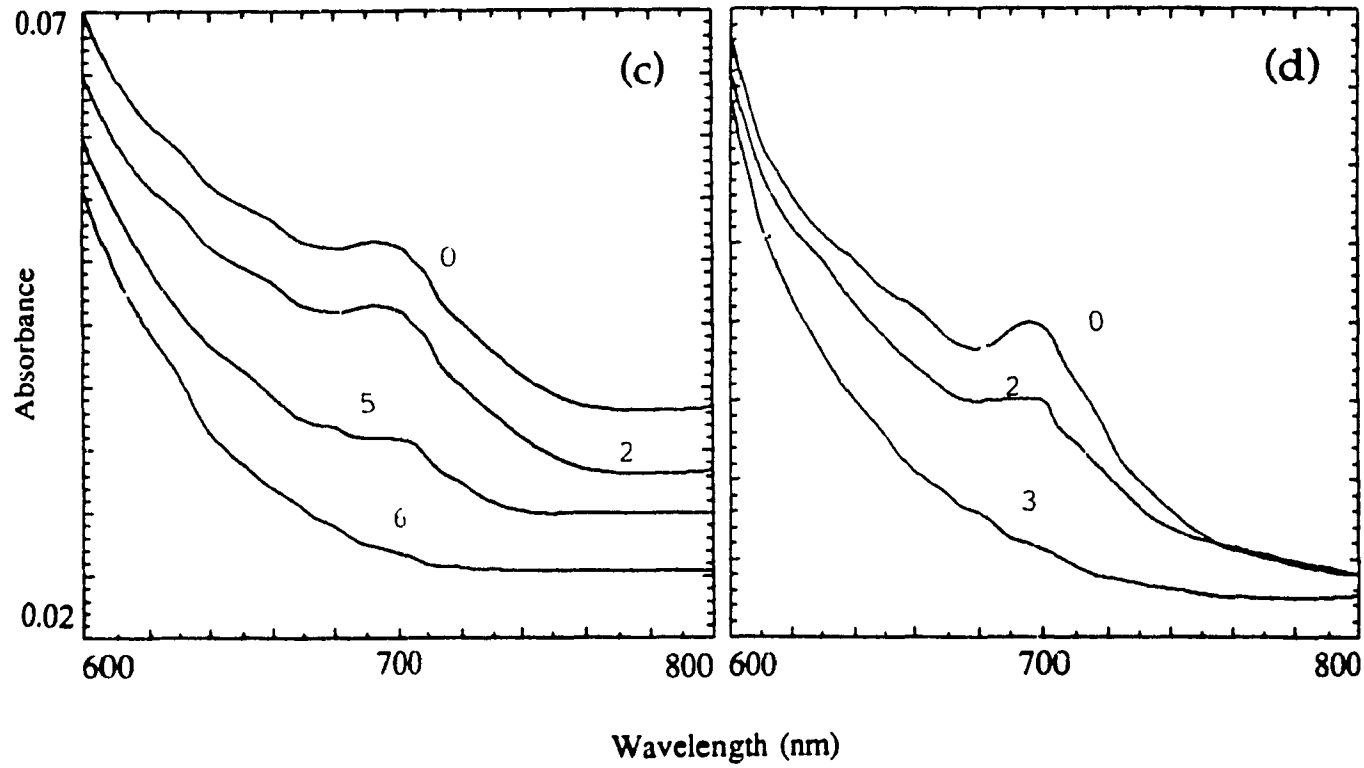
0.07
0.02
Absorbance
(c)
(d)
0
2
5
6
3
600
700
800
Wavelength (nm)

Figure 2.19: Absorption spectra of 30 μM (a) horse, (b) tuna, (c) Candida and (d) Saccharomyces ferricytochromes c in 100 mM sodium phosphate buffer, pH 7.0 containing the guanidine hydrochloride concentrations indicated on the spectra. Scan speed was 250 nm/min, 25 ± 1 °C.

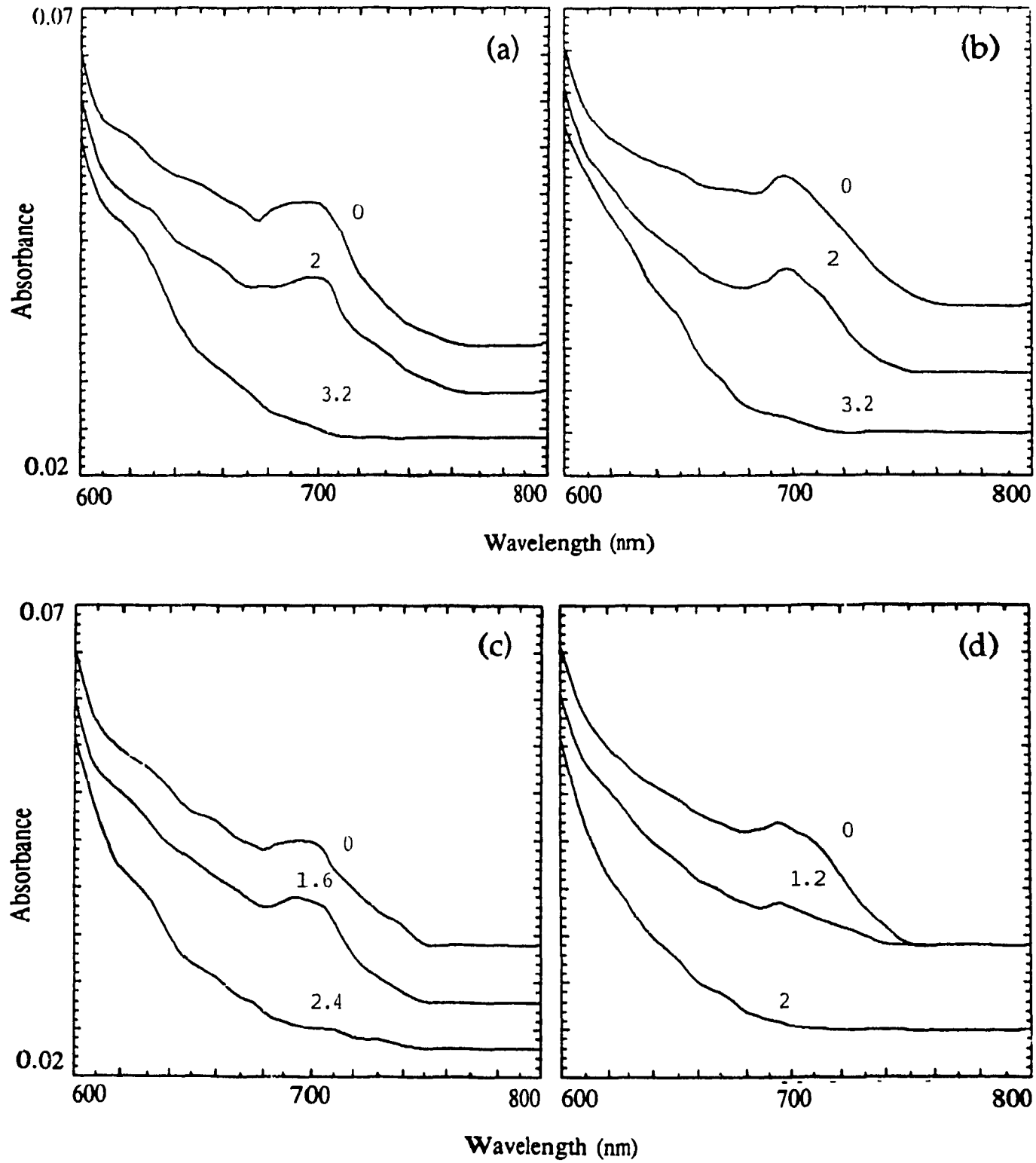
0.07
0.02
Absorbance
(a)
(b)
(c)
(d)
0
2
3.2
1.6
2.4
1.2
600
700
800
Wavelength (nm)

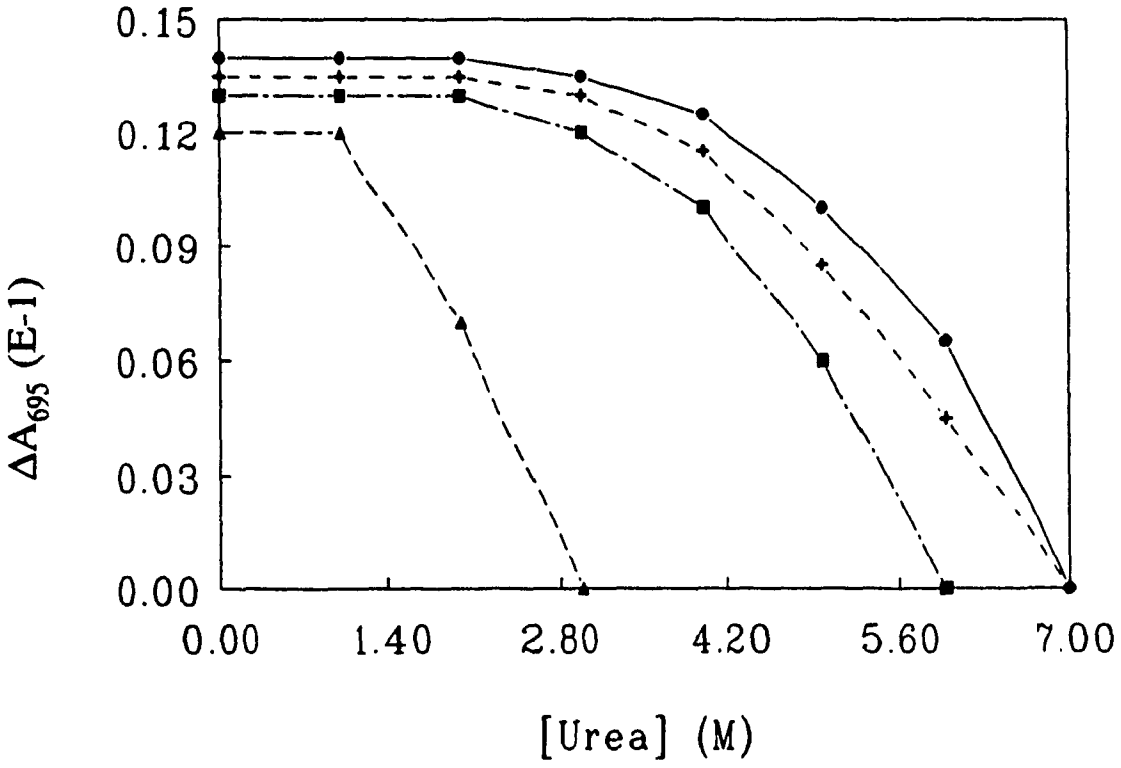

Figure 2.20: Observed absorbance change (ΔA_{695}) at 695-nm of the ferricytochromes c vs. urea concentration. 30 μM horse (●), tuna (+), Candida (■) and Saccharomyces (▲) ferricytochromes c in 50 mM sodium phosphate buffer, pH 7.0, containing 0.2 M KCl. The ΔA_{695} values were determined from the spectra in Figure 2.18 as indicated in Figure 2.17.

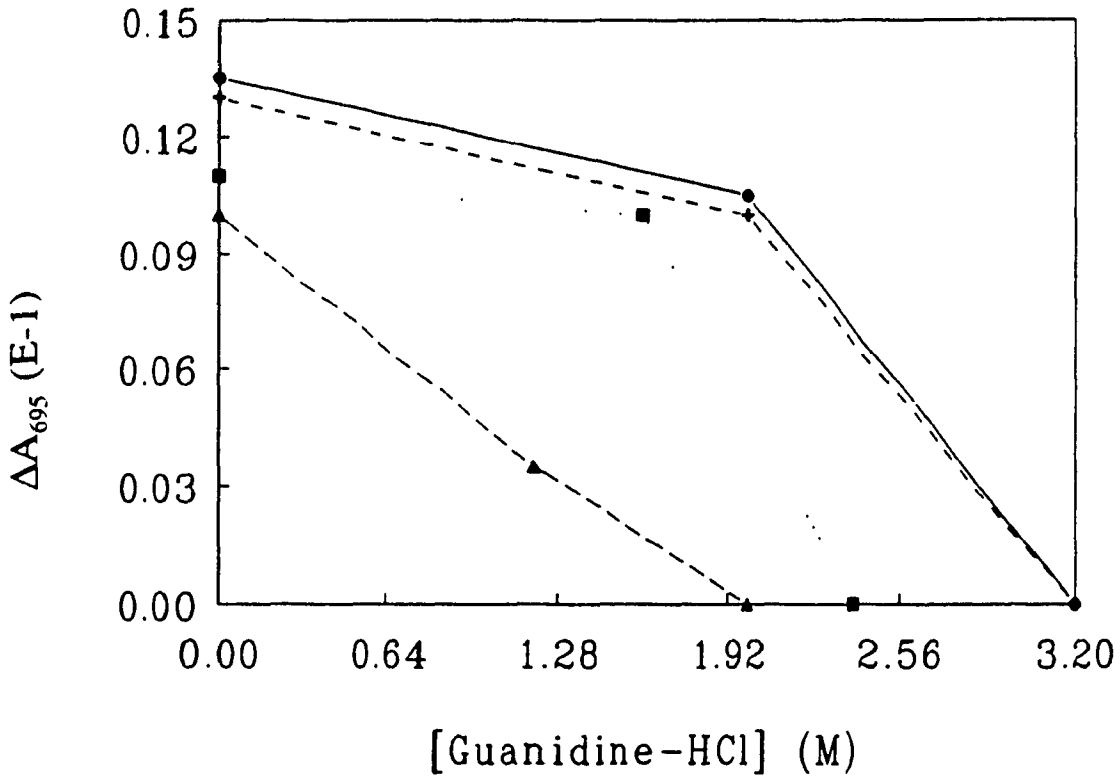

Figure 2.21: Observed absorbance change (ΔA_{695}) at 695-nm of the ferricytochromes c vs. guanidine hydrochloride concentration. 30 μM horse (●), tuna (+), Candida (■) and Saccharomyces (▲) ferricytochromes c in 100 mM sodium phosphate buffer, pH 7.0. The ΔA_{695} values were determined from the spectra in Figure 2.19 as indicated in Figure 2.17.

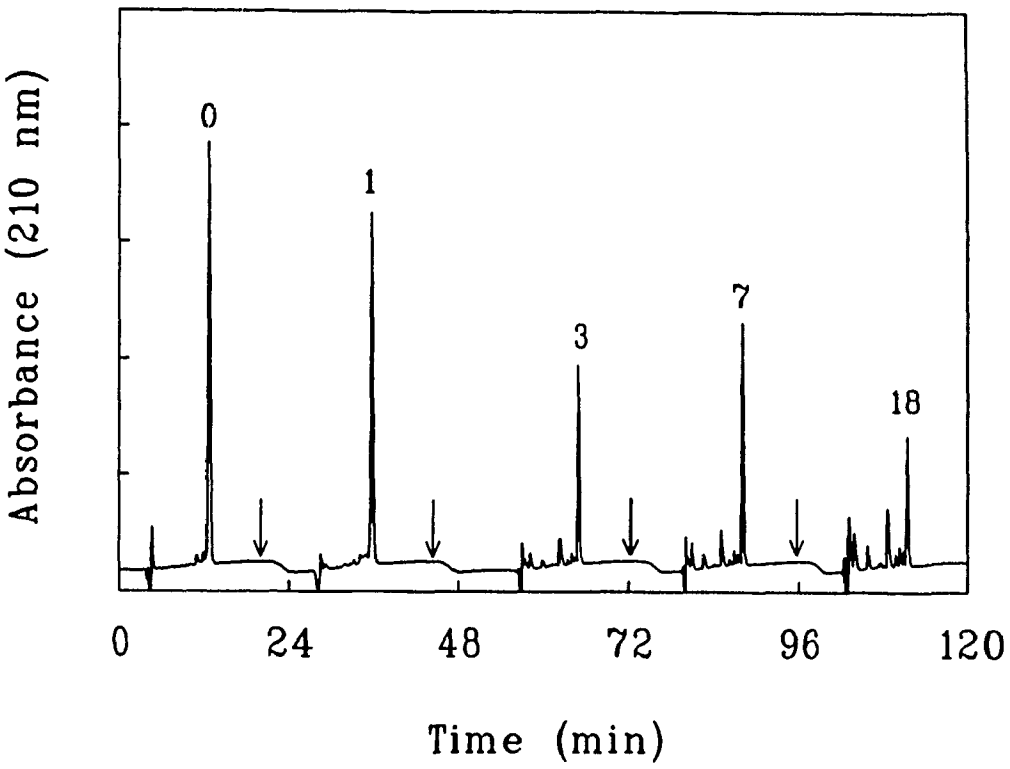

Figure 2.22: Reversed-phase HPLC chromatograms of tryptic digests of horse cytochrome c. The digested (0.05 mg in 100 µl) samples were injected onto the column approximately every 20 min (at the arrows) and the numbers on the main bands indicate the digestion time in hours. Digestion was carried out in 50 mM phosphate buffer, pH 7.0, containing 0.2 M KCl at 37 °C with a trypsin to cytochrome c ratio of 1:50 (W:W). The HPLC column was equilibrated with 20% CH_3CN containing 0.1% TFA (pH 2.5) and elution was with a 20 to 80% CH_3CN gradient in 0.1% TFA within 15 min at a flow rate of 1.0 ml/min. The column was washed with 20% CH_3CN containing 0.1% TFA for ~ 5 min after each 15-min elution.

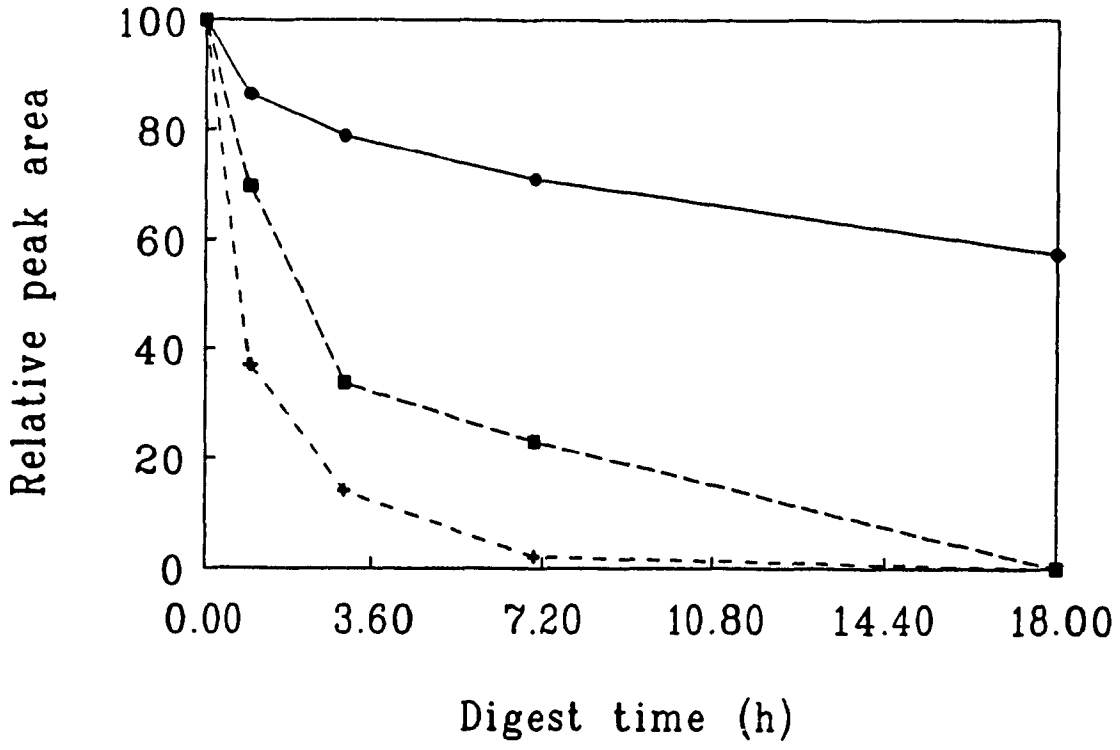

Figure 2.23: Time course of tryptic digestion of cytochromes c at pH 7.0 and 37 °C. Relative peak areas of the HPLC bands containing undigested horse (●), tuna (+) and Candida (■) cytochromes c are plotted vs. time. The areas of bands at 0 h are taken as 100%, and the experimental conditions are given in the caption to Figure 2.22 which shows the HPLC chromatograms for horse cytochrome c.

bands of undigested horse cytochrome c, which were separated by HPLC (Figure 2.22), were collected for MW confirmation by ES-MS, and the mass spectra are shown in Figure 2.24. All five peaks demonstrated very similar spectral behaviour, producing charged states ranging from 10+ to 16+, from which their average MW was found to be 12,359 ± 1, as expected for horse cytochrome c[30]. Thus, the mass spectral data confirm that undigested cytochrome c is separated from the rest of the peaks in the digest by HPLC in 15 min. The mass spectra (Figure 2.24) also show a peak at m/z 748.4 which increases with digestion time (Figure 2.24). Analysis of cytochrome c tryptic peptides using MacProMass software (Version 1.04, Sciex) for protease digest analysis indicated that this peak does not arise from cytochrome c, but from trypsin autoproteolysis.

Figure 2.24: Electrospray mass spectra of HPLC bands containing undigested horse cytochrome c (Figure 2.22) in 10% acetic acid from (a) 0 h, (b) 1 h, (c) 3 h, (d) 7 h and (e) 18 h tryptic digests. The ions carrying 10 to 16 positive charges were used to determine the MWs which are indicated on the spectra. The capillary and orifice voltages were 4.8 kV and 100 V, respectively, and the samples were delivered by a syringe pump at a rate of 2.0 ~ 3.0 µl/min.

(a)

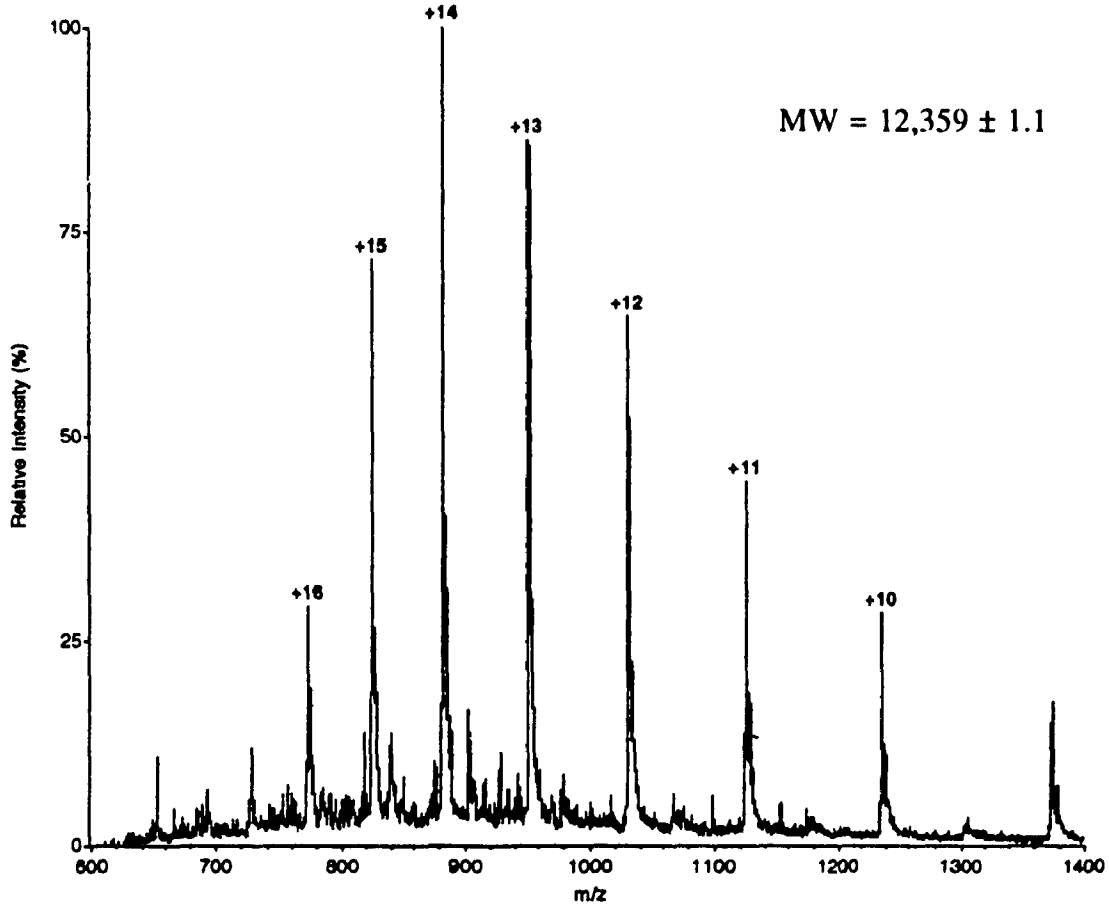
MW = 12,359 ± 1.1
+16
+15
+14
+13
+12
+11
+10
Relative Intensity (%)
m/z
100
75
50
25
0
600
700
800
900
1000
1100
1200
1300
1400

(b)

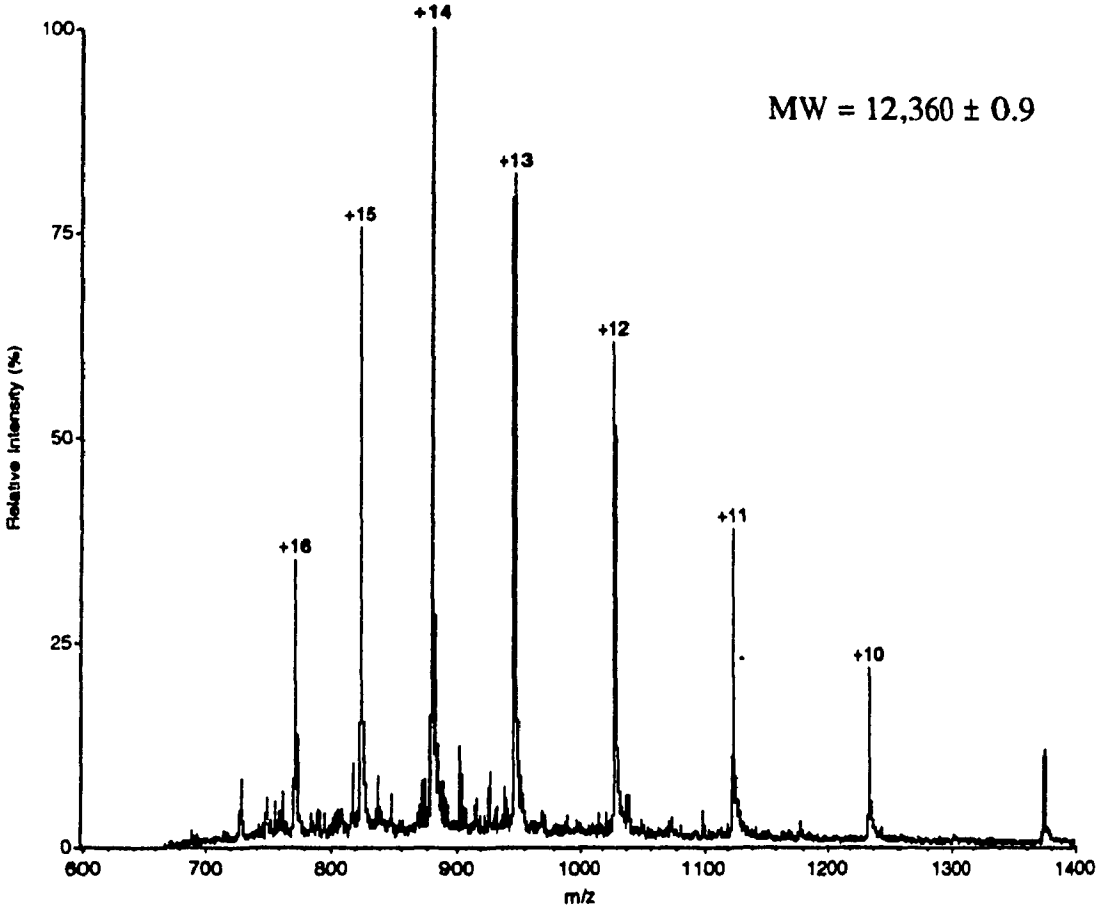
MW = 12,360 ± 0.9
+16
+15
+14
+13
+12
+11
+10
Relative Intensity (%)
100
75
50
25
0
600
700
800
900
1000
1100
1200
1300
1400
m/z

(c)

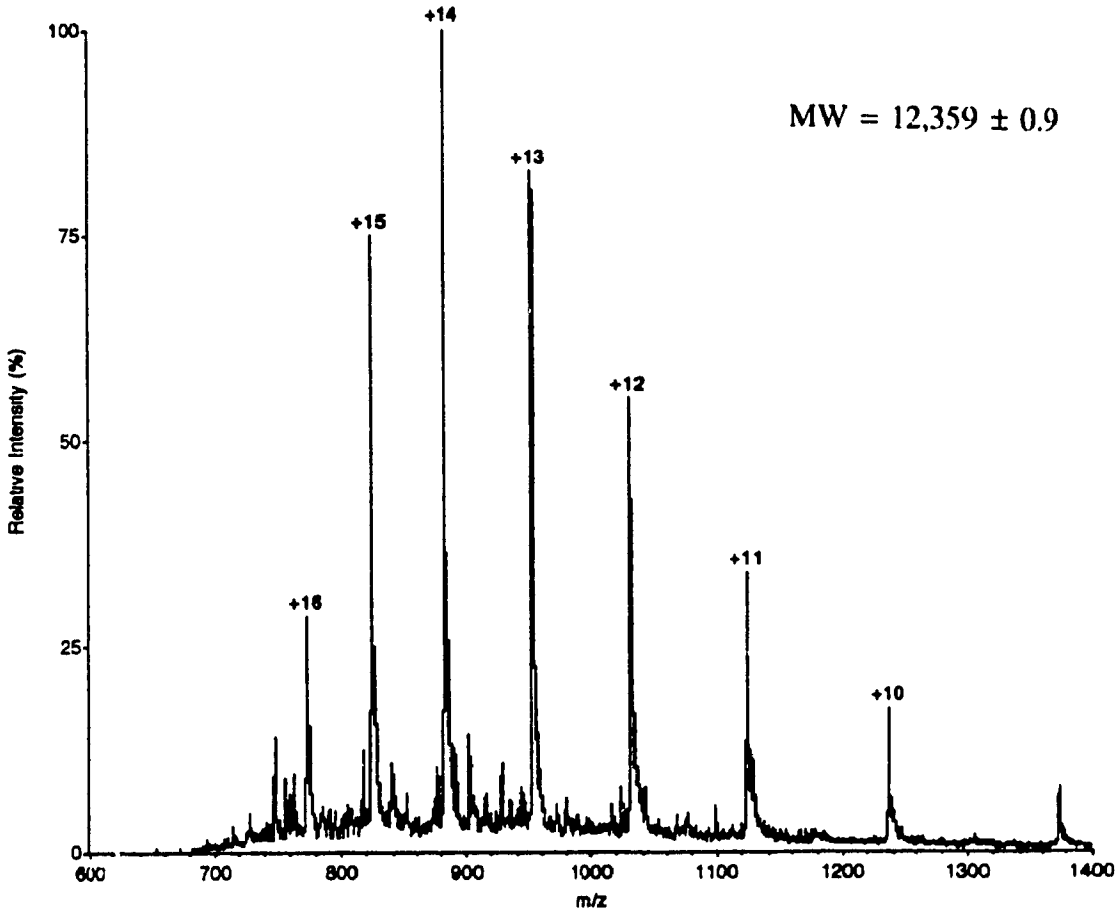
MW = 12,359 ± 0.9
+14
+15
+13
+12
+16
+11
+10
Relative Intensity (%)
100
75
50
25
0
600
700
800
900
1000
1100
1200
1300
1400
m/z

(d)

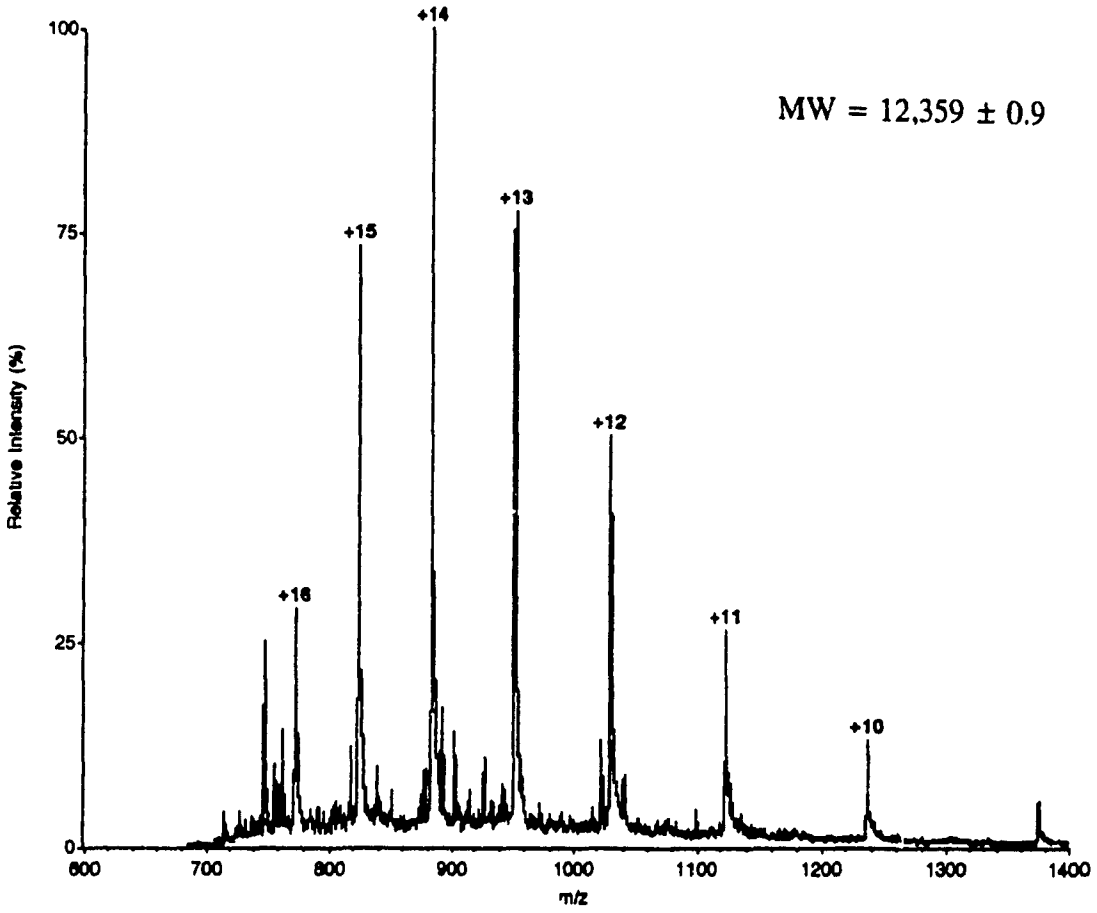
MW = 12,359 ± 0.9
+14
+13
+15
+12
+16
+11
+10
Relative Intensity (%)
100
75
50
25
0
600
700
800
900
1000
1100
1200
1300
1400
m/z

(e)

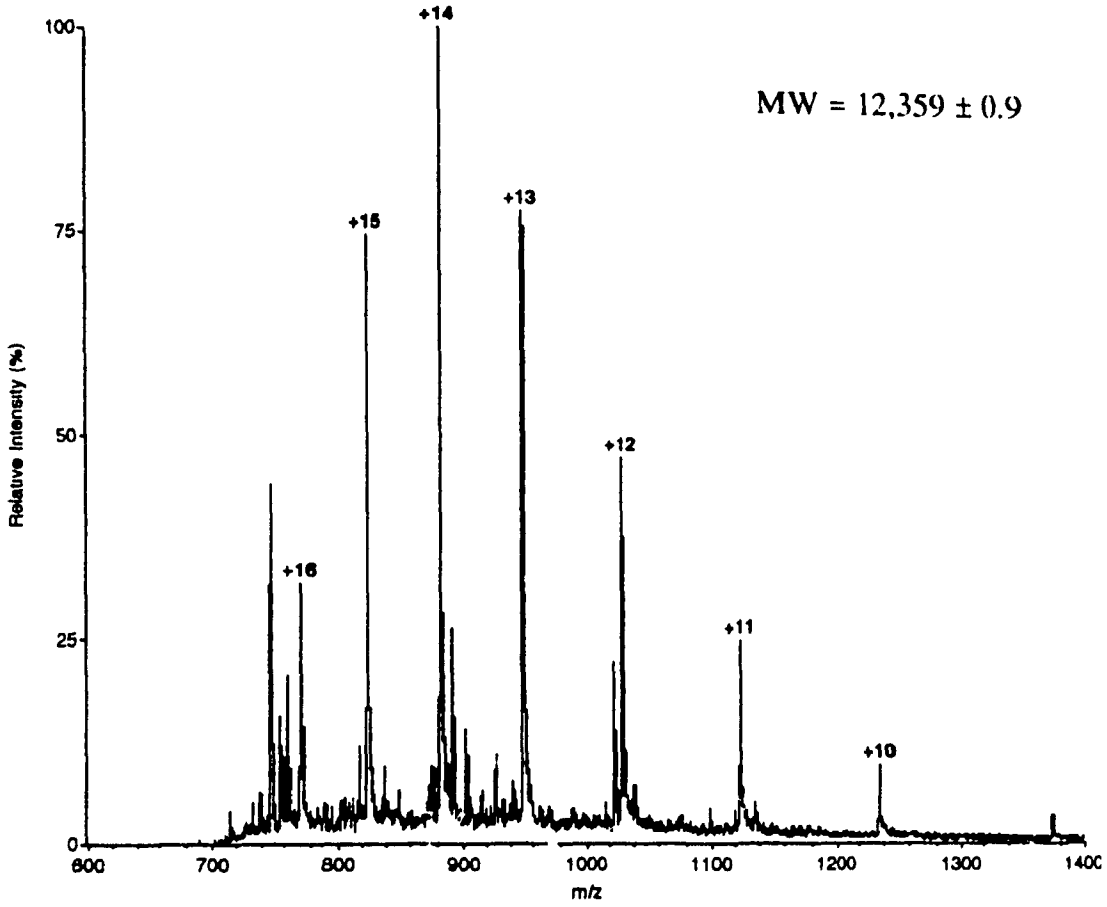
MW = 12,359 ± 0.9
+14
+15
+13
+16
+12
+11
+10
100
75
50
25
0
Relative Intensity (%)
600
700
800
900
1000
1100
1200
1300
1400
m/z

Table 2.1: $\Delta G_{d,aq}$, m values and denaturant concentrations at half maximum fluorescence for native cytochromes c

cytochrome c	urea denaturation				guanidine HCl denaturation			
	$\Delta G_{d,aq}$ [a]	$\Delta\Delta G_{d,aq}$ [b]	m [a]	$[urea]_{1/2}$ [c]	$\Delta G_{d,aq}$ [a]	$\Delta\Delta G_{d,aq}$ [b]	m [a]	$[gdnHCl]_{1/2}$ [c]
horse	9.9±0.5	0	1.4±0.1	6.9±0.1	8.5±0.1	0	3.2±0.1	3.0±0.1
tuna	8.9±0.3	1.0	1.3±0.1	6.9±0.1	8.3±0.2	0.2	3.0±0.1	3.0±0.1
Candida	8.1±0.6	1.8	1.7±0.1	4.9±0.1	6.0±0.2	2.5	2.9±0.1	2.3±0.1
Saccharomyces	2.4±0.1	7.5	1.1±0.1	2.6±0.1	1.7±0.1	6.8	1.6±0.1	1.4±0.1

[a] $\Delta G_{d,aq}$ (kcal/mol) and m (kcal/mol/M) values were obtained from the intercepts and slopes of the plots shown in Figures 2.6 and 2.9. The errors in $\Delta G_{d,aq}$ and m were calculated as indicated in Appendix 5

[b] $\Delta\Delta G_{d,aq}$ (kcal/mol) is the difference between the $\Delta G_{d,aq}$ of horse cytochrome c and the other cytochromes c

[c] $[urea]_{1/2}$ and $[gdn\text{-}HCl]_{1/2}$ (M) are the denaturant concentrations at half maximum fluorescence

Table 2.2: Comparison of denaturant concentration at 50% unfolding and at $\Delta A_{695} = 0$

cytochrome c	urea		guanidine-HCl	
	$\Delta A_{695} = 0$[a]	$[urea]_{1/2}$[b]	$\Delta A_{695} = 0$[a]	$[gdn\text{-}HCl]_{1/2}$[b]
horse	7.0	6.9	3.2	3.0
tuna	7.0	6.9	3.2	3.0
Candida	6.0	4.9	2.4	2.3
Saccharomyces	3.0	2.6	2.0	1.4

[a] $\Delta A_{695} = 0$ is the denaturant concentrations (M) at which the observed 695-nm absorbance reaches zero

[b] $[urea]_{1/2}$ and $[gdn\text{-}HCl]_{1/2}$ (M) are the denaturant concentrations at half maximum fluorescence

2.4 Discussion

The increase in Trp fluorescence is the expected consequence of increasing the average distance between the fluorescent Trp-59 residue (donor) and the heme (quencher). Horse, Candida and Saccharomyces cytochromes c have the same relative fluorescence in 9 M urea (~ 50%) and in 6 M guanidine hydrochloride (~ 70%) relative to free L-Trp. This indicates that the average distance between Trp-59 and the heme is similar in the denatured state of the three cytochromes c, although this distance is larger in 6 M guanidine hydrochloride than in 9 M urea. The cytochromes c are more sensitive to guanidine hydrochloride than to urea, but their fluorescence is still less than 100% relative to L-Trp at high denaturant concentrations, which implies that they maintain some tertiary structure under these conditions. Interpretation of the relative fluorescence of tuna cytochrome c is complicated by the presence of 2 Trp residues in its polypeptide, which leads to relative fluorescence >100% in 6 M guanidine hydrochloride.

The effects of denaturants on proteins are commonly analyzed by assuming a two-state equilibrium between the native state (n), and the denatured state (d). This is supported by the observation that the free energy change of the unfolding process (ΔG_d) often depends linearly on the concentration of the denaturants, as expressed by Equation 2.3. Extrapolation of ΔG_d from the high concentrations of denaturants at which unfolding is observed to the pure aqueous solvent ($\Delta G_{d,aq}$) is justified in a two-state model. The mitochondrial cytochromes c from horse, tuna, Candida and Saccharomyces show different conformational stability as a function of urea, guanidine hydrochloride and heating (Figures 2.4, 2.7 and 2.10). The denaturation of the cytochromes c by urea and

guanidine hydrochloride is assumed to be a reversible two-state transition since ΔG_d, the difference in free energy between the n and d states, varies linearly with denaturant concentration (Figures 2.6 and 2.9).

In Table 2.1, the free energy changes extrapolated to zero urea and guanidine hydrochloride concentration ($\Delta G_{d\,aq}$) are given for the four cytochromes. The $\Delta G_{d,aq}$ values represent the free energy difference between the n and d states in aqueous solution, and thus indicate the order of the overall conformational stability of the different species of cytochrome c. The $\Delta G_{d,aq}$ values for horse and tuna cytochromes c are similar (9.9 and 8.9 kcal/mol in urea; 8.5 and 8.3 kcal/mol in guanidine hydrochloride). Appendix 1 gives the sequences of the four cytochromes c. There are 18 amino acid variants between horse and tuna cytochrome c. Fifteen of these substitutions are on the surface of the proteins (Figure 1.1). Two of the remaining substitutions are partially buried (Thr-9 $\rightarrow$ Ile; Tyr-46 $\rightarrow$ Phe; Figure 1.1) and the final substitution is Val-95 $\rightarrow$ Ile and this residues is in contact with the heme (Figure 1.1). Thus, both cytochromes c contain essentially the same hydrophobic residues surrounding the heme. Since hydrophobic interaction of the polypeptide with heme is important in stabilizing the native conformation of cytochrome c[13], it is not surprising that the horse and tuna cytochromes c possess similar $\Delta G_{d,aq}$ values.

The amino acid sequence of the two species of yeast cytochromes c differ at 25 out of 108 residues (Appendix 1). However, Candida cytochrome c is significantly more stable than Saccharomyces cytochrome c (8.1 and 2.4 kcal/mol from urea denaturation; 6.0 and 1.7 kcal/mol from guanidine hydrochloride denaturation). Similar to the horse

and tuna pair, most (17 out of 21) of the substitutions are on the surface of the yeast cytochromes c. The four nonexposed substitutions are Ile-20 → Val, Val-95 → Ile, Met-98 → Leu and Ser-102 → Cys (Candida → Saccharomyces). The Val-95 → Ile substitution also occurs in the horse and tuna pair; thus the large $\Delta\Delta G_{d,aq}$ (4-6 kcal/mol) between the two yeast cytochromes c must be largely due to the Ile-20 → Val, Met-98 → Leu and Ser-102 → Cys mutation. In fact, the C102T Saccharomyces cytochrome c mutant is reported to have a $\Delta G_{d,aq}$ of 6.4 kcal/mol obtained from denaturation in guanidine hydrochloride[31]. This value obtained for the C102T mutant is quite close to the $\Delta G_{d,aq}$ value of 6.0 kcal/mol obtained in this study for Candida cytochrome c (Table 2.1). The -OH in the side chain of Ser-102 at the C-terminus of Candida cytochrome c provides a hydrogen-bond donor which can form a "helix cap" with Met-98 in the C-terminal helix[31]. Wild type Saccharomyces cytochrome c dimerizes by S-S bond formation between two Cys-102 residues, therefore preventing formation of a C-terminal helix cap. The loss of a helix cap would be a source of instability in wild-type Saccharomyces cytochrome c, and the mutation Cys-102 → Thr or Ser would allow the helix cap to form, thus increasing the conformational stability of the C102T or C102S mutant.

The yeast cytochromes have lower global stability than the horse and tuna cytochromes to denaturation by both urea and guanidine hydrochloride (Table 2.1). For example in guanidine hydrochloride the difference in $\Delta G_{d,aq}$ between the horse, tuna pair and the Candida, C102T Saccharomyces pair is ~2.5 kcal/mol. There are 38 amino acid variants between horse and Saccharomyces cytochromes c, while there are 42 amino acid variants between horse and Candida cytochromes c. Since multiple differences exist, an

interpretation of the effect of specific amino acid substitutions on the relative stabilities of the yeast and horse proteins is difficult. The substitutions in the buried and partially buried residues are highly conservative (e.g. Leu-35 → Ile, Leu-64 → Met and Ile-85 → Leu, where the residue in the horse, tuna pair is given first). Since the hydrophobic cores of the two pairs are similar, the difference in conformational stability may arise from the many substitutions on the surface of the proteins. Although mutagenesis studies have shown that destabilizing substitutions generally occur in the hydrophobic core of proteins, it has recently been shown that mutation of the highly solvent exposed Lys-73 → hydrophobic residues (Met, Trp, Tyr and Phe) results in 1.0 - 1.5 kcal/mol decrease in $\Delta G_{d,aq}$ of C102S Saccharomyces cytochrome c[14]. The large number of hydrophilic to hydrophobic substitutions and also hydrophobic to hydrophilic substitutions in surface exposed residues in the two cytochrome pairs may account for the ~2.5 kcal/mol difference in their $\Delta G_{d,aq}$. Another reason for their lower $\Delta G_{d,aq}$ could be that the yeast cytochromes c have five or six additional N-terminal residues compared to horse and tuna cytochromes c, which may increase the conformational entropy of the unfolded state[32].

The slopes, m, of the ΔG_d vs. denaturant plots (Table 2.1) fall within the expected values for urea (~1 kcal/mol/M) and guanidine hydrochloride (~3 kcal/mol/M). From theoretical analysis[14], m, is proportional to $\Delta A = A_d - A_n$, the difference in the solvent-exposed surface areas of the d and n states. Thus, ΔA, represents the increase in exposure of nonpolar residues to the solvent when the protein unfolds. Since m depends on the amino acid composition, its value should be conserved in a group of homologous proteins such as the cytochromes c. The lower values of m for Saccharomyces cytochrome c,

particularly in guanidine hydrochloride (Table 2.1), implies that the unfolded state of this protein is more compact than that of horse, tuna or Candida cytochrome c.

The data in Table 2.1 compare favourably with a number of published studies on cytochrome c stabilities. Schejter et al.[33] reported an average $\Delta G_{d,aq}$ of 8.96 kcal/mol and a m value of 1.17 kcal/mol/M for the denaturation in urea of a set of mammalian and avian cytochromes c. In guanidine hydrochloride an average of $\Delta G_{d,aq}$ of 7.6 kcal/mol and m = 3.5 kcal/mol/M were reported for various mammalian, chicken and tuna cytochromes c[1]. The reported value for $\Delta G_{d,aq}$ of wild type Saccharomyces cytochrome c and of the protein treated with iodoacetamide, to block the free -SH group of Cys-102, was 2.1 kcal/mol in each case (pH 7.2, 20 °C) from denaturation studies in guanidine hydrochloride[29]. This value is in good agreement with the value in Table 2.1 and significantly lower than the $\Delta G_{d,aq}$ values reported for the C102T[31] and C102S[14] mutants [6.4 (pH 7.2, 27 °C) and 5.7 kcal/mol (pH 7.5, 25 °C)]. The only reported values of $\Delta G_{d,aq}$ and m for Candida cytochrome c were 7.24 kcal/mol and 1.89 kcal/mol/M at pH 6.5 and 25 °C, respectively[9]. These values, which were obtaind from denaturation in guanidine hydrochloride, are between our value in urea and in guanidine hydrochloride at pH 7.0.

The fluorescence emission maxima red-shift with increasing concentrations of denaturant (Figures 2.12 and 2.13). This implies that the environment of Trp-59 changes from hydrophobic to hydrophilic, consistent with unfolding of the polypeptide. Because of very weak fluorescence of the cytochromes c in the folded states, there is a large error in measurement of emission maxima. However, in all cases, except Saccharomyces

cytochrome c in urea, the emission maxima are fully red-shifted to 348 - 350 nm before reaching the denaturant concentrations which result in half maximum fluorescence (Table 2.1). The different behaviour observed for the emission maximum of Saccharomyces cytochrome c in urea (Figure 2.12) is consistent with greater tertiary structure in the denatured state of this protein as reflected in its lower m values (Table 2.1).

Figures 2.14 and 2.15 show that the Soret bands of all cytochromes c blue-shift in denaturants, which implies that some axial ligand exchange is occurring. The Soret bands of horse, Candida and Saccharomyces cytochromes c shift only slightly to blue, while the tuna cytochrome c band is significantly more blue-shifted at high concentrations of denaturants. Tuna cytochrome c has a Soret maximum at 402 nm at high denaturant concentrations suggesting that the Fe(III) may be 5-coordinate, high-spin, or 6-coordinate, high spin with Met-80(S) displaced by a weak field ligand such as water. The latter is more likely since 5-coordinate high spin hemes have a shoulder at the high frequency side of the Soret band[34] but no such shoulder is seen in Figure 2.26. Thus, the Soret data suggest that the heme axial ligation is significantly different in tuna cytochrome c and the other cytochromes c, which probably possess two strong field ligands from the polypeptide. Since in each cytochrome His-18 is adjacent to Cys-17, which is covalently bonded to the heme (Figure 1.1), His-18 is a likely axial ligand. Bis-histidine heme complexes are known to be stable, so coordination of a second histidine to the heme Fe in the unfolded state is a definite possibility. An examination of Appendix 1 reveals that tuna cytochrome c has only His-26 in addition to His-18, whereas the horse and yeast cytochromes have two (His-26, His-33) and three (His-26, His-33, His-39) extra

histidines, respectively. The large difference in Soret maximum between the tuna and the other cytochromes suggests that His-26 may be too close to His-18 (Figure 1.1) to form a stable bis-histidine complex.

There is a large body of evidence which indicates that the 695-nm band is associated with the heme Fe(III)-S(Met-80) bond in native ferricytochrome c and that its presence is a measure of the integrity of this bond[35,15,18]. The 695-nm band disappears on denaturation, on the binding of exogenous ligands and on reduction of ferricytochrome c[17]. The value of 695-nm absorbance reaches zero in high concentration of denaturants as shown in Figures 2.18 and 2.19. Thus, the fact that this absorbance is completely quenched by denaturants implies that at pH 7.0 the Met-80(S) ligand is displaced by another axial ligand. The Fe(III)-S bond is cleaved ($\Delta A_{695} = 0$) at approximately the denaturant concentration of half maximum fluorescence (Table 2.2), thus loss of the 695-nm band probably occurs simultaneously with gross distortion of the protein's native conformation.

The fluorescence of L-Trp shows strong temperature dependence (Figure 2.11) with the intensity decreasing by ~1% per degree increase in temperature. There are also large fluorescence increases associated with the conformational changes induced in the cytochromes on increasing temperature. However, thermal parameters were not calculated from the present results since the relative fluorescence (%) of the unfolded states is poorly defined. Nonetheless, the data indicate that the relative thermal stabilities of the cytochromes follow the same order as their stabilities in denaturants: horse > tuna > Candida > Saccharomyces.

Time dependent protease digestion of the cytochromes c was used to probe their local stabilities. Saccharomyces cytochrome c was not included in this study because tryptic digestion of the protein was complicated by dimer formation as mentioned previously. Trypsin, which specifically cleaves peptide bonds on the C-terminal side of Lys and Arg residues, was used here because cytochromes c contain a large number of these residues which are highly surface exposed[8]. Phosphate buffer (pH 7.0) was used as a replacement for the normal ammonium bicarbonate buffer (pH 8.0) since only partial digestion of the samples was desirable to allow evaluation of local stabilities. The reversed-phase HPLC chromatograms of the tryptic digests of horse cytochrome c display intense peaks at different digestion times (Figure 2.22), which were analyzed by ES-MS. The results (Figure 2.23) indicate that the MWs of all species fall within 12,359 ± 1 Da, confirming that the intense peaks arise from undigested cytochrome c, even after 18 hours. Figure 2.23 summarizes the time course of tryptic digestion of horse, tuna and Candida cytochromes c. From these data it can be seen that the local stabilities of the cytochromes follow the order: horse > Candida > tuna. This order is the same as that reported in the literature[3], where the same digestion conditions were used but the digested samples were separated on a HPLC gel-permeation column instead of the C-18 column used here.

The $\Delta G_{d,aq}$ values from the fluorescence data, which represent the global conformational stability of the cytochromes, decrease in the order: horse > tuna > Candida > Saccharomyces (Table 2.1). Thus, the global and local stabilities do not follow the same order. Clearly, tuna cytochrome c is digested by trypsin at 37 °C much faster than

horse cytochrome c (Figure 2.23) although their $\Delta G_{d,aq}$ at values at 25 °C are similar (Table 2.1). The higher susceptibility of tuna cytochrome c to trypsin compared to horse cytochrome c can not be simply explained by the number of susceptible sites for trypsin since horse has 21 Arg + Lys residues, while tuna cytochrome c has only 17. The difference in local stability must reflect differences in the surface properties of the two proteins due to changes in primary structure, since 18 out of 103 residues are variant and 15 of these are found on the surface. In fact, there is experimental evidence that the heme crevice of tuna c is less stable than that of horse c[19]. At pH 8.0, the formal potentials of the horse and tuna cytochromes are clearly biphasic, indicating a conformational change at high temperature. The breaks occur at 30 and 40 °C for tuna and horse c, respectively, well below the complete unfolding transition observed by calorimetry at 75 and 84 °C[19], and have been associated with opening of the heme crevice. Thus, the lower break temperature for tuna c indicates that the local stability of its heme crevice is less stable than in horse c. Since the heme crevice is surrounded by a ring of Lys residues, decreased local stability in this region is expected to give rise to greater susceptibility to trypsin proteolysis as observed in Figure 2.23.

Candida cytochrome c, which has a lower global stability than tuna cytochrome c (Table 2.1), and has almost the same number of susceptible sites (16) to trypsin, also exhibits higher local stability than tuna cytochrome c. This suggests that Candida c has a more stable heme crevice than tuna c despite its lower overall conformational stability.

2.5 References

1) McLendon G. and Smith, M. *J. Biol. Chem.* **1978**, *253*, 4004.

2) Cohen, J.S.; Fisher, W.R. and Schechter, A.N. *J. Biol. Chem.* **1974**, *249*, 1113.

3) Endo, S.; Nagayama, K. and Wada, A. *J. Biomol. Struct. Dynam.* **1985**, *3*, 409.

4) Murphy, M.E.P.; Nall, B.T. and Brayer, G.D. *J. Mol. Biol.* **1992**, *227*, 160.

5) Sherman, F.; Stewart, J.W.; Parker, J.H.; Inhaber, E.; Shipman, N.A.; Putterman, G.J.; Gardisky, R.L. and Margoliash, E. *J. Biol. Chem.* **1968**, *243*, 5446.

6) Hampsey, D.M.; Das, G. and Sherman, F. *J. Biol. Chem.* **1986**, *261*, 3259.

7) Holzschu, D.; Principio, L.; Conklin, K.T. Hichey, D.R.; Short, J.; Rao, R.; McLendon, G. and Sherman, F. *J. Biol. Chem.* **1987**, *262*, 7125.

8) Moore, G.R. and Pettigrew, G.W. *Cytochromes c - Evolutionary, Structural and Physicochemical Aspects*. Springer-Verlag, New York. **1990**.

9) Knapp, J.A. and Pace, C.N. *Biochem.* **1974**, *13*, 1289.

10) Myer, Y.P.; Pande, A. and Saturno, A.F. *J. Biol. Chem.* **1981**, *256*, 1576.

11) Nall, B.T. and Landers, T.A. *Biochem.* **1981**, *20*, 5402.

12) Corbett, R.J.T. and Roche, R.S. *Biochem.* **1984**, *23*, 1888.

13) Caffrey, M.S.; Daldal, F.; Holden, H.M. and Cusanovish, M.A. *Biochem.* **1991**, *30*, 4119.

14) Bowler, B.E.; May, K.; Zaragoza, T.; York, P.; Dong, A. and Caughey, W.S. *Biochem.* **1993**, *32*, 183.

15) Schejter, A. and George, P. *Biochem.* **1964**, *3*, 1045.

16) Sreenathan, B.R. and Taylor, C.P.S. *Biochem. Biophys. Res. Commun.* **1971**, *42*, 1122.

17) Wilson, M.T. and Greenwood, C. *Eur. J. Biochem.* **1971**, *22*, 11.

18) Myer, Y.P.; MacDonald, L.H.; Verma, B.C. and Pande, A. *Biochem.* **1980**, *19*, 199.

19) Yuan, X. and Hawkridge, F.M. *J. Electroanal. Chem.* **1993**, *350*, 29.

20) Darbre, A. *Practical Protein Chemistry - A Handbook.* Wiley, New York. **1988**. p. 132.

21) Palmero, S.; de Marchis, M.; Parti, M. and Fugassa, E. *Anal. Biochem.* **1992**, *202*, 152.

22) Larsen, B.S. and McEwen, C.N. *J. Am. Soc. Mass Spectrom.* **1991**, *2*, 205.

23) Feng, R. and Konishi, Y. *Anal. Chem.* **1992**, *64*, 2090.

24) Babul, G. and Stellwagen, E. *Biochem.* **1972**, *11*, 1195.

25) Tsong, T.W. *Biochem.* **1975**, *14*, 1542.

26) Hickey, D.R.; McLendon, G. and Sherman, F. *J. Biol. Chem.* **1988**, *263*, 18298.

27) Creighton, T.E. *Proteins: Structure and Molecular Properties (2nd ed.)* W.H. Freeman and Company, New York. **1993**. p. 287.

28) Lakowicz, J.R. *Principles of Fluorescence Spectroscopy.* Plennum, New York. **1983**. p. 44.

29) Zuniga, E.H. and Nall, B.T. *Biochem.* **1983**, *22*, 1430.

30) McLuckey, S.A.; Van Berkel, G.J. and Glish, G.I. *J. Am. Chem. Soc.* **1990**, *112*, 5668.

31) Betz, S.F. and Pielak, G.J. *Biochem.* **1992**, *31*, 12337.

32) Kawaguchi, H. and Noda, H. *J. Biochem.* **1977**, *81*, 1307.

33) Schejter, A.; Luntz, T.L.; Koshy, T.I. and Margoliash, E. *Biochem.* **1992**, *31*, 8336.

34) Yonetani, T. and Anni, H. *J. Biol. Chem.* **1987**, *262*, 9547.

35) Kaminsky, L.S.; Miller, V.J.and Davison, A.J. *Biochem.* **1973**, *12*, 2215.

36) Ferrin, T.E.; Huang, C.C.; Jarvis, L.E. and Landgridge, R. *J. Mol. Graphics.* **1988**, *6*, 13.

3.0 Relative stabilities of iron, cobalt, zinc and porphyrin horse cytochromes c

3.1 Introduction

Recently there has been a great deal of interest in the synthesis of metal-substituted enzymes and in the study of their physical, chemical and biochemical properties[1]. Because the heme in hemoglobin and myoglobin is held to the globin only by noncovalent forces and can be readily removed by acidification, metal substituted derivatives of myoglobin and hemoglobin have been extensively studied. Metal substitution has also been accomplished for cytochrome c. Since the heme is covalently bound by sulfur linkages to the polypeptide chain (Figure 1.1), it cannot be removed without denaturation[2]. However, the iron can be "extracted" from the porphyrin ring on exposure to HF leaving porphyrin cytochrome c (por-cyt c) into which the desired metal can be incorporated. Using this procedure Co(III)[3], Zn(II)[4], Sn(IV)[5], Cu(II)[6], Mn(III)[7] and Ni(II)[8] derivatives of cytochrome c have been prepared.

Cobalt(III) cytochrome c (Co-cyt c) has been shown to have Met-80 and His-18 as axial ligands like the native species[3,9]. Zinc is present in cytochrome c as mixture of five- and six-coordinate metal ions at 27 °C where ~66% of Zn-cyt c molecules possess Met-80 ligation[4,10]. Thus, Zn-cyt c should show altered denaturation if the strength of the sixth ligand plays a significant role in the stabilization of the native form of the

polypeptide. Zn-cyt c has been used as probe for native cytochrome c since studies have shown that its structure is similar to native cytochrome c[11,12]. Only small conformational differences between Fe-cyt c and Zn-cyt c, which appear to be on a similar scale to the native redox-state conformation change, have been reported[5,11].

This work probes whether the nature of the central metal influences the unfolding of the horse cytochrome c polypeptide by using Trp-59 fluorescence. A comparison of the denaturation process of native Fe(III) cytochrome c (Fe-cyt c), por-cyt c, Co-cyt c and Zn-cyt c in the presence of various concentrations of urea is presented. To compare the local stability of Fe-cyt c and its derivatives, HPLC was used to analyze the time dependence of tryptic digestion of the proteins. The preparation of por-, Zn- and Co-cyts c and their characterization by ES-MS are also described.

3.2 Experimental

3.2.1 Materials

Ammonium acetate and zinc acetate [$Zn(CH_3CO_2)_2.2H_2O$; FW. 219.48] were obtained from Caledon and J.T. Baker, respectively. Sodium chloride, sodium phosphate and acetic acid were purchased from American Chemicals, Anachemia and Omega, respectively. Cobalt acetate [$Co(CH_3CO_2)_2.4H_2O$; FW. 249.1] was purchased from Sigma. Porphyrin cytochrome c (crude) was provided by Dr. Jack Kornblatt (Concordia), and Craig Fenwick and Dr. Jim Wishart (Brookhaven).

3.2.2 Methods

FPLC purification of por-cyt c: 500 µl of por-cyt c (2.0 mM) were loaded on

the FPLC cation-exchange Mono S 10/10 column and elution was carried out using a 20 mM sodium phosphate buffer, pH 7.0, with a gradient of 0 to 1.0 M KCl at a flow rate of 1.0 ml/min.

Preparation of Zn-cyt c: 1.0 ml of 2.0 mM por-cyt c was added to a ten-fold molar excess of zinc acetate in 10 ml of 0.1 M ammonium acetate buffer, pH 5.0. This solution was stirred for a period of 3 h at 25 °C in the dark. The uptake of zinc was followed by removing aliquots of the reaction mixture and monitoring the visible absorption spectrum. The reaction was considered over when the Soret band of por-cyt c at 404 nm was displaced to 424 nm (Figure 3.1). Excess zinc acetate was removed by dialysis against nanopure water for at least 1 h, and followed by 20 h dialysis against 20 mM phosphate buffer, pH 7.0, at 4 °C in the dark. Zn-cyt c was concentrated by ultrafiltration using an Amicon stirred cell (10 ml) with a YM-10 filter and transferred to 0.1 M phosphate buffer, pH 7.0, and purified by FPLC using the system described in Section 2.2.2. Prior to FPLC, samples were filtered through 0.45-μm syringe filters (Gelman Sciences) and buffers were also filtered with 0.45-μm filters (Gelman Sciences), and degassed under vacuum for 30 min. Cation-exchange FPLC was performed using a Mono S 10/10 column. A 500-μl filtered Zn-cyt c solution (0.5 mM) was introduced into the FPLC system and elution was carried out using 20 mM phosphate buffer (pH 7.0) with a 0 to 0.6 M KCl gradient at a flow rate of 1.0 ml/min.

Preparation of Co-cyt c: In a 5-ml flask 58 mg of NaCl, 14 mg of $NaH_2PO_4.H_2O$, 25 mg of $Co(OAc)_2.4H_2O$, 0.1 ml of acetic acid, and 0.9 ml of nanopure water were combined. Stirring and crushing were required to get all the salts into

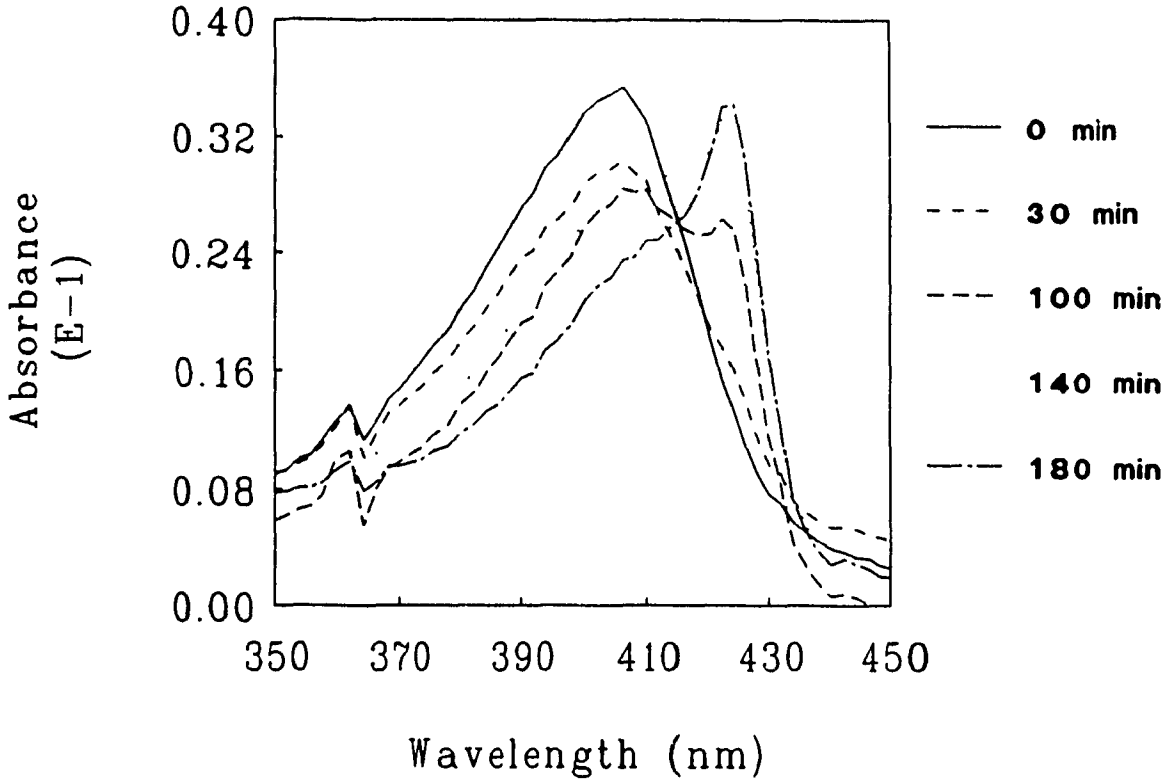

Figure 3.1: Preparation of Zn-cyt c. The reaction solution (10 ml) was prepared by mixing 1.0 ml of por-cyt c (2.0 mM in pH 7.0) with 9.0 ml of ~ 2.5 M zinc acetate in 0.1 M NH_4AC buffer, pH 5.0. The reaction was carried out at 25 ± 1 °C in the dark with stirring, and the Soret absorption was recorded at the various reaction times indicated above.

solution. To this mixture was added 1 ml of por-cyt c (1.25 mM) in 0.02 M phosphate buffer, pH 8.0, and the flask was suspended in a stirred water bath at 71 ± 1 °C. The reaction was complete after about 30 min. The progress of cobalt insertion was monitored by adding 10 µl of the reaction mixture to 990 µl of 0.1 M phosphate buffer (pH 7.0), and observing the shift of the por-cyt c Soret band from 404 nm to 426 nm, which is the Soret maximum for Co-cyt c (Figure 3.2). The crude Co-cyt c was concentrated by ultrafiltration using an Amicon stirred cell (10 ml) with a YM-10 filter, transferred to 0.1 M phosphate buffer (pH 7.0), and purified by cation-exchange FPLC on the Mono S 10/10 column. 500 µl of filtered Co-cyt c (0.5 mM) were loaded on the FPLC column in the presence of 40-fold excess ascorbic acid to reduce any Fe(III)-cyt c impurity to Fe(II)-cyt c since Fe(II)-cyt c but not Fe(III)-cyt c can be separated from Co(III)-cyt c on the Mono S column. Elution was carried out using degassed 20 mM sodium phosphate buffer, pH 7.0, with a 0 to 0.6 M KCl gradient at a flow rate of 1.0 ml/min.

ES-MS of the horse cytochrome c derivatives: The API III mass spectrometer described in Section 2.2.2 was used for all samples. Mass spectra were obtained as outlined in Section 2.2.2. The m/z scale was checked with lysozyme (14,310 Da), and MW determinations on Fe-cyt c (0.67 mg/ml), por-cyt c (0.35 mg/ml), Zn-cyt c (0.43 mg/ml) and Co-cyt c (0.28 mg/ml) in 10% acetic acid (pH 2.2) were performed using the same instrument parameters given in Section 2.2.2.

Denaturation of Fe-cyt c and its derivatives in urea: Protein concentrations were determined on a Hewlett Packard 8451A diode array spectrophotometer (± 2 nm)

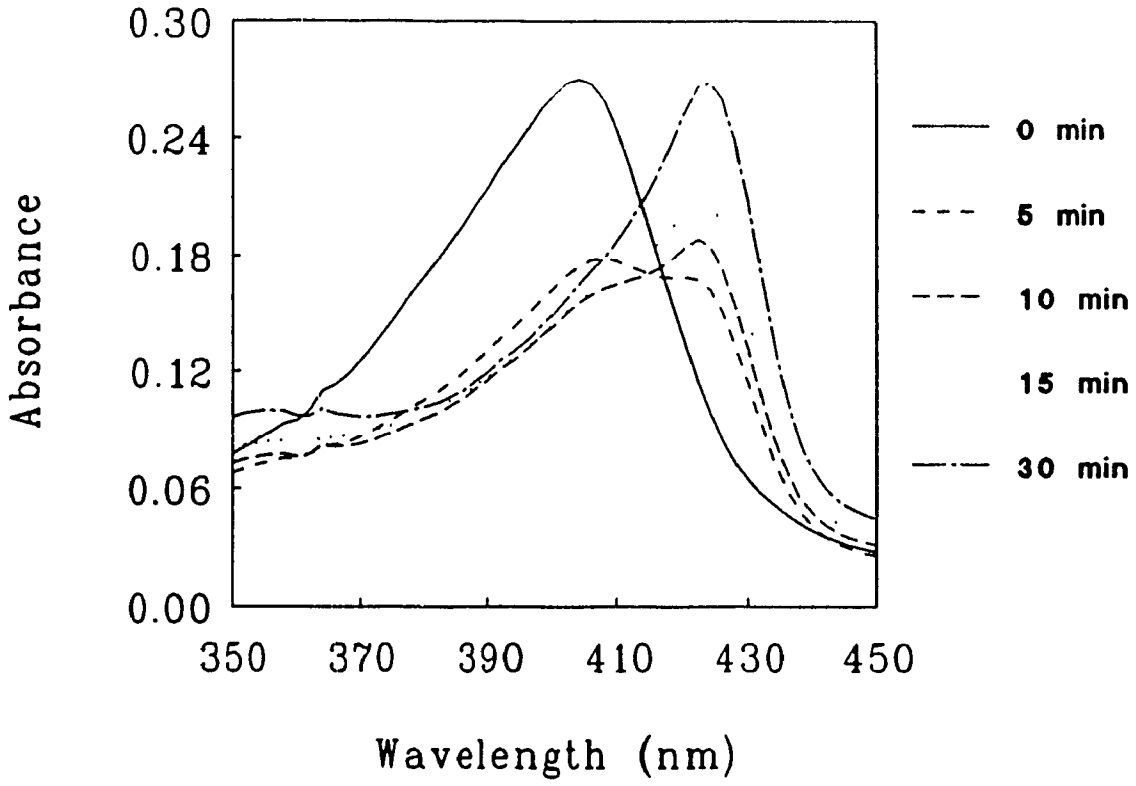

Figure 3.2: Preparation of Co-cyt c. The reaction solution contained 58 mg NaCl, 14 mg $NaH_2PO_4H_2O$, 25 mg $Co(OAc)_2.4H_2O$, 0.1 ml acetic acid, 0.9 ml water and 1.0 ml of a por-cyt c (1.25 mM) solution in 20 mM sodium phosphate buffer, pH 8.0. The reaction was carried out at 71 ± 1 °C and the Soret absorption was recorded at the various reaction times indicated above.

using the following Soret millimolar extinction coefficients $(mM\ cm)^{-1}$: Fe-cyt c, 106 at 410 nm[14]; por-cyt c, 160 at 404 nm[15]; Zn-cyt c, 243 at 424 nm[5]; and Co-cyt c, 106.1 at 426 nm[3]. The concentration of L-Trp was determined using an extinction coefficient of 5.6 $(mM\ cm)^{-1}$ at 280 nm. Urea concentrations were determined by weight. In all denaturation experiments, the cytochrome and L-Trp concentrations were 2.0 μM, and all measurements were carried out in 50 mM sodium phosphate buffer (pH 7.0), containing 0.2 M KCl at 25 °C. The cytochromes c were allowed to denature for at least 10 min in the presence of urea prior to measuring fluorescence and absorption spectra.

Reversibility of denaturation Fe-cyt c and its derivatives: To test the reversibility of unfolding, Fe-cyt c was unfolded in 8.0 M urea and dialyzed with 50 mM sodium phosphate buffer (pH 7.0) for 3 days. The buffer was changed three times during this period to remove urea and refold the protein. Denaturation of refolded Fe-cyt c was examined as a function of urea concentration from 0 to 9.0 M. Por-, Zn- and Co-cyts c were unfolded in 8.0 M urea, the post-transition region. After 1 h the urea concentration was diluted to those found in the pre-transition and transition regions and within 7 days fluorescence was measured as described in the next section.

Fluorescence of Fe-cyt c its derivatives in urea: All fluorescence measurements were performed on a Shimadzu Model RF-5000 fluorometer using excitation and emission slits of 5 nm. The excitation wavelength used for all samples was 280 nm and integrated emission intensities from 315 to 400 nm were determined. The integrated emission of the blank was subtracted from that of the protein samples, and corrections for inner filter effects were accomplished using Equation 2.5. The integrated intensity obtained for 2.0

μM L-Trp in the same concentration of urea was taken to be 100%.

Analysis of the local stabilities of Fe-cyt c and its derivatives by HPLC: The digestion buffer was 50 mM sodium phosphate buffer, pH 7.0 containing 0.2 M KCl. Trypsin dissolved in 10 mM HCl and the cytochromes c dissolved in the digestion buffer were mixed and incubated at 37 °C for 0, 1, 4, 7 and 15 h. The concentrations of Fe-, por-, Zn- and Co-cyts c in the digestion were 2.0, 1.1, 2.7 and 1.1 mg/ml, respectively, and the cytochrome to trypsin ratio was 50:1 (W:W) for each sample. 100 μl of digested Fe-cyt c and its derivatives were injected on the HPLC system as described in Section 2.2.2. The eluent was 0.1% trifluoroacetatic acid (pH 2.5) with a 20 to 80% acetonitrile gradient over 15-min. Samples were eluted at a flow rate of 1.0 ml/min at room temperature (25 °C) and 12 ± 0.2 MPa pressure. The eluted samples were detected by their absorbance at 210 nm and at their Soret band maxima.

3.3 Results

FPLC purification of por-cyt c: Figure 3.3 shows that the cation-exchange (Mono S) chromatogram of por-cyt c displays 2 peaks at 0.48 and 0.54 M KCl. The Soret absorption maximum of both peaks is 404 nm (Figure 3.4), but the ratio (R) of 404 nm to 280 nm absorbance for peak 1 (R = 6.5) is higher than that of peak 2 (R = 2.5). Since R = 4.3[16] for Fe-cyt c, R = 6.5 is expected for por-cyt c because of its higher Soret extinction coefficient, so peak 1 was collected and concentrated.

FPLC purification of Zn-cyt c: The FPLC purification of the Zn-cyt c reaction mixture also resulted in two peaks eluting from the cation-exchange column at 0.33 and

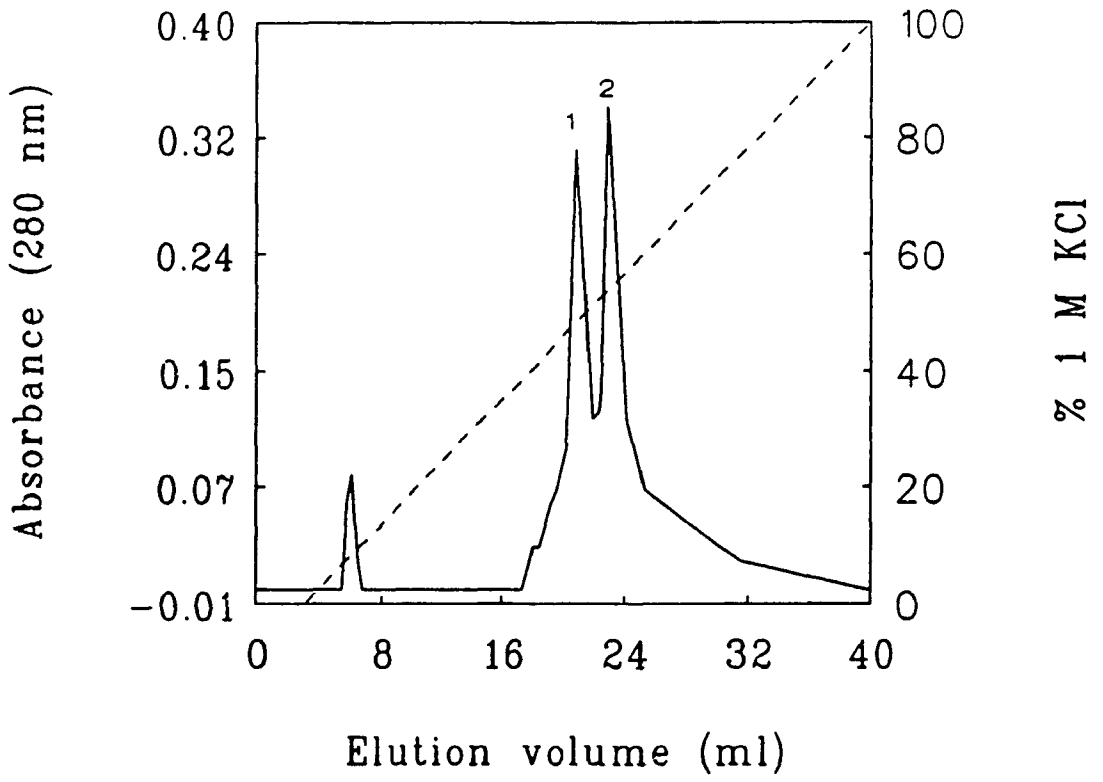

Figure 3.3: FPLC purification of por-cyt c. 12 mg por-cyt c in 500 µl were injected onto the FPLC Mono S 10/10 cation-exchange column equilibrated with 20 mM sodium phosphate buffer, pH 7.0. The sample was eluted in the same buffer with a 0 to 1.0 M KCl gradi nt (dashed line) at a flow rate of 1.0 ml/min and 25 ± 1 °C. Both peaks 1 and 2 were collected.

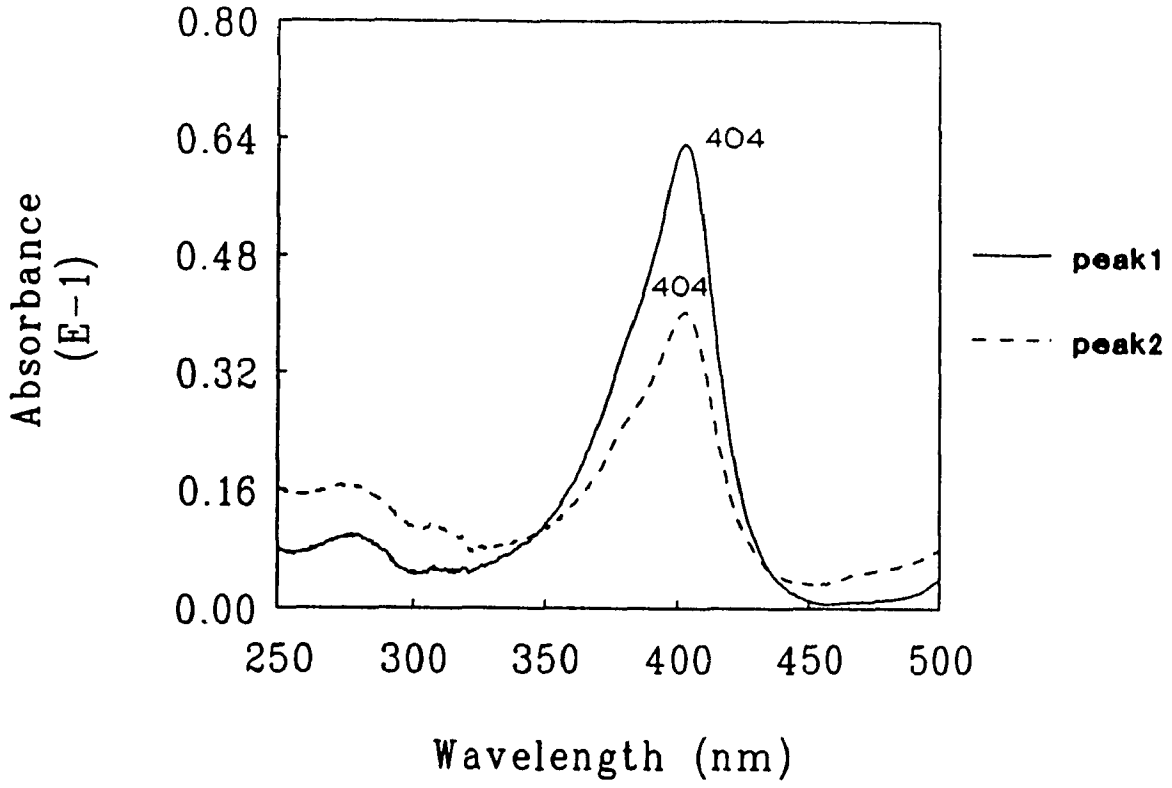

Figure 3.4: Absorption of the peaks in the FPLC chromatogram of por-cyt c. The two peaks are those labelled in Figure 3.3, and their spectra were recorded in 50 mM sodium phosphate buffer, pH 7.0, containing 0.2 M KCl at 25 ± 1 °C.

0.36 M KCl (Figure 3.5). The Soret absorption is shown in Figure 3.6 for both peaks. The maximum for peak 1 is 424 nm which is that expected for Zn-cyt c, and peak 2 has a maximum at 410 nm corresponding to Fe-cyt c.

FPLC purification of Co-cyt c: The FPLC Mono S elution profile (Figure 3.7) of the Co-cyt c reaction mixture displays 4 distinct protein peaks (1 to 4), and ascorbic acid was eluted before the first protein peak. Peak 1 contains a small amount of protein but no heme as indicated by the absorption spectrum shown in Figure 3.8a. The Soret absorption of peaks 2, 3 and 4, which are shown in Figure 3.8b, c and d, are similar, and have R values of 2.0, 5.0, 3.5, respectively. Since peak 3 has R = 5.0 and a Soret maximum at 426 nm, as expected for Co-cyt c, this peak was collected and concentrated.

MWs of horse cytochrome c derivatives from ES-MS: Figure 3.9 shows the mass spectra of Fe-, por-, Zn- and Co-cyts c in 10% acetic acid (pH 2.2). All four samples demonstrated similar spectral behaviour, producing charged states ranging from 10+ to 17+, from which their average MWs were determined. Table 3.1 compares the MWs obtained by ES-MS and those calculated from changes in the expected MW of the porphyrin prosthetic group at pH 2.2. At low pH all four pyrrole N atoms are protonated, and spectral studies with model porphyrins generally show a single transition between the tetraprotonated and the neutral diprotonated forms[17,15]. A single pK_a of 2.5 has been reported for deprotonation of tetraprotonated por-cyt c[18]; however, the formation of an intermediate triprotonated form with a pK_a of 1.3 has also been reported[15] but no pH titration data were shown. The MW of 12,307 given in Table 3.1 is exactly that excepted for the tetraprotonated form of por-cyt c. Substitution of Zn (AW = 65) for Fe (AW = 56)

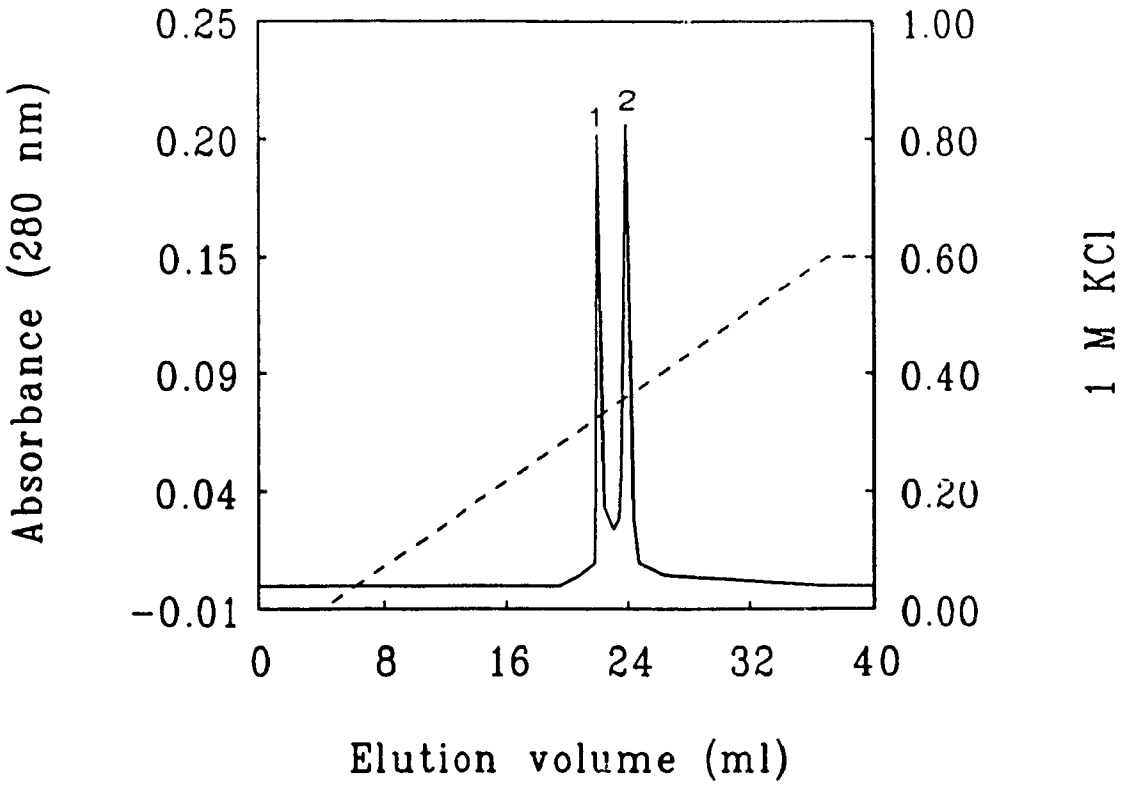

Figure 3.5: FPLC purification of Zn-cyt c. 3.0 mg Zn-cyt c in 500 µl were injected onto the FPLC Mono S 10/10 cation-exchange column equilibrated with 20 mM sodium phosphate buffer, pH 7.0. The sample was eluted in the same buffer with a 0 to 0.6 M KCl gradient (dashed line) at a flow rate of 1.0 ml/min and 25 ± 1 °C. Both peaks 1 and 2 were collected.

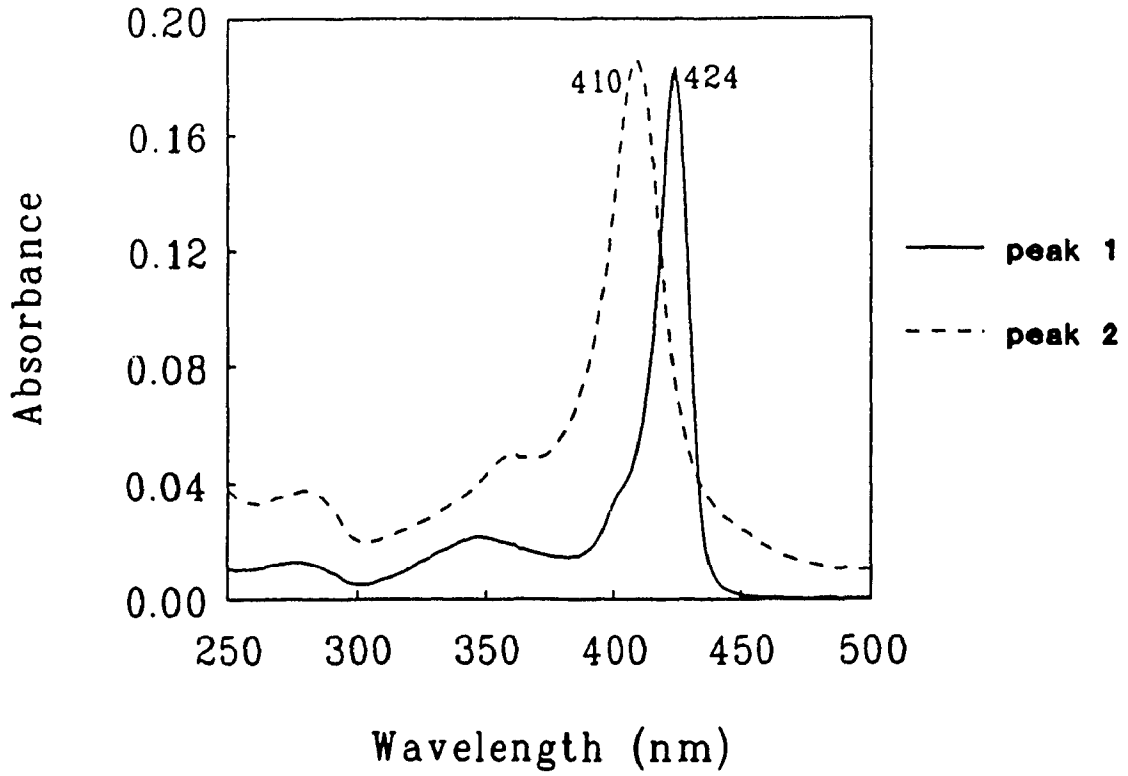

Figure 3.6: Absorption of peaks in the FPLC chromatogram of Zn-cyt c. The two peaks are those labelled in Figure 3.5 and their spectra were recorded in 50 mM sodium phosphate buffer, pH 7.0, containing 0.2 M KCl at 25 ± 1 °C.

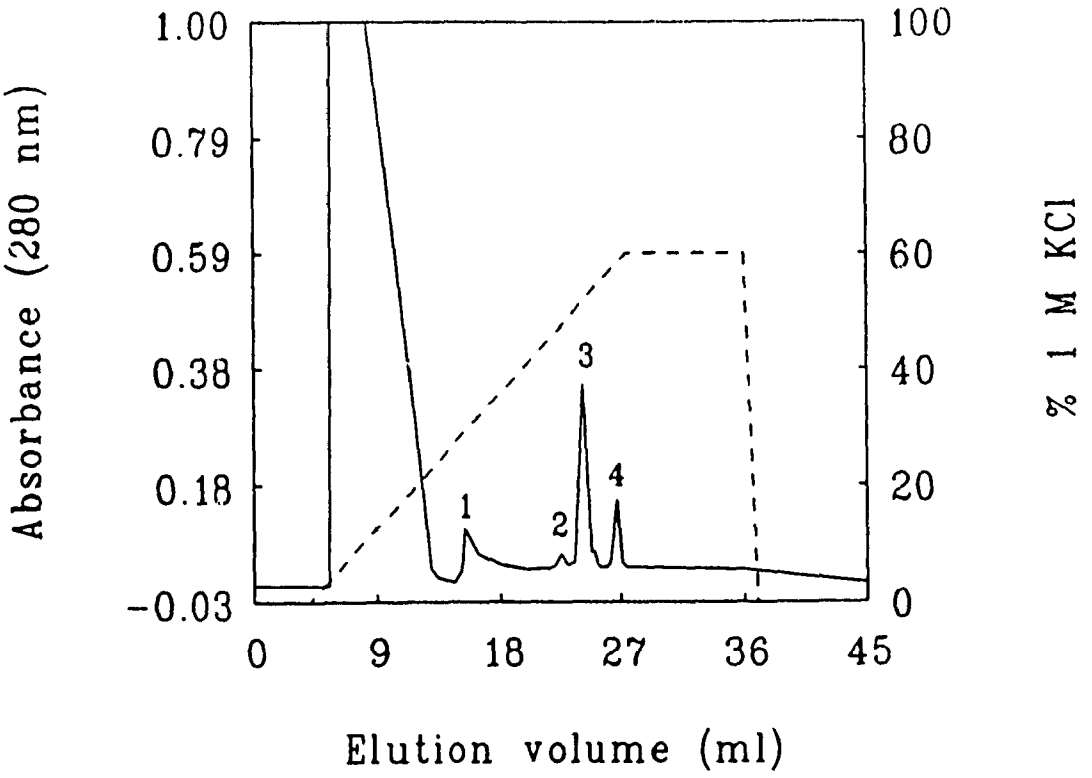

Figure 3.7: FPLC purification of Co-cyt c. 3.0 mg in 500 µl were injected onto the FPLC Mono S 10/10 cation-exchange column equilibrated with 20 mM sodium phosphate buffer, pH 7.0. The sample was eluted in the same buffer with a 0 to 0.6 M KCl gradient (dashed line) at a flow rate of 1.0 ml/min and 25 ± 1 °C. Peaks 1 to 4 were collected; the intense peak at ~ 9 ml contains ascorbic acid which was added to reduce Fe(III)-cyt c to Fe(II)-cyt c.

Figure 3.8: Absorption of the peaks in the FPLC chromatogram of Co-cyt c. The four peaks are those labelled in Figure 3.7, and their spectra were recorded 50 mM sodium phosphate buffer, pH 7.0, containing 0.2 M KCl at 25 ± 1 °C. (a) peak 1; (b) peak 2; (c) peak 3 and (d) peak 4.

(a)

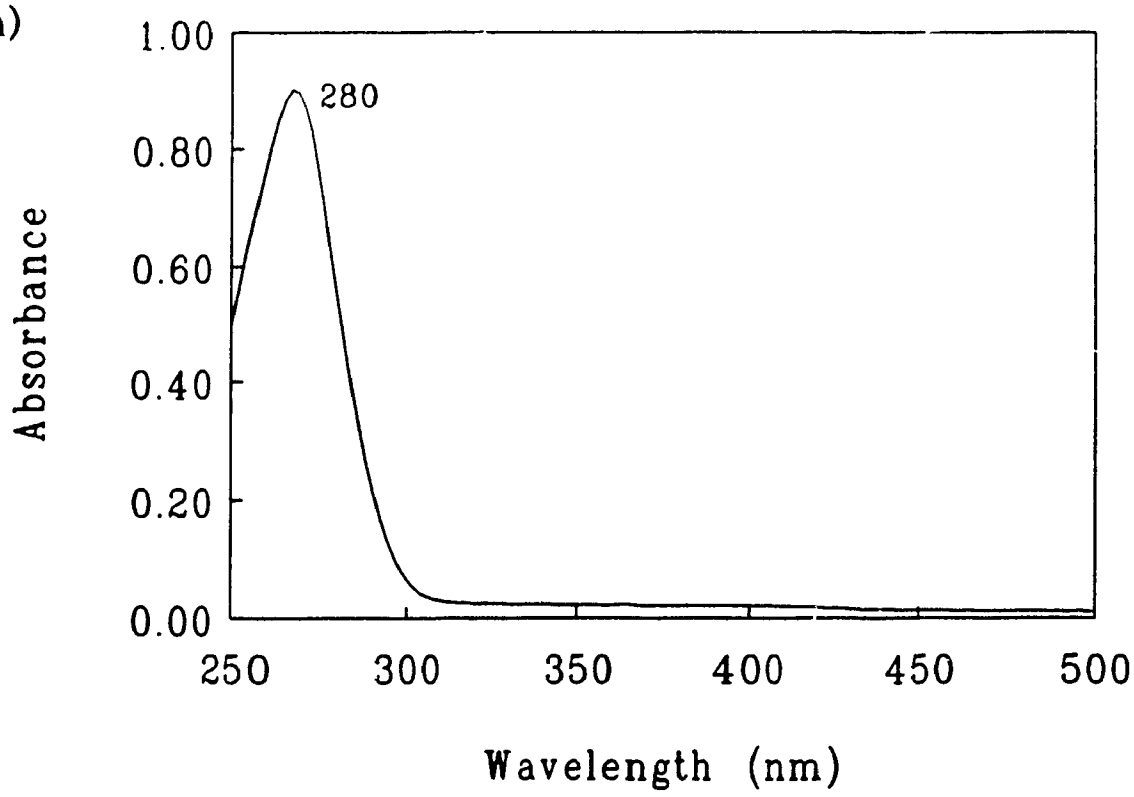
1.00
0.80
0.60
0.40
0.20
0.00
Absorbance
280
250
300
350
400
450
500
Wavelength (nm)

(b)

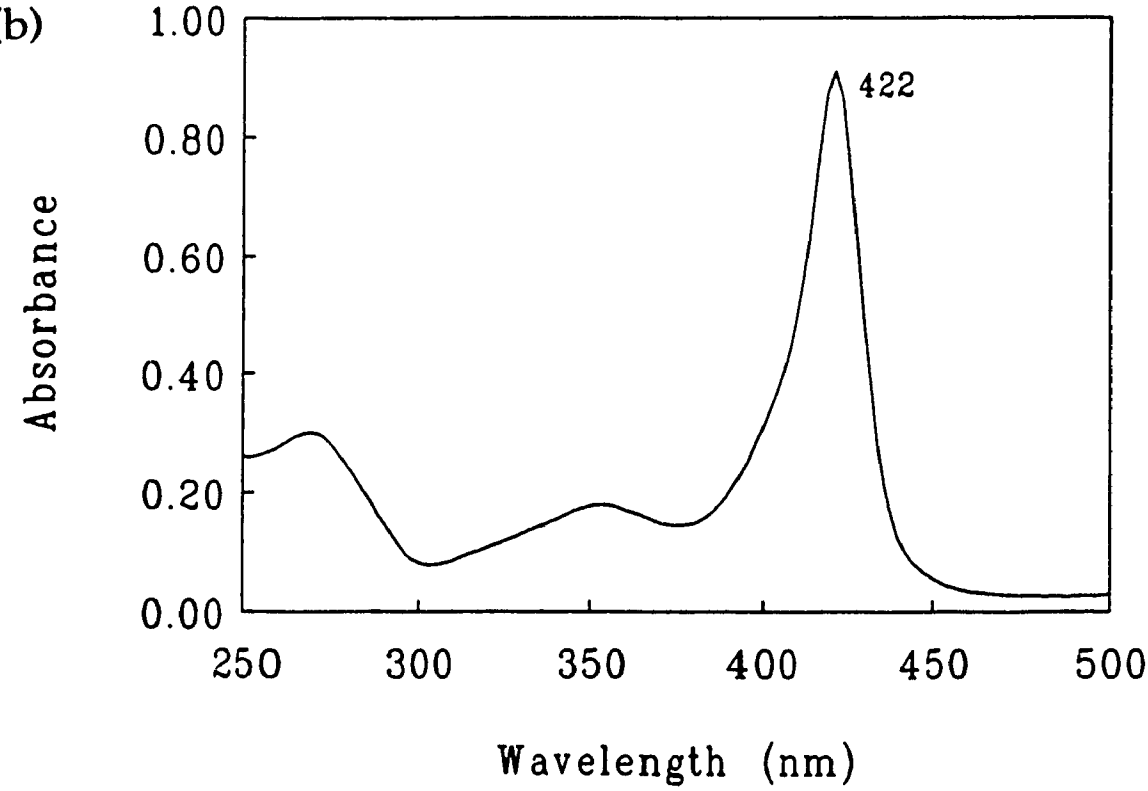
1.00
0.80
0.60
0.40
0.20
0.00
Absorbance
422
250
300
350
400
450
500
Wavelength (nm)

(c)

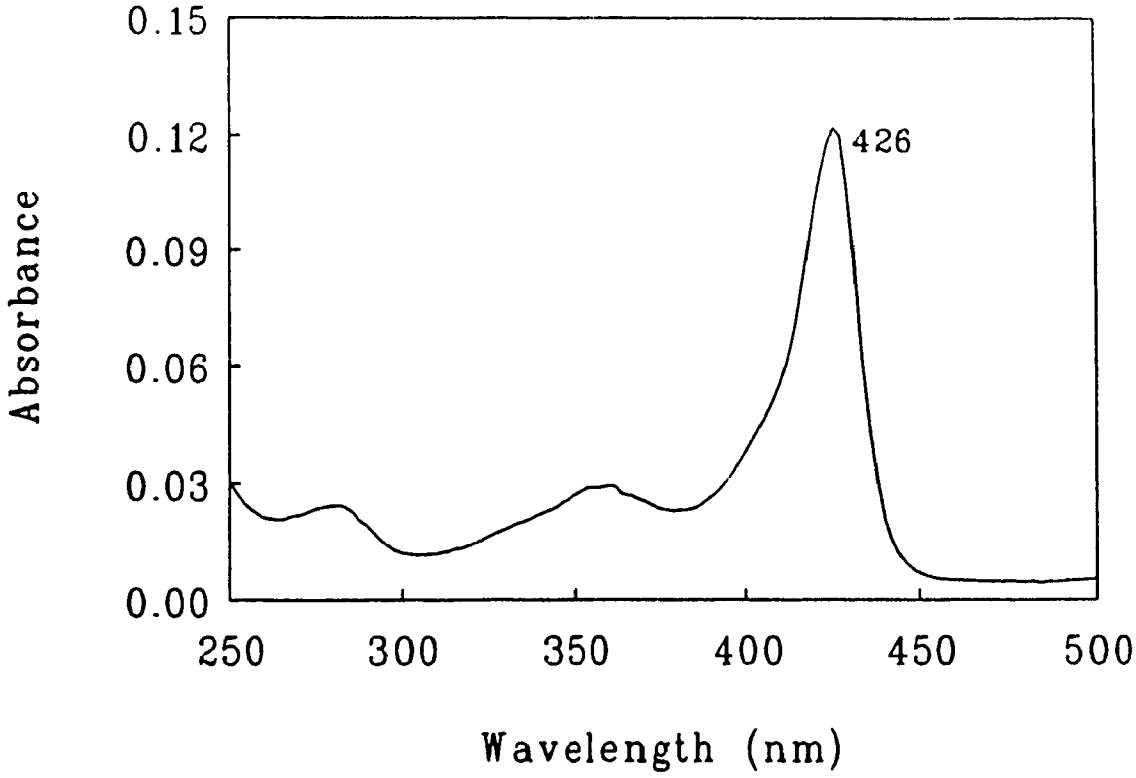
0.15
0.12
0.09
0.06
0.03
0.00
Absorbance
426
250
300
350
400
450
500
Wavelength (nm)

(d)

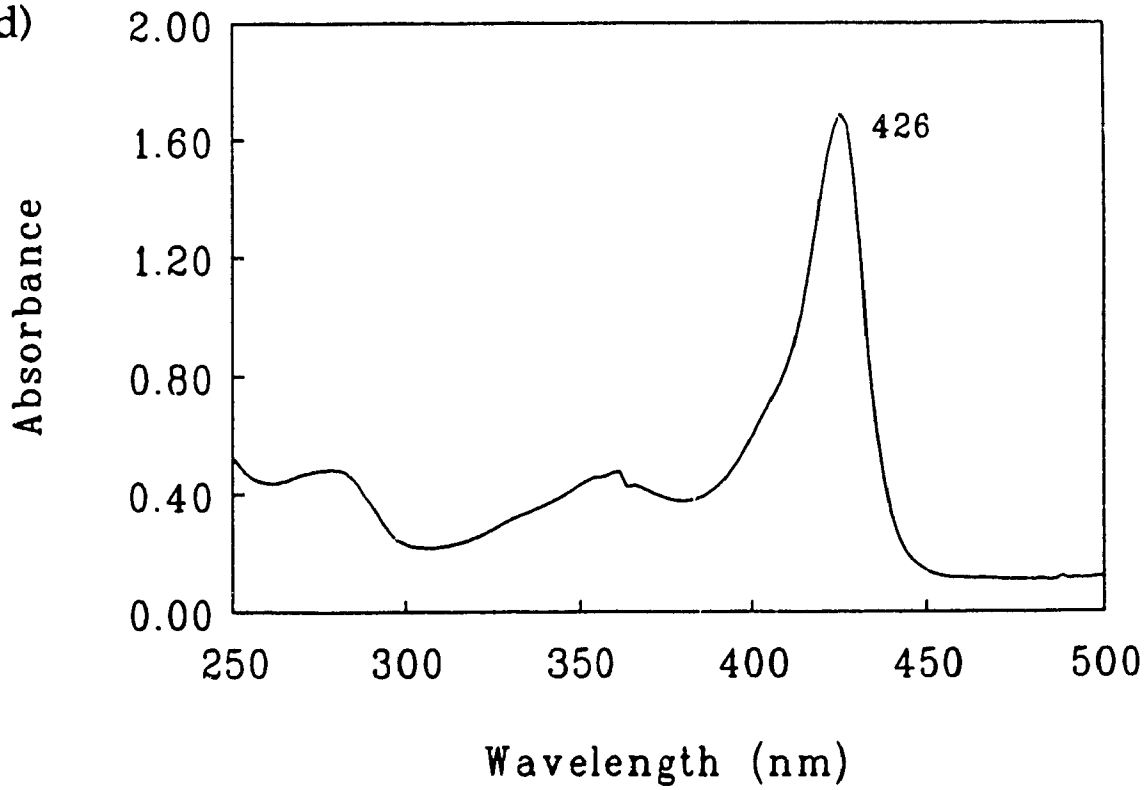
2.00
1.60
1.20
0.80
0.40
0.00
Absorbance
426
250
300
350
400
450
500
Wavelength (nm)

Figure 3.9: Electrospray mass spectra of (a) Fe-cyt c, (b) por-cyt c, (c) Zn-cyt c and (d) Co-cyt c (1 ~ 5 μg/μl) in 10% acetic acid. The ions carrying +10 ~ +17 positive charges were used to determine the MWs which are indicated on the spectra. See caption to Figure 2.24 for further experiment details.

(a)

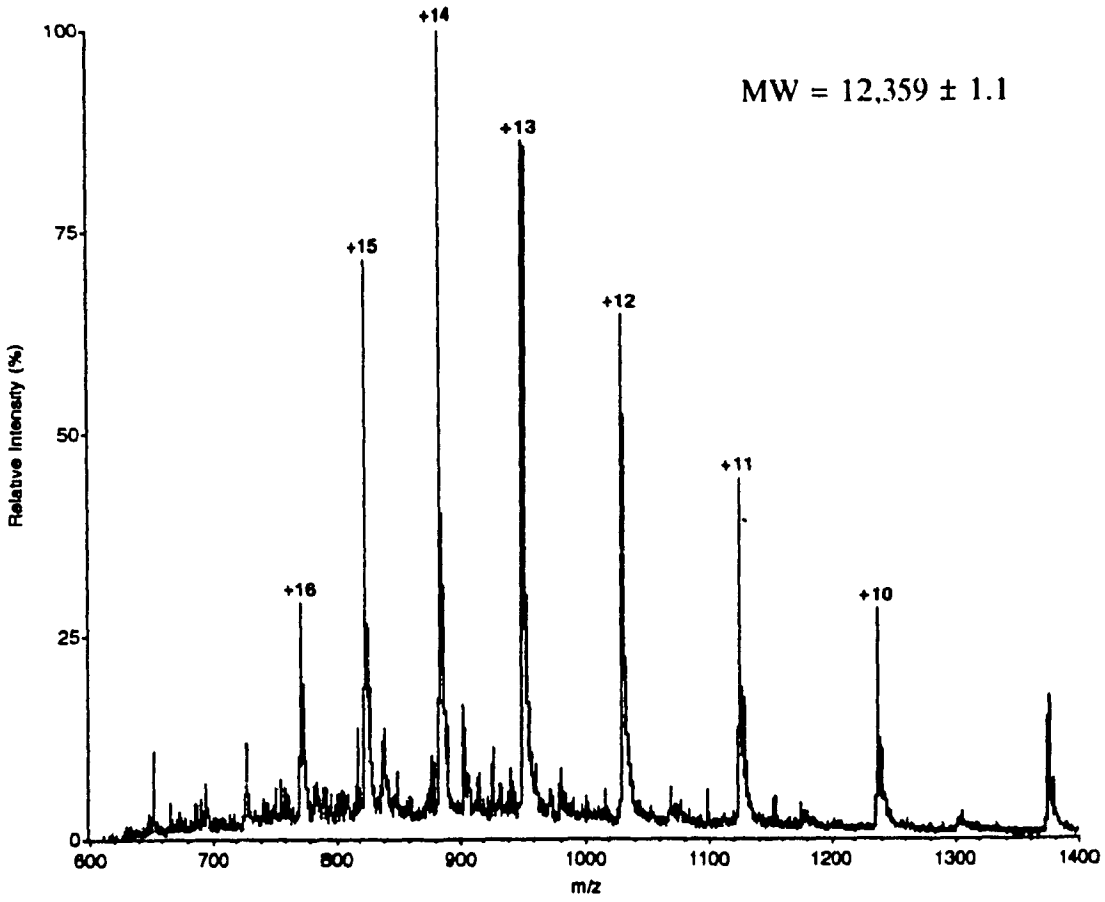
MW = 12,359 ± 1.1
+16
+15
+14
+13
+12
+11
+10
Relative Intensity (%)
m/z
100
75
50
25
0
600
700
800
900
1000
1100
1200
1300
1400

(b)

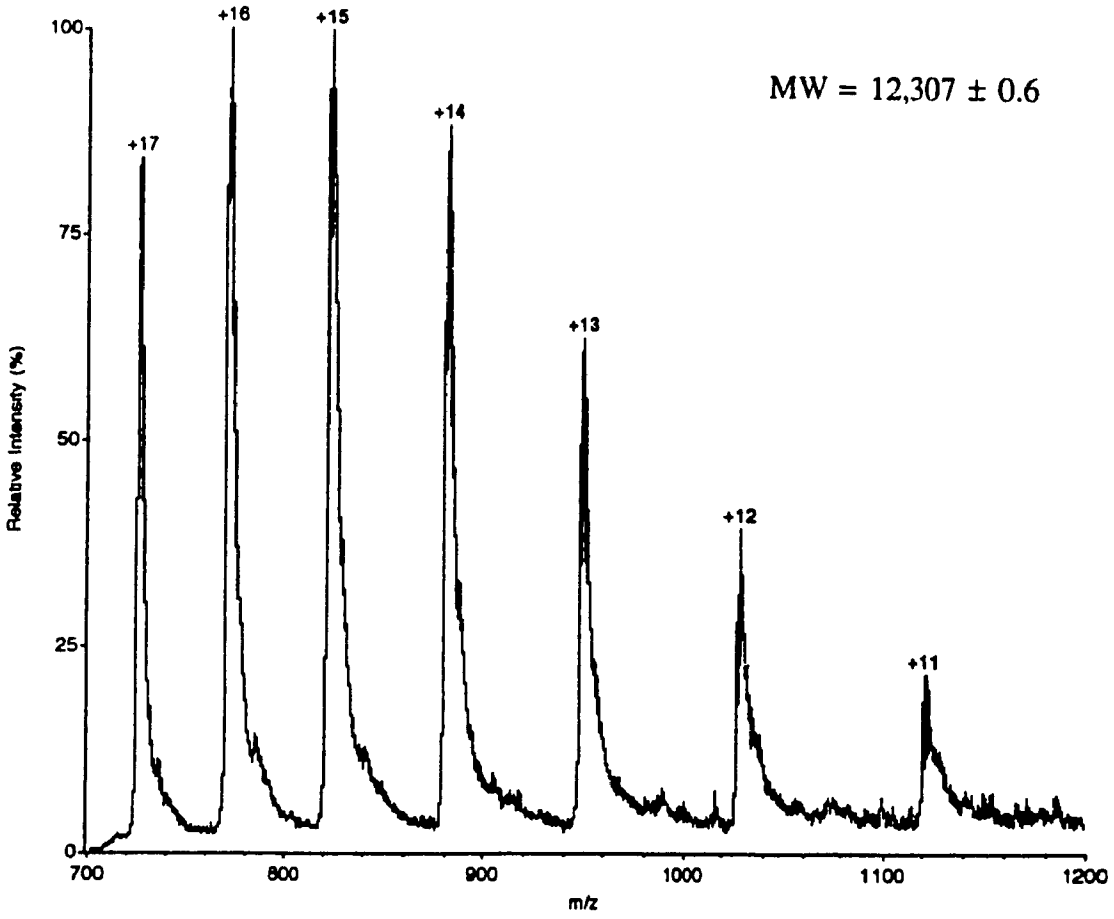
MW = 12,307 ± 0.6
+17
+16
+15
+14
+13
+12
+11
100
75
50
25
0
Relative Intensity (%)
700
800
900
1000
1100
1200
m/z

(c)

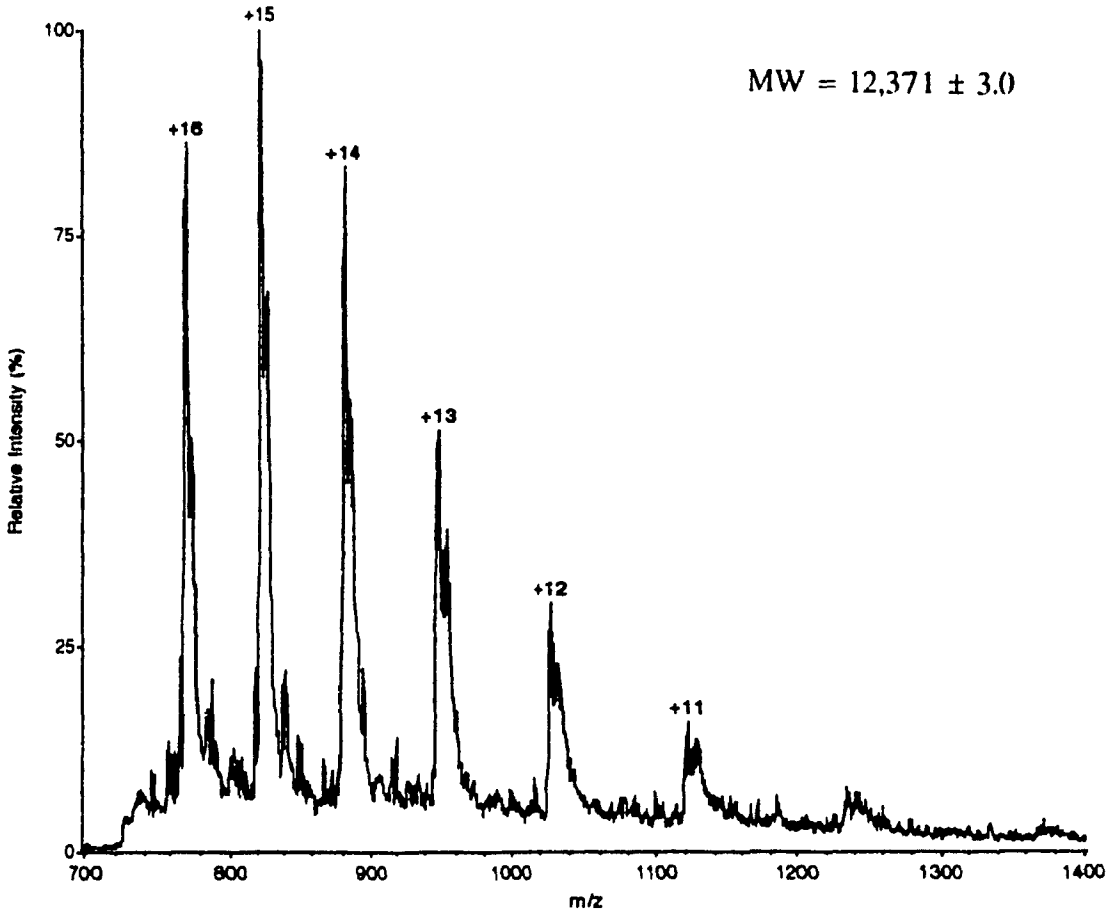
MW = 12,371 ± 3.0
+15
+16
+14
+13
+12
+11
100
75
50
25
0
Relative Intensity (%)
700
800
900
1000
1100
1200
1300
1400
m/z

(d)

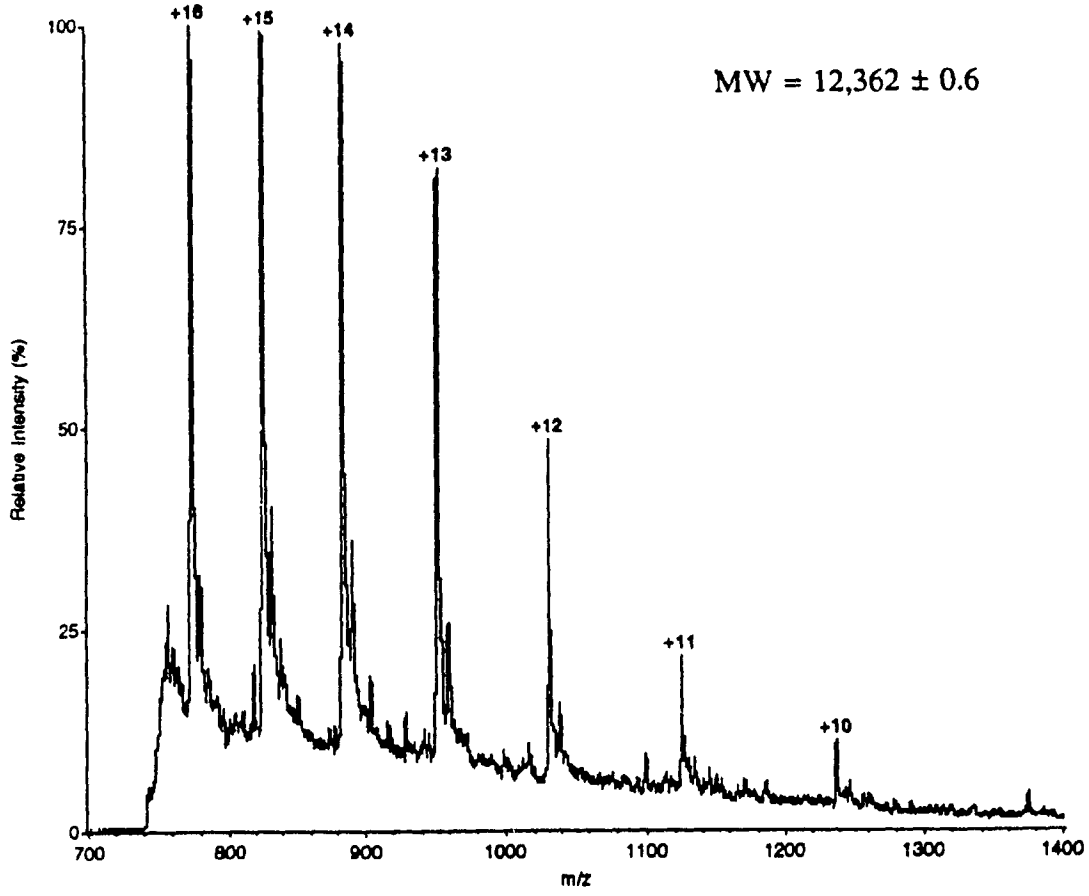
MW = 12,362 ± 0.6
+16
+15
+14
+13
+12
+11
+10
100
75
50
25
0
Relative Intensity (%)
700
800
900
1000
1100
1200
1300
1400
m/z

in the porphyrin should yield an observed MW of 12,368. However, the average observed MW is 12,371 which is 3 Da higher than predicted. Zn-cyt c is acid-labile and Zn is released from the porphyrin at low pH; thus, at pH 2.2 protons may compete with the Zn (II) ion for some of the pyrrole N atoms and each substitution would give rise to a mass increase of 1 Da. Substitution of Co (AW = 59) for Fe (AW = 56) in cyt c is excepted to give a MW of 12,362 which is precisely the value observed (Table 3.1). From the excellent agreement between the observed and anticipated MWs, we conclude that por-cyt c, Zn-cyt c and Co-cyt c have been formed with no alteration of the polypeptide. Extra peaks are clearly visible in the por- and Zn-cyt c mass spectra (Figure 3.9b, c). These peaks arise from a species with a MW of 12,324, so it is possible that Na (AW = 23) adducts of por-cyt c are formed.

Reversibility of denaturation of Fe-cyt c and its derivatives: The fluorescence of refolded Fe-cyt c, which has been unfolded in urea, is compared in Figure 3.10 with that of native Fe-cyt c. Results for both the native and refolded cytochromes are superimposable which indicates that unfolding of Fe-cyt c in urea is reversible. The results in Figures 3.11, 3.12 and 3.13 show that unfolding of the cytochrome c derivatives in urea is also reversible. However, the time required for the 8-M urea denatured derivatives to renature was about 7 days at 4 °C, while unfolding in 8 M urea takes only ~10 min at room temperature.

Free energy of denaturation of Fe-cyt c and its derivatives: To examine the relative stabilities of Fe-cyt c and its derivatives, fluorescence-monitored urea denaturation was carried out, and the data are listed in Appendix 3 and plotted in Figure 3.14. As

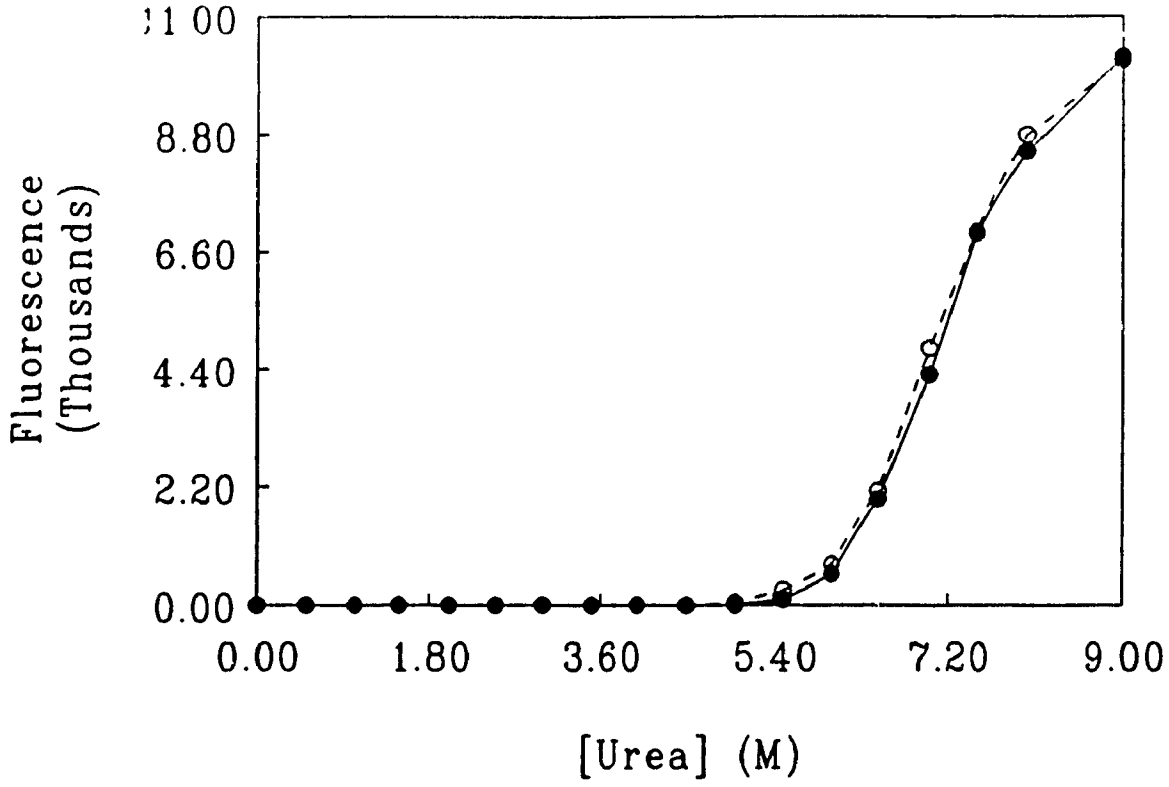

Figure 3.10: Integrated fluorescence of 2.0 μM native (● solid line) and refolded (o dashed line) horse Fe-cyt c vs. urea concentration at pH 7.0. Prior to these measurements refolded Fe-cyt c has been exposed to 8.0 M urea which was removed by dialysis (see text). See caption to Figure 2.4 for further experimental details.

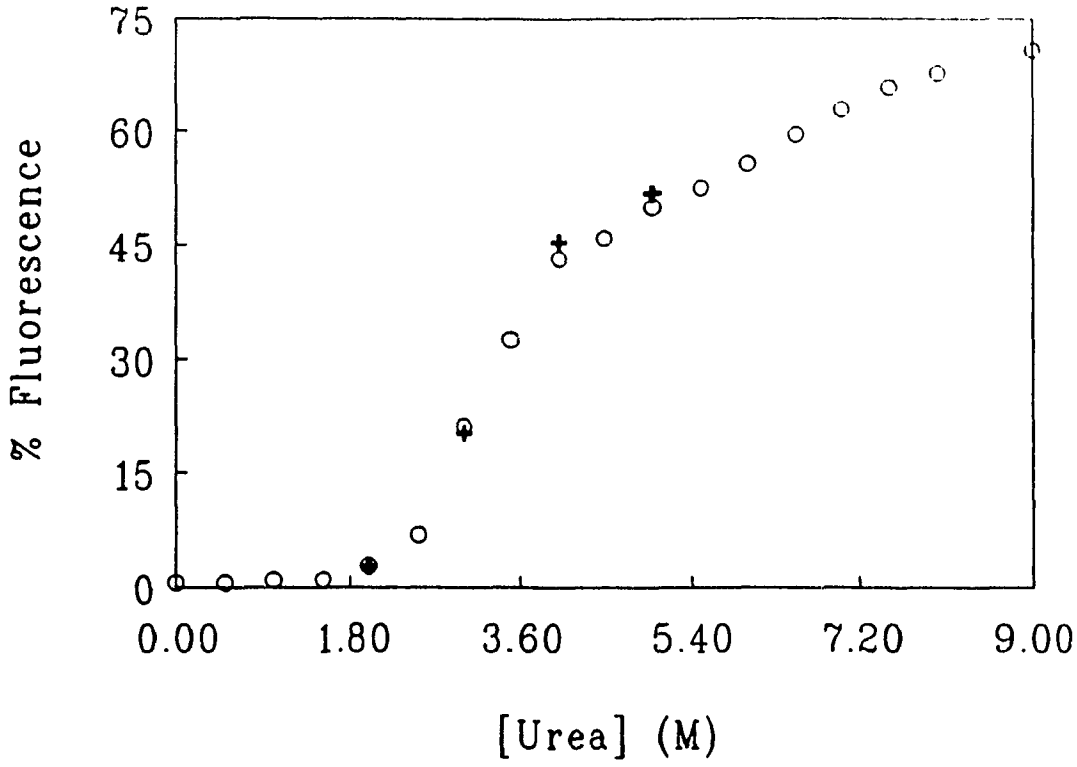

Figure 3.11: Relative integrated fluorescence (%) of 2.0 μM native (o) and partially refolded (+) por-cyt c vs. urea concentration at pH 7.0. Partially refolded por-cyt c was exposed to 8.0 M urea prior to dilution to the urea concentrations indicated here. The fluorescence of 2.0 μM L-Trp at the same concentration of urea was taken as 100%. See caption to Figure 2.4 for further experimental details.

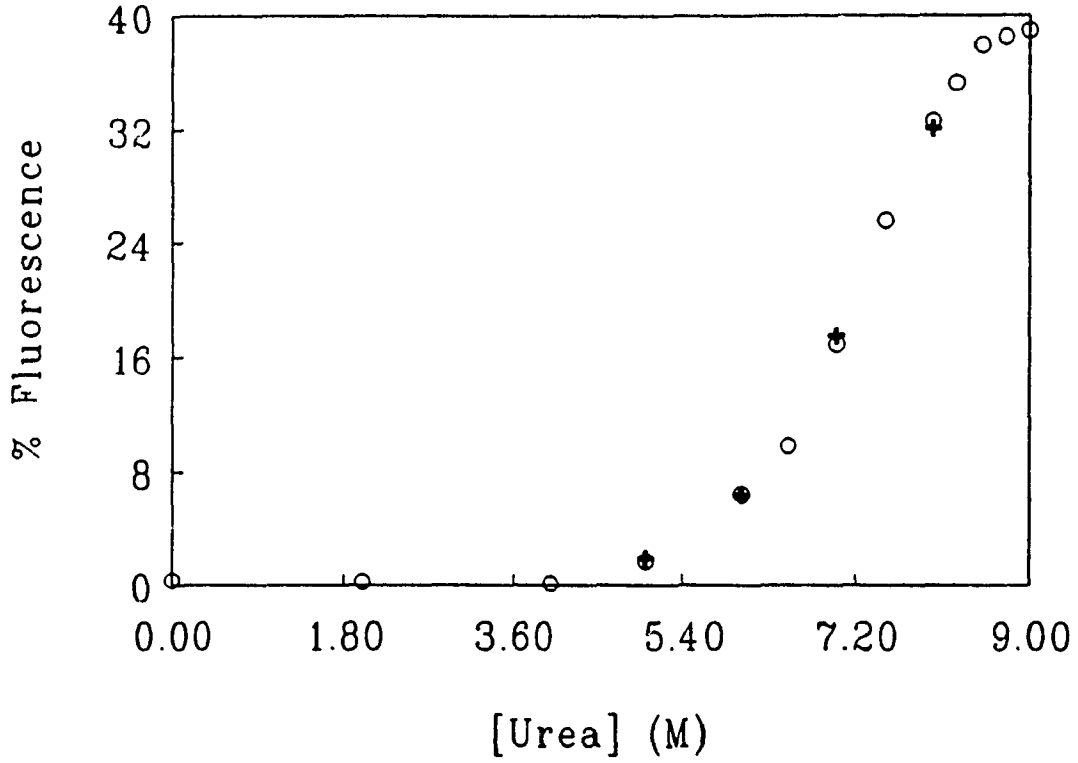

Figure 3.12: Relative integrated fluorescence (%) of 2.0 μM native (o) and partially refolded (+) Zn-cyt c vs. urea concentration at pH 7.0. See caption to Figures 2.4 and 3.11 for further experimental details.

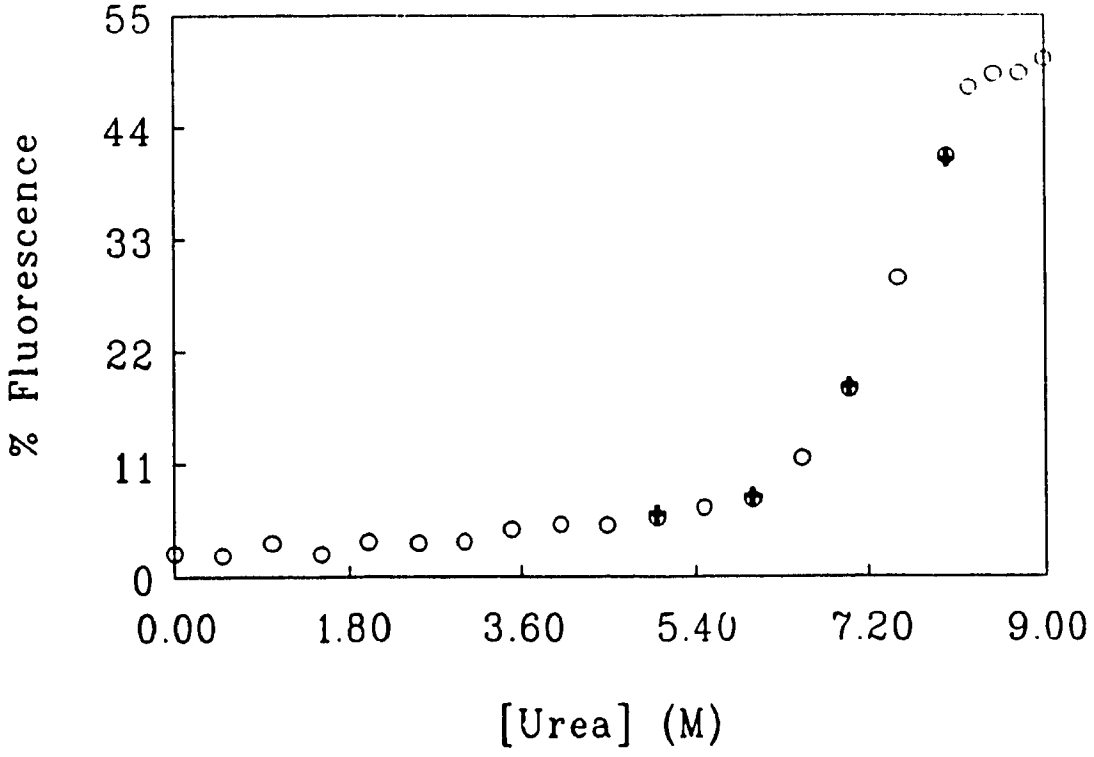

Figure 3.13: Relative integrated fluorescence (%) of 2.0 μM native (o) and partially refolded (+) Co-cyt c vs. urea concentration at pH 7.0. See caption to Figures 2.4 and 3.11 for further experimental details.

before (Section 2.2), the relative integrated emission from 315 to 400 nm vs. urea concentration was recorded for each sample and the data were analyzed in terms of a two-state mechanism as outlined in Section 2.2.2. Plots of the standard free energy change of denaturation (ΔG_d) vs. urea concentration (Equation 2.3) are shown in Figure 3.15. The Y-intercepts ($\Delta G_{d,aq}$), and slopes (m) of these plot are presented in Table 3.2. From these data it can be seen that the global stabilities of Fe-cyt c and its derivatives decrease in the order: Co-cyt c > Fe-cyt c > Zn-cyt c > por-cyt c.

Analysis of local stability of Fe-cyt c and its derivatives by HPLC: The time dependence of tryptic digestion of the cytochromes c was analyzed by HPLC and Figure 3.16 shows the chromatograms obtained for Zn-cyt c. These are similar to those shown in Figure 2.22 for Fe-cyt c, and also similar to the chromatograms obtained for por- and Co-cyts c (not shown). Clearly, HPLC successfully separates the tryptic digests in only 15 min. From the absorbance at 210 nm of the bands corresponding to undigested protein, the time course of tryptic digestion of Fe-cyt c and its derivatives is plotted in Figure 3.17, taking the absorbances at 210 nm at zero digestion time as 100%. The results parallel those from the fluorescence data, since the local stabilities of Fe-cyt c and its derivatives follow the same trend as the global stabilities: Co-cyt c > Fe-cyt c > Zn-cyt c > por-cyt c.

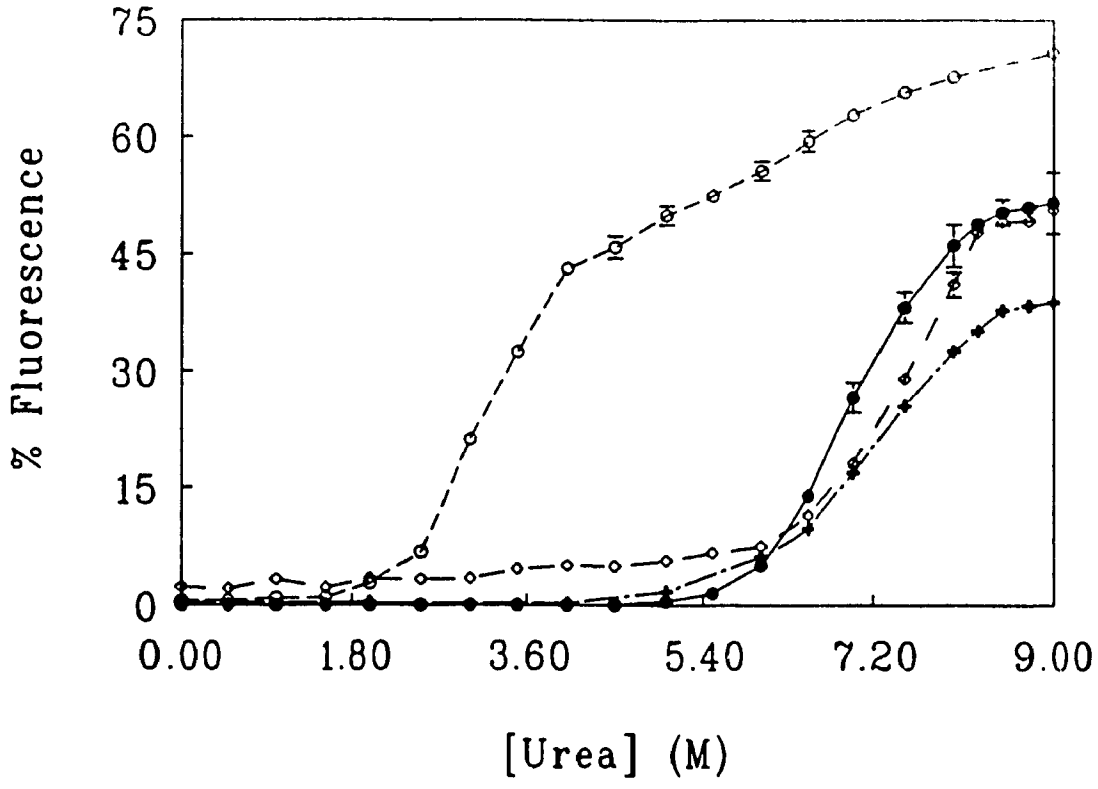

Figure 3.14: Comparison of relative integrated fluorescence (%) of 2.0 μM Fe- (●), por- (○), Zn- (+) and Co- (◇) cyt c vs. urea concentration at pH 7.0. The fluorescence of 2.0 μM L-Trp at the same concentration of urea was taken as 100%. See caption to Figure 2.4 for further experimental details. The error bars were obtained from an average of 3 to 5 trials.

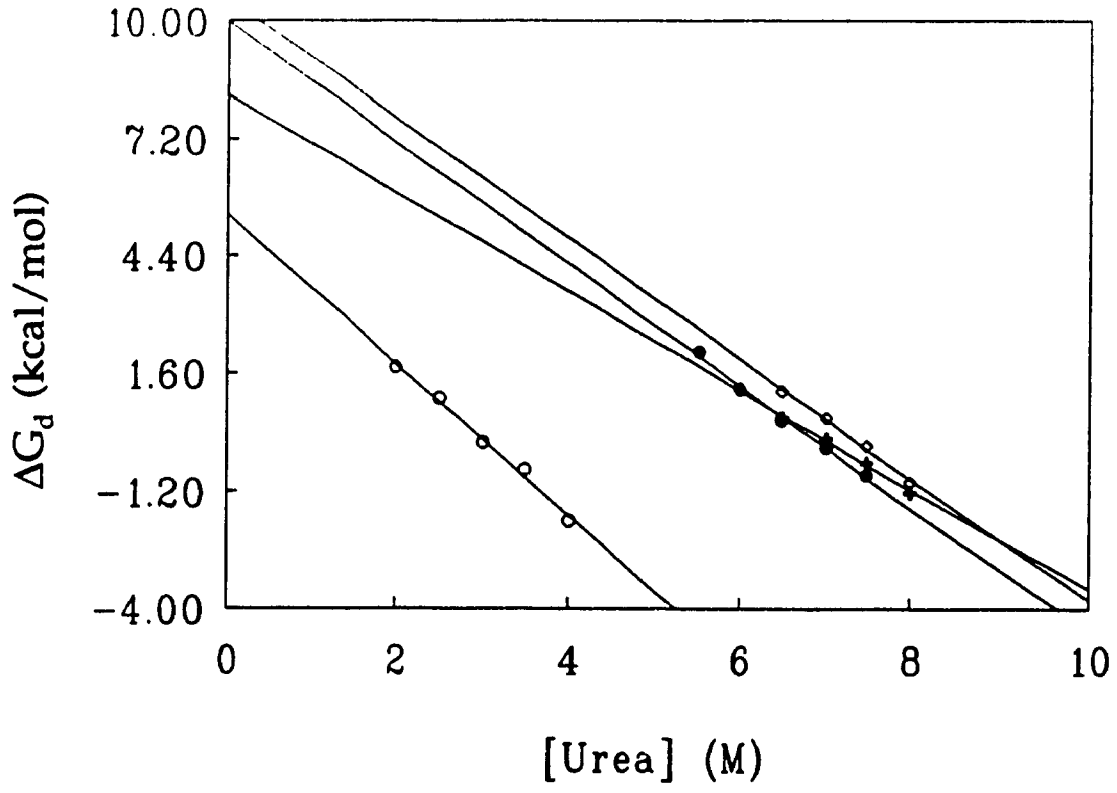

Figure 3.15: Free energies of denaturation (ΔG_d) of Fe- (●), por- (○), Zn- (+), Co- (◇) cyt c vs. urea concentration. ΔG_d values were calculated using Equation 2.4 and the data in Appendix 3. The intercept and slope of each plot gives $\Delta G_{d,aq}$ and m, respectively (Equation 2.3).

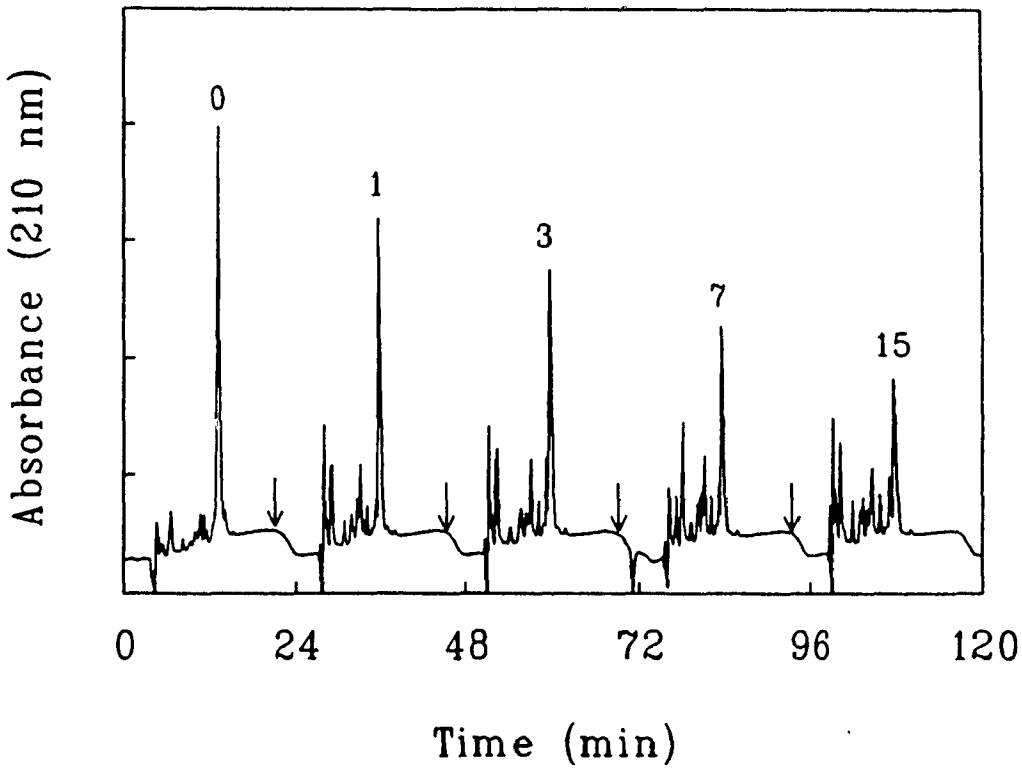

Figure 3.16: Reversed-phase HPLC chromatograms of tryptic digests of Zn cyt c. The digests (0.05 mg in 100 µl) of Zn-cyt c were injected onto the column approximately every 20 min (at the arrows) and the numbers on the main bands indicate the digestion time in hours. Digestion was carried out in 50 mM phosphate buffer (pH 7.0), containing 0.2 M KCl at 37 °C with a trypsin to Zn-cyt c ratio of 1:50 (W:W). The HPLC column was equilibrated with 20% CH_3CN containing 0.1% TFA (pH 2.5) and elution was with a 20 to 80% CH_3CN gradient in 0.1% TFA within 15 min at a flow rate of 1.0 ml/min. The column was washed with 20% CH_3CN containing 0.1% TFA for ~ 5 min after each 15-min elution.

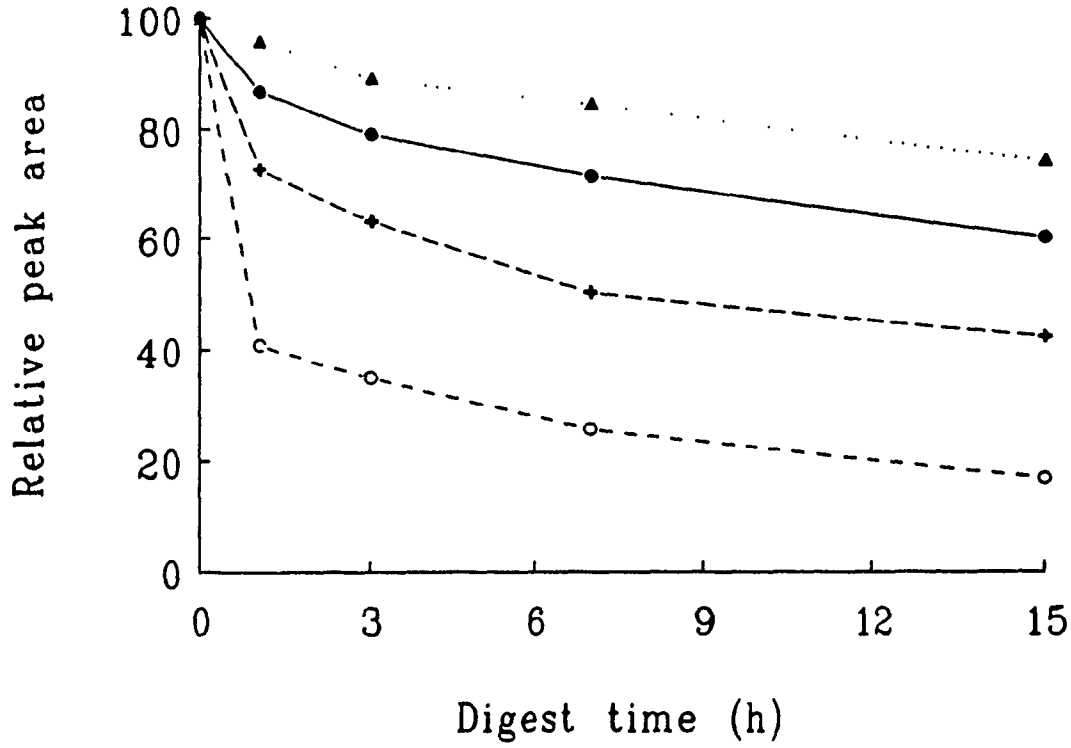

Figure 3.17: Time course of tryptic digestion of horse cytochrome c and its derivatives at pH 7.0 and 37 °C. Relative peak areas of the HPLC bands containing undigested Fe- (●), por- (○), Zn- (+) and Co- (▲) cyts c are plotted vs. digestion time. The areas of the bands at 0 h are taken as 100%, and the experimental conditions are given in the caption to Figure 3.16, which shows the HPLC chromatograms for Zn-cyt c.

Table 3.1: MWs of Fe-cyt c and its derivatives observed by ES-MS

species	obs. MW[a]	calc. MW[b]
Fe-cyt c	12,359±1.1	
por-cyt c	12,307±0.6	12,307
Zn-cyt c	12,371±3.0	12,368
Co-cyt c	12,362±0.6	12,362
Na-cyt c	12,324±1.3	12,326

[a] MWs observed by ES-MS

[b] MWs calculated from changes in the expected MW of the porphyrin prosthetic group at pH 2.2 (see text)

Table 3.2: $\Delta G_{d,aq}$, m values and urea concentrations at half maximum fluorescence for Fe-, por-, Zn-, and Co-cyts c

species	$\Delta G_{d,aq}$[a] (kcal/mol)	$\Delta\Delta G_{d,aq}$[b] (kcal/mol)	m[a] (kcal/mol/M)	$[urea]_{1/2}$[c] (M)
Fe-cyt c	9.9±0.5	0	1.4±0.1	6.9±0.1
por-cyt c	5.4±0.2	4.5	1.8±0.1	2.7±0.1
Zn-cyt c	8.2±0.3	1.7	1.2±0.1	7.0±0.1
Co-cyt c	10.5±0.4	-0.6	1.4±0.1	7.2±0.1

[a] $\Delta G_{d,aq}$ and m values were obtained from the intercepts and slopes of the plots shown in the Figure 3.15. The errors in $\Delta G_{d,aq}$ and m were calculated as indicated in Appendix 5

[b] $\Delta\Delta G_{d,aq}$ is the difference between the $\Delta G_{d,aq}$ of horse cytochrome c and its derivative

[c] $[urea]_{1/2}$ is the urea concentration at half maximum fluorescence

3.4 Discussion

The horse cytochrome c derivatives were purified by cation-exchange FPLC and characterized by Soret absorption and ES-MS. The Soret maximum of por-cyt c is at 404 nm, which shifts to 424 and 426 nm upon incorporation of Zn and Co, respectively, into the porphyrin core. The ES-MS results demonstrate that the MWs of the derivatives are in excellent agreement with those calculated using the expected MWs of the porphyrin prosthetic groups (Table 3.1). These results indicate that HF exposure to remove the iron from the porphyrin ring leaves a significant fraction of the polypeptide unaltered. Likewise, the procedures used to insert zinc or cobalt into the porphyrin yield a large amount of the metalloderivative with the polypeptide in its native form. The ES-MS results presented here confirm, for the first time, that metal-free and metalloderivatives of horse cytochrome c can be readily prepared without alteration of the polypeptide. Furthermore, the data in Table 3.1 indicate the power of ES-MS in protein characterization. Although the MW difference between Fe-cyt c and Co-cyt c is only 3 Da, ES-MS still distinguishes between these two derivatives. The ES-MS results also show that por-cyt c forms Na adducts (Figure 3.9), and that Zn is lost from Zn-cyt c at low pH.

Denaturation of Fe-cyt c and its derivatives is reversible. After a few hours exposure to 8.0 M urea, it was found that the proteins refold completely under dialysis or dilution in 3 - 7 days. Thus, the equilibrium between the folded (native) and unfolded (denatured) states is reversible. The fluorescence-monitored denaturation data are summarized in Figure 3.14. Using Trp-59 fluorescence as a probe, the midpoint for urea

denaturation of por-cyt c is at 2.7 M (Table 3.2). In contrast, the same transition in Fe-cyt c and its Zn and Co metalloderivatives is centred at 7 M urea. Analysis of each transition in terms of a two-state model predicts that the free energy change in aqueous buffer ($\Delta G_{d,aq}$) between the native and denatured states are the following (kcal/mol): 5.4 (por-cyt c), 8.2 (Zn-cyt c), 9.9 (Fe-cyt c) and 10.5 (Co-cyt c). The higher sensitivity of por-cyt c to urea may be due to increased conformational flexibility of the polypeptide caused by the loss of the metal axial ligands since their presence increases the midpoint of the denaturation transition observed for the derivatives (Figure 3.14).

The estimated differences in the conformational stability of the proteins in the absence of denaturant are in agreement with expectations based on the strength of the axial ligands. Both Met-80 and His-18 are axial ligands in Fe-cyt c, Co-cyt c[9], and Zn-cyt c, but only ~66% of the Zn-cyt c molecules possess a Zn(II)-S(Met-80) bond[10]. Fe-cyt c is more stable than Zn-cyt c by 1.7 kcal/mol ($\Delta\Delta G_{d,aq}$; Table 3.2); however, Fe(II)-cyt c, which has a neutral prosthetic group like Zn-cyt c, is ~0.6 kcal/mol more stable than Fe(III)-cyt c[19]. So, the difference in conformational free energy between the Fe(II)- and Zn(II)-cyts c is ~2.3 kcal/mol. A heme crevice stability of 1.2 kcal/mol was estimated from thermal titration of the 695-nm band of horse Fe-cyt c[20]. It is well known that the Fe(II)-S(Met-80) bond is more stable than the Fe(III)-S(Met-80) bond[21] which will increase the stability of the heme crevice in Fe(II)-cyt c relative to Fe(III)-cyt c. Thus, the $\Delta\Delta G_{d,aq}$ of 2.3 kcal/mol between Zn- and Fe(II)-cyts c could be largely due to the increased stability of the closed heme crevice in Fe(II)-cyt c, compared to the partially open crevice in Zn-cyt c, which has a weak sixth axial ligand. Clearly the axial ligands

are important in stabilizing the tertiary structure of cytochrome c. However, since por-cyt c is more sensitive to urea denaturation than Zn-cyt c, the contribution of the M-S(Met-80) bond to the global stability of cytochrome c must be less important than that of the M-N(His-18) bond.

The fluorescence results show that Co-cyt c is more stable than Fe-cyt c to urea denaturation ($\Delta\Delta G_{d,aq}$ = -0.6 kcal/mol; Table 3.2). Proton NMR studies have shown local conformational changes in Co-cyt c compare to Fe-cyt c; in particular, the peptide chain segment 78-82 is closer to the porphyrin in Co-cyt c[10]. This indicates that the Co(III)-S(Met-80) bond is stronger than the Fe(III)-S(Met-80), which could result in the greater conformational stability of Co-cyt c.

The slope of the ΔG_d vs. urea plot gives the m values for denaturation. As mentioned in Chapter 2, m is a function of ΔA, a parameter that represents the increase in exposure of nonpolar residues to the solvent in the denatured state of a protein. Since m depends on the amino acid composition, its value was expected to be the same for all the horse cytochrome c derivatives. Examination of Figure 3.14 shows that the derivatives exhibit the following maximum relative fluorescence values (%F) in 9 M urea: 40% (Zn-cyt c), 50% (Fe- and Co-cyts c) and 70% (por-cyt c). This variation in maximum %F indicates that the denatured states of derivatives have different degrees of tertiary structure, with Zn-cyt c having the most compact structure and por-cyt c having the least compact structure. This is consistent with the small m value for Zn-cyt c (1.2 kcal/mol/M) and the large m value for por-cyt c (1.8 kcal/mol/M), indicating that the exposure of nonpolar residues is greater in the denatured state of por-cyt c. The Soret

maxima of the derivatives show 2-4 nm blue shifts in the denatured states which could reflect changes in porphyrin environment or in axial ligation in the case of Zn- and Co-cyts c.

Time-controlled tryptic digestion was used to probe the relative local stabilities of Fe-cyt c and its derivatives at pH 7.0 and 37 °C. Reversed-phase HPLC was used to analyze the digests and the results are summarized in Figure 3.17. As can be seen from this figure, the order of the local stabilities is as follows: Co-cyt c > Fe-cyt c > Zn-cyt c > por-cyt c. This order is the same as that found for the global stabilities from the fluorescence experiments. Since a large number of Lys residues surround the exposed heme edge (Figure 3.18), conformational flexibility or instability in this region should increase the susceptibility of the derivatives to tryptic digestion. Weakening or total removal of the axial ligands is expected to destabilize regions of the polypeptide surrounding the ligating residues, His-18 and Met-80. Since His-18 is adjacent to Cys-17, which is covalently bonded to the heme, the conformational flexibility of this region is expected to be limited even in the absence of His-18 metal ligation. The Met-80 residue is part of a loop between the α-helix 70-75 and the stable C-terminal α-helix 87-102. Loss of Met-80 metal ligation is expected to greatly increase the conformational flexibility of segment 75-87 which contains Lys-79, 86 and 87 (Figures 1.1 and 3.18). Thus, the absence of the two axial ligands in por-cyt c should result in a derivative with the most conformational flexibility around the heme; the weak Met-80 ligation should make the conformational flexibility of segment 75-87 greater in Zn-cyt c than in Fe-cyt c, whereas the strong axial ligation in Co-cyt c should decrease the conformational flexibility in the

heme region of this derivative. The observed local stabilities follow the same order as predicted for the local conformational stabilities of the polypeptide in the heme region. Thus, we conclude from our investigations on the horse cytochrome c derivatives that axial ligation plays a key role in determining both the local and global relative conformational stabilities.

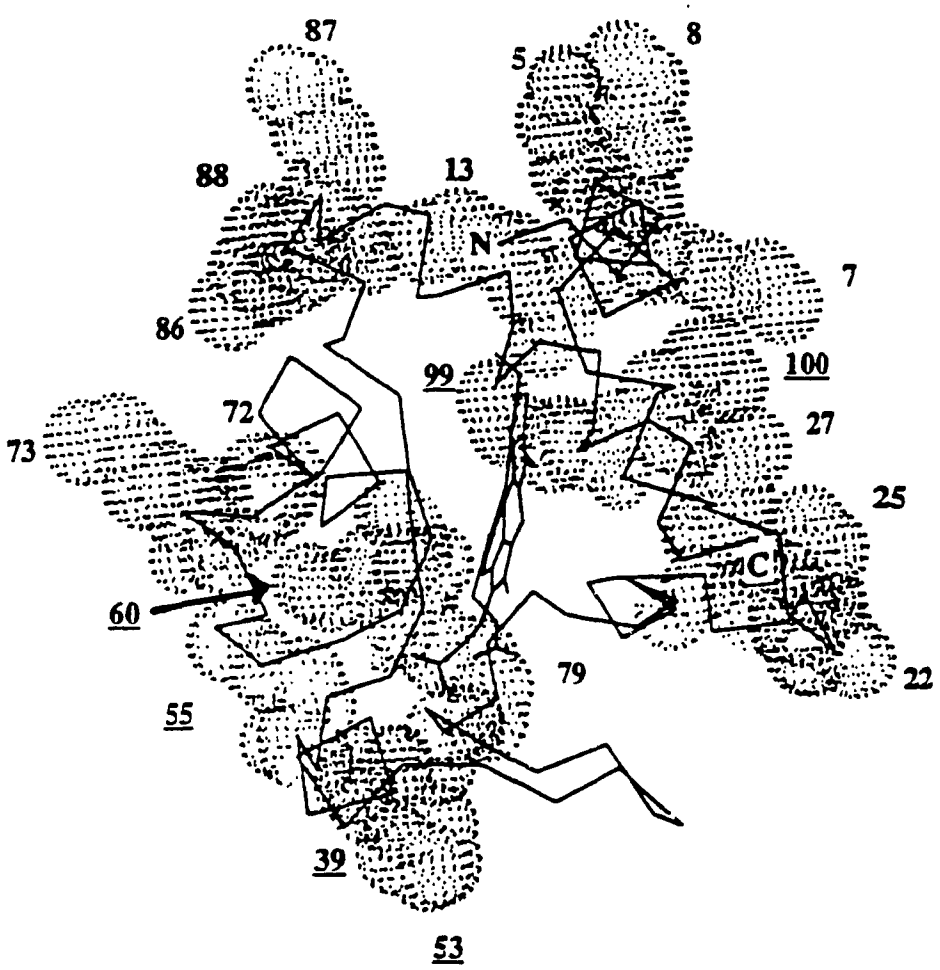

Figure 3.18: Computer graphics display of the C_α backbone of horse Fe-cyt c showing the location of the heme and the Van der Waals surfaces of the 19 Lys residues. Lys on the back surface are underlined. The amino and carboxyl terminals are designated by N and C. This molecular graphics image was produced using MidasPlus software[22] from the Computer Graphics Laboratory, University of California, San Francisco.

3.5 References

1) Dickinson, L.C. *J. Chem. Ed.* **1976**, *53*, 381.

2) Fisher, W.R.; Taniuchi, H. and Anfinsen, C.B. *J. Biol. Chem.* **1973**, *248*, 3188.

3) Dickinson, L.C. and Chien, J.C.W. *Biochem.* **1975**, *14*, 3526.

4) Vos, K.; Laane, C.; Weijers, S.R.; Van Hoek, A.; Veeger, C. and Visser, A.J.W.G. *Eur. J. Biochem.* **1978**, *169*, 259.

5) Vanderkooi, J.M.; Adar, F. and Erecinska, M. *Eur. J. Biochem.* **1976**, *64*, 381.

6) Findlay, M.C.; Dichinson, L.C. and Chien, J.C.W. *J. Am. Chem. Soc.* **1977**, *99*, 5168.

7) Dickinson, L.C. and Chien, J.C.W. *J. Biol. Chem.* **1977**, *252*, 6156.

8) Findlay, M.C. and Chien, J.C.W. *Eur. J. Biochem.* **1977**, *76*, 79.

9) Dickinson, L.C. and Chien, J.C.W. *Biochem.* **1975**, *14*, 3534.

10) Moore, G.R.; Williams, R.J.P.; Chien, J.C.W. and Dickson, L.C. *J. Inor. Biochem.* **1980**, *12*, 1.

11) Dixit, B.P.S.D.; Moy,V.T. and Vanderkooi, J.M. *Biochem.* **1984**, *23*, 2103.

12) Vanderkooi, J.M.; Moy, V.T.; Maniara, G. and Koloczek, H. *Biochem.* **1985**, *24*, 7931.

13) Horie, T.; Maniara, G. and Vanderkooi, J.M. *FEBS.* **1993**, *177*, 287.

14) Babul, G. and Stellwagen, E. *Biochem.* **1972**, *11*, 1195.

15) Strottman, J.M.; Stellwagen, A.; Bryant, C. and Stellwagen, E. *J. Biol. Chem.* **1984**, *259*, 6931.

16) Margoliash, E. and Walasek, O.F. *Cytochrome c from Vertebrate and Invertebrate Sources*. Estabrook, R.W. and Pullman, M.E. (ed.). *Methods in Enzymology*. Academic

Press, New York. **1967**, *10*, p. 339.

17) Falk, J.E. *Porphyrins and Metalloporphyrins - Their General, Physical and Coordination Chemistry, and Laboratory Methods*. Elsevier Publishing Company, New York. **1964**, p. 10.

18) Vanderkool, J.M. and Erecinska, M. *Eur. J. Biochem.* **1975**, *60*, 199.

19) McLendon, G. and Smith, M. *J. Biol. Chem.* **1978**, *253*, 4004.

20) Osheroff, N.; Borden, D.; Koppenol, W.H. and Margoliash, E. *J. Biol. Chem.* **1980**, *255*, 1689.

21) Takano, T and Dickerson, R.E. *Conformational Differences Between Ferri- and Ferrocytochrome c*. Chien Ho (ed.). *Electron Transport and Oxygen Utilization*. Elsevier North Holland Inc. **1982**, p. 17.

22) Ferrin, T.E.; Huang, C.C.; Jarvis, L.E. and Landgridge, R. *J. Mol. Graphics*. **1988**, *6*, 13.

4.0 Comparison of stabilities of native and derivatives of cytochrome c

The results in Chapter 2 show that the global conformational stabilities of the different native cytochromes c vary considerably. The order of global stabilities was found to be as follows: horse > tuna > Candida > Saccharomyces (Table 2.1). The results presented in Chapter 3 reveal that the order of the global stabilities for the horse cytochrome c derivatives are as follows: Co-cyt c > Fe-cyt c > Zn-cyt c > por-cyt c (Table 3.2). It is of interest that the free energy of denaturation in urea of the native cytochromes c exhibit a broader range of values ($\Delta\Delta G_{d,aq}$ = 7.5 kcal/mol; Table 2.1) compared to the derivatives ($\Delta\Delta G_{d,aq}$ = 5.1 kcal/mol; Table 3.2). However, as discussed in Chapter 2, the low $\Delta G_{d,aq}$ for wild type Saccharomyces cytochrome c may be largely due to the presence of Cys-102 in the C-terminal. The C102T and C102S mutants have reported $\Delta G_{d,aq}$ values from guanidine denaturation studies similar to that found here for Candida c. Thus, if we assume that the $\Delta G_{d,aq}$ value for the C102T mutant from urea denaturation is also similar to that for Candida c from urea denaturation, then the $\Delta\Delta G_{d,aq}$ range is only 2-3 kcal/mol instead of 7.5 kcal/mol. Hence, removal of the heme axial ligands has a larger effect on the global stability than substitution of ~40 amino acid residues when C-terminal helix capping is present in the four native cytochromes c. This underscores the importance of the axial ligands in stabilizing the tertiary structure of

cytochrome c. From the relative global stabilities of Zn- and por-cyts c (Table 3.2), it is clear that His-18 ligation has a larger stabilizing effect on the folded conformation of cytochrome c than Met-80 ligation. This is probably due to the greater strength of M-N(His-18) bond compared to the M-S(Met-80) bond[1].

The native cytochromes c showed blue-shifted Soret maxima in 9 M urea and 6 M guanidine hydrochloride which were interpreted as arising from changes in heme axial ligation on protein denaturation. Loss of the 695-nm absorption in high denaturant concentration confirms that the Fe(III)-S(Met-80) bond is cleaved under these conditions. Blue-shifted Soret maxima were also observed for the horse cytochrome c derivatives in 9 M urea. Since por-cyt c cannot form axial ligands, the ~2-nm blue shift in the Soret maximum in urea must be due to changes in the porphyrin environment. However, for Zn- and Co-cyts c, the ~4-nm blue shift can arise from changes in axial ligation or porphyrin environment or from both. Confirmation of changes in axial ligation by absorption is not possible for these metalloderivatives since a direct probe, such as the 695-nm band for native cytochromes c, has not been identified in the spectra of the derivatives. From the denaturation results, similar maximum relative fluorescence values (%F) were observed for the native cytochromes c (~50%) and for the metalloderivatives (40-50%) indicating residual tertiary structure in each case, which may arise from similar axial ligation in the denatured state.

Comparison of the m values for urea denaturation between the native and nonnative cytochromes c is also informative. The m values for urea denaturation are centred around 1.4 kcal/mol/M with the exception of Saccharomyces and Zn-cyt c, and

Candida and por-cyt c which exhibit m values of 1.1-1.2 and 1.7-1.8 kcal/mol/M, respectively (Tables 2.1 and 3.2). Thus, the sensitivity of the proteins to urea appears to be dependent on the 20 amino acid substitutions between the yeast proteins as well as on axial ligation.

The urea concentrations at half maximum fluorescence are also a measure of the relative conformational stabilities of cytochromes c. From the $[urea]_{1/2}$ values in Tables 2.1 and 3.2, we can see that with the exception of the yeast cytochromes c, the native cytochromes c and the metalloderivatives all have $[urea]_{1/2}$ values of ~7 M. The closeness of the $[urea]_{1/2}$ values and the corresponding $\Delta G_{d,aq}$ values (9.4 ± 1.0 kcal/mol) indicate that stabilities of this group of cytochromes c fall within a narrow range. The Saccharomyces cytochrome c and por-cyt c have essentially the same $[urea]_{1/2}$ values (2.6 M), but por-cyt c has a higher conformational stability ($\Delta G_{d,aq}$ = 5.4 kcal/mol) than the Saccharomyces protein ($\Delta G_{d,aq}$ = 2.3 kcal/mol), which is a consequence of the large difference in m values between the two proteins (1.8 vs. 1.1 kcal/mol/M). Clustering of hydrophobic residues in the denatured state of Saccharomyces c would reduce both its $\Delta G_{d,aq}$ and m values.

For the derivatives of horse cytochrome c the local stabilities correlate with the global stabilities, both decreasing in the order: Co-cyt c > Fe-cyt c > Zn-cyt c > por-cyt c. Inspection of Figure 3.17 reveals a large spread in digestion time; for example, 20% digestion of Co-, Fe-, Zn- and por-cyts c occurs in ~15 h, ~3 h, ~1 h, and ~30 min, respectively. We conclude that this large spread in digestion time reflects an equally large spread in the local conformational stabilities of the polypeptide involved in axial

ligation, especially the Met-80 loop (segment 75-87) as discussed in Chapter 3. For the native cytochromes c (Figure 2.23), 20% digestion of the horse, Candida and tuna proteins occurs in ~3 h, ~1 h and ~30 min, respectively. These results, which are in excellent agreement with those published by Endo *et al.*,[2] reveal a much smaller range in digestion time for the native proteins (6-fold variation) compared to the derivatives (30-fold variation). In Chapter 2, we pointed out that the local stabilities of the horse and tuna cytochromes c reflect the local stabilities of their heme crevices. Since the native or closed-heme crevice structure of cytochrome c involves Fe(III)-S(Met-80) ligation, the local stability of the Met-80 loop will vary in the same manner as the heme crevice stability. Thus, we conclude that the variation in local stabilities of the native cytochromes c also reflects the stabilities of their Met-80 loops.

Protease digestion is believed to occur sequentially, with the most unstable local region of the polypeptide being the first target of the protease. Hence, our conclusion above implies that the Met-80 loop is the most susceptible region to tryptic digestion. Is there a physiological reason for high local conformational flexibility in the Met-80 loop? The physiological role of cytochrome c is electron transfer to and from its biological partners such as cytochrome c oxidase and cytochrome c reductase in mitochondria[1]. This involves cycling of the heme Fe between +2 and +3 oxidation states. Superimposition of the high resolution crystal structures of oxidized and reduced tuna cytochrome c shows that there are no significant alterations in main-chain conformation between the two forms. However, small but significant conformational changes can be seen on the Met-80 side of the heme crevice[4]. Thus, control of the flexibility in the Met-

80 loop should control maximum electron-transfer rates between cytochrome c and its physiological partners. In support of this view, reductases from various sources, which rapidly reduce native cytochrome c, do not reduce Co-cyt c although reduction is thermodynamically favourable[5]. This implies that the reduction of Co-cyt c is kinetically infeasible, which could be due to the high stability and rigidity of the porphyrin crevice in Co-cyt c, as reflected in its high local stability.

4.1 References

1) Dikerson, R.E.; Takano, T.; Eisenberg, D.; Kallai, O.B.; Samson, L.; Cooper, A. and Margliash, E. *J. Biol. Chem.* **1971**, *246*, 1511.

2) Endo, S.; Nagayama, K. and Wada, A. *J. Biomol. Struct. Dynam.* **1985**, *3*, 409.

3) Moore, G.R. and Pettigrew, G.W. *Cytcohromes c - Evolutionary, Structural and Physicochemical Aspects*. Springer-Verlag, New York. **1990**, p. 363.

4) Takano, T. and Dickerson, R.E. *Conformational Differences Between Ferri- and Ferrocytochrome c*. Chien Ho (ed.). *Electron Transport and Oxygen Utilization*. Elsevier North Holland Inc. **1982**, p. 17.

5) Dickinson L.C. and Chien, J.C.W. *Biochem.* **1975**, *14*, 3526.

5.0 Suggestions for future work

1) Fluorescence-monitored denaturation only detects the distance between the heme and Trp-59. Circular dichroism (CD) studies should be undertaken to monitor the secondary structure (α-helix and β-sheet) of the cytochromes c as a function of denaturant concentration. A comparison of the CD and fluorescence results would also reveal the validity of the two-state denaturation model used here.

2) The fluorescence and CD of the ferrocytochromes c vs. denaturant concentration should be investigated to compare relative stabilities of the reduced and oxidized forms of the native cytochromes.

3) The tryptic digests of the native cytochromes c and of the derivatives should be analyzed at shorter time intervals to confirm the initial site(s) of tryptic degradation from the peptides produced.

4) Mutants of Saccharomyces cytochrome c should be prepared to test the effects of helix capping of the C-terminal on the global and local conformational stability of cytochrome c.

5) Saccharomyces mutants should also be used to probe the effects of surface mutations on the global and local stability.

Appendix 1: Primary sequence alignment for cytochromes c[a]

	1									10
Horse	gly-	asp-	val-	glu-	lys-	gly-	lys-	lys-	ile-	phe-
Tuna	gly-	asp-	val-	ala-	lys-	gly-	lys-	lys-	thr-	phe-
Sacch.	TEFKA-	gly-	ser-	ala-	lys-	lys-	gly-	ala-	thr-	leu-
Can.	PAPFEQ-	gly-	ser-	ala-	lys-	lys-	gly-	ala-	thr-	leu-

	20									30
Horse	val-	glu-	lys-	gly-	gly-	lys-	his-	lys-	thr-	gly-
Tuna	val-	glu-	asn-	gly-	gly-	lys-	his-	lys-	val-	gly-
Sacch.	val-	glu-	lys-	gly-	gly-	pro-	his-	lys-	val-	gly-
Candida	ile-	glu-	ala-	gly-	gly-	pro-	his-	lys-	val-	gly-

	40									50
Horse	pro-	asn-	leu-	his-	gly-	leu-	phe-	gly-	arg-	lys-
Tuna	pro-	asn-	leu-	trp-	gly-	leu-	phe-	gly-	arg-	lys-
Sacch.	pro-	asn-	leu-	his-	gly-	ile-	phe-	gly-	arg-	his-
Candida	pro-	asn-	leu-	his-	gly-	ile-	phe-	ser-	arg-	his-

	60									70
Horse	thr-	gly-	gln-	ala-	pro-	gly-	phe-	thr-	tyr-	thr-
Tuna	thr-	gly-	gln-	ala-	glu-	gly-	tyr-	ser-	tyr-	thr-
Sacch.	ser-	gly-	gln-	ala-	glu-	gly-	tyr-	ser-	tyr-	thr-
Candida	ser-	gly-	gln-	ala-	glu-	gly-	tyr-	ser-	tyr-	thr-

	80									90
Horse	asp-	ala-	asn-	lys-	asn-	lys-	gly-	ile-	thr-	trp-
Tuna	asp-	ala-	asn-	lys-	ser-	lys-	gly-	ile-	val-	trp-
Sacch.	asp-	ala-	asn-	ile-	lys-	lys-	asn-	val-	leu-	trp-
Candida	asp-	ala-	asn-	lys-	arg-	ala-	gly-	val-	glu-	trp-

	100									
Horse	lys-	glu-	glu-	thr-	leu-	met-	glu-	tyr-	leu-	glu-
Tuna	asn-	asn-	asp-	thr-	leu-	met-	glu-	tyr-	leu-	glu-
Sacch.	asp-	glu-	asn-	asn-	met-	ser-	glu-	tyr-	leu-	thr-
Candida	ala-	glu-	pro-	thr-	met-	ser-	asp-	tyr-	leu-	glu-

	110									120
Horse	asn-	pro-	lys-	lys-	tyr-	ile-	pro-	gly-	thr-	lys-
Tuna	asn-	pro-	lys-	lys-	tyr-	ile-	pro-	gly-	thr-	lys-
Sacch.	asn-	pro-	xxx-	lys-	tyr-	ile-	pro-	gly-	thr-	lys-
Candida	asn-	pro-	xxx-	lys-	tyr-	ile-	pro-	gly-	thr-	lys-

	130									140
Horse	met-	ile-	phe-	ala-	gly-	ile-	lys-	lys-	lys-	thr-
Tuna	met-	ile-	phe-	ala-	gly-	ile-	lys-	lys-	lys-	gly-
Sacch.	met-	ala-	phe-	ala-	gly-	leu-	lys-	lys-	glu-	lys-
Candida	met-	ala-	phe-	ala-	gly-	leu-	lys-	lys-	ala-	lys-

	150									160
Horse	glu-	arg-	glu-	asp-	leu-	ile-	ala-	tyr-	leu-	lys-
Tuna	glu-	arg-	gln-	asp-	leu-	val-	ala-	tyr-	leu-	lys-
Sacch.	asp-	arg-	asn-	asp-	leu-	ile-	thr-	tyr-	leu-	lys-
Candida	asp-	arg-	asn-	asp-	leu-	val-	thr-	tyr-	met-	leu-

	170									180
Horse	lys-	ala-	thr-	asn-	glu					
Tuna	ser-	ala-	thr-	ser						
Sacch.	lys-	ala-	cys-	glu						
Candida	glu-	ala-	ser-	lys						

[a] Moore, G.R. and Pettigrew, G.W. *Cytcohromes c - Evolutionary, Structural and Physicochemical Aspects*. Springer-Verlag, New York. **1990**, p. 115.

Appendix 2: Relative fluorescence (%F) of native cytochromes c in urea

Observed integrated fluorescence (%F) vs. urea concentration for horse cytochrome c relative to L-Trp[a]

[urea] (M)	F_1	F_2	F_3	F_4	F_5	Avg. F ± SD[b]
0	0	0	0	0	0	0
0.5	0	0	0	0	0	0
1.0	0	0	0	0	0	0
1.5	0	0	0	0	0	0
2.0	0	0	0	0	0	0
2.5	0	0	0	0	0	0
3.0	0	0	0	0	0	0
3.5	0	0	0	0	0	0
4.0	0	0	0	0	0	0
4.5	0	0	0	0	0	0
5.0	0.22	1.58	0.50	0	0	0.5 ± 0.6
5.5	1.33	2.72	2.30	0.9	0.3	1.5 ± 1.0
6.0	4.43	4.91	6.30	5.1	4.5	5.1 ± 0.7
6.5	14.7	13.69	15.20	13.2	13.0	14.0 ± 0.9
7.0	26.67	24.09	29.57	26.3	27.0	26.7 ± 1.9
7.5	37.94	36.27	41.00	36.9	39.2	38.3 ± 1.9
8.0	44.08	45.36	50.82	44.9	45.8	46.2 ± 2.7
8.25						48.9
8.5						50.4
8.75						51.0
9.0	48.26	49.38	56.09	48.5	55.6	51.6 ± 3.9

[a] 2 μM horse cytochrome c in 50 mM phosphate buffer (pH 7.0) with 0.2 M KCl, 25±1 °C and 2 μM L-Trp in the same buffer.

[b] F_d = 2.4 [urea] + 3.0 (from avg. F values in 8.5-9.0 M urea); F_n = 0.

Observed integrated fluorescence (%F) vs. urea concentration for tuna cytochrome c relative to L-Trp[a]

[urea] (M)	F_1	F_2	F_3	Avg. F ± SD[b]
0	1.1	1.9	3.9	2.6 ± 1.4
0.5	1.2	2.8	3.4	2.5 ± 1.1
1.0	1.5	2.2	2.9	2.2 ± 0.7
1.5	1.8	2.9	2.7	2.5 ± 0.6
2.0	1.8	2.1	2.7	2.2 ± 0.4
2.5	1.3	2.6	2.4	2.1 ± 0.7
3.0	1.7	2.3	2.1	2.0 ± 0.3
3.5	2.0	2.2	2.1	2.1 ± 0.1
4.0	2.4	2.6	2.5	2.5 ± 0.1
4.5	2.7	2.8	2.6	2.7 ± 0.1
5.0	3.0	2.8	2.9	2.9 ± 0.1
5.5	4.2	4.9	4.7	4.6 ± 0.4
6.0	7.8	8.1	10.2	8.7 ± 1.3
6.5	17.5	22.1	18.2	19.3 ± 2.5
7.0	37.6	40.5	36.3	38.1 ± 2.2
7.5	49.7	52.5	54.9	52.4 ± 2.6
8.0	63.3	65.9	67.5	65.6 ± 2.1
8.25				69.8
8.5				71.8
8.75				75.5
9.0	76.5	76.8	75.1	76.1 ± 0.9

[a] 2 μM tuna cytochrome c in 50 mM phosphate buffer (pH 7.0) with 0.2 M KCl, 25±1 °C and 2 μM L-Trp in the same buffer.

[b] F_d = 10.7 [urea] - 19.1 (from avg. F values in 8.5-9.0 M urea); F_n = 2.3 (from avg. F in 0-3.5 M urea)

Observed integrated fluorescence (%F) vs. urea concentration for Candida cytochrome c relative to L-Trp[a]

[urea] (M)	F_1	F_2	F_3	Avg. F ± SD[b]
0	0.9	3.1	1.1	1.7 ± 1.2
0.5	1.2	3.7	1.8	2.2 ± 1.3
1.0	1.1	3.9	1.9	2.2 ± 1.4
1.5	1.1	3.4	1.6	2.0 ± 1.2
2.0	1.5	4.1	2.7	2.8 ± 1.3
2.5	1.2	4.9	2.4	2.8 ± 1.9
3.0	2.5	4.9	2.9	3.4 ± 1.3
3.5	3.6	6.8	4.3	4.9 ± 1.7
4.0	7.2	7.4	7.3	7.3 ± 0.1
4.5	13.5	17.2	14.9	15.2 ± 1.9
5.0	26.8	29.6	27.4	27.9 ± 1.5
5.5	38.0	40.5	39.3	39.3 ± 1.2
6.0	44.9	45.1	45.0	45.0 ± 1.0
6.5	45.1	46.7	45.4	45.7 ± 0.9
7.0	45.2	47.7	46.6	46.5 ± 1.2
7.5	47.3	48.1	46.9	47.4 ± 0.6
8.0	48.0	48.6	48.4	48.3 ± 0.3
9.0	48.9	49.9	49.2	49.3 ± 0.5

[a] 2 μM Candida cytochrome c in 50 mM phosphate buffer (pH 7.0) with 0.2 M KCl, 25±1 °C and 2 μM L-Trp in the same buffer.

[b] F_d = 1.49 [urea] + 36.12 (from avg. F values in 6.0-9.0 M urea); F_n = 0.49 [urea] + 1.7 (from avg. F values in 0-3.0 M urea).

Observed integrated fluorescence (%F) vs. urea concentration for Saccharomyces cytochrome c relative to L-Trp[a]

[urea] (M)	F_1	F_2	F_3	Avg. F ± SD[b]
0	1.4	1.3	1.7	1.5 ± 0.2
0.5	2.5	2.4	2.9	2.6 ± 0.3
1.0	4.3	4.8	7.3	5.5 ± 1.6
1.5	9.2	9.5	12.2	10.3 ± 1.7
2.0	14.1	15.6	17.7	15.8 ± 1.8
2.5	24.1	22.9	26.5	24.5 ± 1.8
3.0	34.4	34.1	32.3	33.6 ± 1.1
3.5	35.5	37.7	39.3	37.5 ± 1.9
4.0	39.7	41.5	43.3	41.5 ± 1.8
4.5	42.3	43.3	43.6	43.1 ± 1.0
5.0	42.5	43.7	46.0	44.1 ± 1.8
5.5	44.9	46.9	47.7	46.5 ± 1.4
6.0	47.4	47.8	50.8	48.7 ± 1.8
6.5	49.1	49.9	52.6	50.5 ± 1.8
7.0	50.0	51.1	52.6	51.2 ± 1.3
7.5	50.2	52.5	53.4	52.0 ± 1.6
8.0	52.7	52.8	55.1	53.5 ± 1.3
9.0	52	53.9	54.6	53.5 ± 1.3

[a] 2 μM Saccharomyces cytochrome c in 50 mM phosphate buffer (pH 7.0) with 0.2 M KCl, 25±1 °C and 2 μM L-Trp in the same buffer.

[b] F_d = 2.54 [urea] + 32.56 (from avg. F values in 4.5-9.0 M urea); F_n = 1.5 for $\%F_n$ determinations.

Appendix 3: Relative fluorescence (%F) of horse cytochrome c derivatives in urea

Observed integrated fluorescence (%F) vs. urea concentration for por-cyt c relative to L-Trp[a]

[urea] (M)	F_1	F_2	F_3	Avg. F ± SD[b]
0	0.6	0.7	0.5	0.6 ± 0.1
0.5	0.7	0.5	0.6	0.6 ± 0.1
1.0	1.0	0.9	0.8	0.9 ± 0.1
1.5	1.2	1.0	0.8	1.0 ± 0.2
2.0	2.7	2.9	2.8	2.8 ± 0.1
2.5	6.6	7.0	6.9	6.8 ± 0.2
3.0	20.7	21.7	21.1	21.2 ± 0.5
3.5	32.4	32.2	32.8	32.5 ± 0.3
4.0	42.8	43.1	43.7	43.2 ± 0.5
4.5	46.5	47.0	44.3	45.9 ± 1.4
5.0	49.9	51.3	47.8	50.0 ± 1.2
5.5	52.7	52.1	52.8	52.5 ± 0.4
6.0	54.4	56.8	56.0	55.7 ± 1.2
6.5	57.9	60.4	60.1	59.5 ± 1.4
7.0	62.3	63.8	62.2	62.8 ± 0.9
7.5	65.1	66.3	66.1	65.8 ± 0.6
8.0	67.4	67.9	67.7	67.7 ± 0.3
9.0	70.9	71.1	70.3	70.8 ± 0.4

[a] 2 μM por-cyt c in 50 mM phosphate buffer (pH 7.0) with 0.2 M KCl, 25±1 °C and 2 μM L-Trp in the same buffer.

[b] F_d = 5.52 [urea] + 22.96 (from avg. F values in 5.0-9.0 M urea); F_n = 0.3 [urea] + 0.55 (from avg. F values in 0-1.5 M urea).

Observed integrated fluorescence (%F) vs. urea concentration for Zn-cyt c relative to L-Trp[a]

[urea] (M)	F_1	F_2	F_3	Avg. F ± SD[b]
0	0.5	0.4	0.3	0.4 ± 0.1
0.5				
1.0				
1.5				
2.0	0.2	0.4	0.3	0.3 ± 0.1
2.5				
3.0				
3.5				
4.0	0.1	0.3	0.2	0.2 ± 0.1
4.5				
5.0	1.7	1.6	1.8	1.7 ± 0.1
5.5				
6.0	6.3	6.1	6.2	6.2 ± 0.1
6.5	9.4	10.1	9.8	9.8 ± 0.3
7.0	16.1	18.1	16.5	16.9 ± 1.0
7.5	25.6	25.2	25.9	25.6 ± 0.3
8.0	32.2	33.2	32.9	32.7 ± 0.6
8.25				35.3
8.5				37.9
8.75				38.5
9.0	38.2	39.5	39.1	38.9 ± 0.7

[a] 2 μM Zn-cyt c in 50 mM phosphate buffer (pH 7.0) with 0.2 M KCl, 25±1 °C and 2 μM L-Trp in the same buffer.

[b] F_d = 1.94 [urea] + 21.46 (from avg. F values in 8.5-9.0 M urea); F_n = -0.05 [urea] + 0.35 (from avg. F values in 0-4.0 M urea).

Observed integrated fluorescence (%F) vs. urea concentration for Co-cyt c relative to L-Trp[a]

[urea] (M)	F_1	F_2	F_3	Avg. F ± SD[b]
0	2.1	2.5	2.2	2.3 ± 0.2
0.5	2.3	2.0	1.9	2.1 ± 0.2
1.0	3.7	2.3	4.0	3.3 ± 0.9
1.5	2.2	2.4	2.3	2.2 ± 0.1
2.0	2.9	3.5	3.8	3.4 ± 0.5
2.5	3.3	3.1	3.5	3.3 ± 0.2
3.0	3.3	3.4	3.5	3.4 ± 0.1
3.5	4.0	4.7	5.2	4.6 ± 0.6
4.0	4.4	5.2	5.8	5.1 ± 0.7
4.5	5.1	4.8	5.2	5.0 ± 0.2
5.0	5.8	5.6	5.7	5.7 ± 0.1
5.5	6.4	7.0	6.8	6.7 ± 0.3
6.0	7.5	7.6	7.4	7.5 ± 0.1
6.5	11.4	11.6	11.5	11.5 ± 0.1
7.0	18.0	17.9	18.7	18.2 ± 0.4
7.5	29.1	28.9	29.4	29.1 ± 0.2
8.0	39.6	42.8	41.1	41.2 ± 1.6
8.25				47.9
8.5				49.2
8.75				49.3
9.0	50.6	51.4	50.1	50.7 ± 0.6

[a] 2 μM Co-cyt c in 50 mM phosphate buffer (pH 7.0) with 0.2 M KCl, 25±1 °C and 2 μM L-Trp in the same buffer.

[b] F_d = 3.0 [urea] + 23.48 (from avg. F values in 8.25-9.0 M urea); F_n = 0.84 [urea] + 1.66 (from avg. F values in 0-6.0 M urea).

Appendix 4: Relative fluorescence (%F) of native cyt c in guanidine hydrochloride

Observed integrated fluorescence (%F) vs. guanidine hydrochloride concentration for horse cytochrome c relative to L-Trp[a]

[Gdn-HCl) (M)	F_1	F_2	F_3	Avg. F ± SD[b]
0	0	0	0	0
0.2				
0.4	0	0	0	0
0.6				
0.8	0	0	0	0
1.0				
1.2	0	0	0	0
1.4				
1.6	0	0	0	0
1.8	0.6	1.1	0.4	0.7 ± 0.4
2.0	1.6	1.5	1.7	1.6 ± 0.1
2.2	5.3	4.7	4.5	4.8 ± 0.4
2.4	10.1	9.9	10.9	10.3 ± 0.5
2.6	23.8	26.1	25.5	25.1 ± 1.2
2.8	40.3	38.7	40.8	39.9 ± 1.1
3.0	47.6	49.7	50.5	49.3 ± 1.5
4.0	63.2	62.7	61.1	62.3 ± 1.1
5.0	70.1	68.5	70.7	69.8 ± 1.0
5.25				70.7
5.5				72.4
5.75				74.0
6.0	75.1	74.7	76.1	75.3 ± 0.7

[a] 2 μM horse cytochrome c in 100 mM phosphate buffer (pH 7.0), 25±1 °C and 2 μM L-Trp in the same buffer.

[b] F_d = 6.5 [gdn-HCl] + 36.6 (from avg. F values in 5.5-6.0 M gdn-HCl); F_n = 0.

Observed integrated fluorescence (%F) vs. guanidine hydrochloride concentration for tuna cytochrome c relative to L-Trp[a]

[Gdn-HCl] (M)	F_1	F_2	F_3	Avg. F ± SD[b]
0	1.5	1.6	1.7	1.6 ± 0.1
0.2				
0.4	1.9	2.0	1.8	1.9 ± 0.1
0.6				
0.8	2.0	2.2	2.1	2.1 ± 0.1
1.0				
1.2	2.1	2.2	2.3	2.2 ± 0.1
1.4				
1.6	2.4	2.0	2.6	2.3 ± 0.3
1.8	3.4	2.6	3.8	3.3 ± 0.6
2.0	3.0	3.9	4.0	3.6 ± 0.5
2.2	5.7	6.1	5.6	5.8 ± 0.3
2.4	10.1	9.5	12.3	10.6 ± 1.5
2.6	25.0	24.8	25.4	25.1 ± 0.3
2.8	42.1	44.8	41.8	42.9 ± 1.7
3.0	63.7	63.6	63.8	63.7 ± 0.1
4.0	86.1	87.0	83.4	85.5 ± 1.9
5.0	102.1	101.7	102.3	102.0 ± 0.3
5.25				104.1
5.5				106.3
5.75				108.4
6.0	108.6	113.3	109.7	110.5 ± 2.4

[a] 2 μM tuna cytochrome c in 100 mM phosphate buffer (pH 7.0), 25±1 °C and 2 μM L-Trp in the same buffer.

[b] F_d = 8.4 [gdn-HCl] + 60.1 (from avg. F values in 5.5-6.0 M gdn-HCl); F_n = 2.0 (from avg. F values in 0-1.6 M gdn-HCl).

Observed integrated fluorescence (%F) vs. guanidine hydrochloride concentration for Candida cytochrome c relative to L-Trp[a]

[Gdn-HCl] (M)	F_1	F_2	F_3	Avg. F ± SD[b]
0	1.2	0.8	1.4	1.1 ± 0.3
0.2				
0.4	1.0	1.6	1.8	1.5 ± 0.4
0.6				
0.8	2.1	1.9	2.0	2.0 ± 0.1
1.0				
1.2	2.9	3.0	2.6	2.8 ± 0.2
1.4	4.2	4.1	4.3	4.2 ± 0.1
1.6	6 0	5.6	6.3	6.0 ± 0.3
1.8	10.3	10.0	10.4	10.2 ± 0.2
2.0	19.1	17.8	19.6	18.8 ± 0.9
2.2	37.9	39.9	37.2	38.3 ± 1.4
2.4				
2.6				
2.8				
3.0	47.9	47.7	47.8	47.8 ± 0.1
4.0	52.6	52.7	52.5	52.6 ± 0.1
5.0	59.6	59.7	59.8	59.7 ± 0.1
6.0	63.9	66.2	64.5	64.9 ± 1.2

[a] 2 μM Candida cytochrome c in 100 mM phosphate buffer (pH 7.0), 25±1 °C and 2 μM L-Trp in the same buffer.

[b] F_d = 5.84 [gdn-HCl] + 29.97 (from avg. F values in 3.0-6.0 M gdn-HCl); F_n = 1.4 [gdn-HCl] + 1.01 (from avg. F values in 1-1.2 M gdn-HCl).

Observed integrated fluorescence (%F) vs. guanidine hydrochloride concentration for Saccharomyces cytochrome c relative to L-Trp[a]

[Gdn-HCl] (M)	F_1	F_2	F_3	Avg. F ± SD[b]
0	1.3	1.1	1.2	1.2 ± 0.1
0.2	2.5	2.6	2.4	2.5 ± 0.1
0.4	6.3	4.4	7.1	5.9 ± 1.4
0.6	13.1	12.3	15.3	13.6 ± 1.5
0.8	17.3	16.6	19.8	17.9 ± 1.7
1.0	23.0	23.9	25.2	24.0 ± 1.1
1.2	28.7	28.1	31.0	29.3 ± 1.5
1.4				
1.6	43.2	41.9	44.3	43.1 ± 1.2
1.8				
2.0	48.7	49.1	51.1	49.6 ± 1.3
2.2				
2.4	53.3	52.1	55.0	53.5 ± 1.5
2.6				
2.8				
3.0	59.4	58.9	59.6	59.3 ± 0.4
4.0	64.1	62.9	65.0	64.0 ± 1.1
5.0	70.7	70.1	71.7	70.8 ± 0.8
6.0	75.9	76.1	78.6	76.9 ± 1.5

[a] 2 μM Saccharomyces cytochrome c in 100 mM phosphate buffer (pH 7.0), 25±1 °C and 2 μM L-Trp in the same buffer.

[b] F_d = 5.96 [gdn-HCl] + 40.93 (from avg. F values in 3.0-6.0 M gdn-HCl); F_n = 1.2 for $\%F_n$ determinations.

Appendix 5: Determination of $\Delta G_{d,aq}$ and m values

1) F_d and F_n values were determined as indicated in Figure 2.2 and the least squares parameters are given in Footnotes (b) to the tables in Appendices 2, 3 and 4.

2) ΔG_d values were calculated from the F_d, F_n and %F values given in the tables in Appendices 2, 3 and 4 using Equation 2.4.

3) Least squares analysis of the ΔG_d values (calculated from each %F in the transition region) vs. denaturant concentration (Equation 2.3) was carried out using Statview software (Macintosh). The least squares parameters $G_{d,aq}$ (intercept) and m (slope) and their standard deviations, which are given in Tables 2.1 and 3.2, were obtained as output from Statview.